

***Theoretical investigations on inelastic processes  
in ion-ion/atom collisions at intermediate and  
high energies***

THE THESIS SUBMITTED TO  
JADAVPUR UNIVERSITY FOR THE AWARD OF THE DEGREE  
OF DOCTOR OF PHILOSOPHY IN SCIENCE

BY

**RAKESH SAMANTA**



DEPARTMENT OF PHYSICS

JADAVPUR UNIVERSITY

KOLKATA- 700 032

INDIA

2013

DEDICATED  
TO MY PARENTS

## CERTIFICATE FROM THE SUPERVISOR(S)

This is to certify that the thesis entitled "*Theoretical investigations on inelastic processes in ion-ion/atom collisions at intermediate and high energies*" submitted by Sri Rakesh Samanta, who got his name registered on 21.03.2011 for the award of Ph. D. (Science) degree of Jadavpur University, is absolutely based upon his own work under the supervision of Dr. Malay Purkait, Reader, Dept. of Physics, Ramakrishna Mission Residential College (Autonomous), Narendrapur and Dr. C. R. Mandal, Professor, Dept. of Physics, Jadavpur University and that neither this thesis nor any part of it has been submitted for either any degree/ diploma or any other academic award anywhere before.

*CM*  
01.11.13  
(Prof. C.R. Mandal)

**Dr. Chitta Ranjan Mandal**  
Professor (Retired)  
Department of Physics  
Jadavpur University  
Kolkata - 700032

*Malay Purkait*  
01.11.13  
(Dr. Malay Purkait)

*Dr. Malay Purkait*  
Reader  
Dept. of Physics  
R.K. Mission Residential College  
Narendrapur, Kolkata-103

# **ACKNOWLEDGMENTS**

I accord my pious feelings, heartfelt gratitude and all time indebtedness to my honorable teachers, Dr. Malay Purkait and Prof. C. R. Mandal, under whose ingenious supervision this work has been accomplished. Their guidance and eternal interest and strong support during this dissertation have been indispensable to me. It goes without saying that without their involvement at all stages; the thesis would not have reached the present form.

During the eventful journey I was fortunate to gather numerous well-wishers, supporters, friends, seniors and of course my beautiful colleagues.

Among them I would like to thank, revered Maharaj, Swami Suparnananda, the former Principal, for his affection and inspiration.

Respected Maharaj, Swami Bhudevananda, the Principal, was always friendly and helpful to me. I thank him for his supports.

Finally, an obvious thanks goes to my parents for their invariable supports and love, unuttered scarification and devotion, and of course for their patience.

Some of my friends have their individual contributions, so it would be a great mistake if I don't remember Sujoy, Manash da, Amit da, Sarat da, Pinaki da, Subhendu da and Suman da.

Thanks to my friends and well-wishers through the globe who are not listed over here. I cordially beg apology to them.

I also gratefully acknowledge UGC, New Delhi for fellowships.

**Kolkata,  
November, 2013**

**(Rakesh Samanta)  
Dept. of Physics,  
Jadavpur University**

# CONTENTS

	<b>Page no.</b>
SUMMARY	9
LIST OF PUBLICATIONS	12

## CHAPTER-1

### **I. GENERAL INTRODUCTION** 13

1.1	Basic definitions	17
1.2	Application Areas	20
	1.2.1 Radiation Therapy	21
	1.2.2 Electron collision cross section data in plasma physics	22
	1.2.3 Needs for cross sections in different types of plasmas	23
	1.2.4 Cross sections for electron interactions with radical species	24
	1.2.5 X-Ray LASER development	25
1.3	Formal Theory of Quantum Scattering	25
	1.3.1. Perturbation Series with the correct boundary conditions	29
	1.3.2. The Lippmann-Schwinger equations	30
	1.3.3. The Born expansions with the correct boundary conditions	31
	1.3.4. Boundary Corrected Continuum Intermediate State (BCCIS) Approximation	32
	1.3.5. Continuum Distorted Wave (CDW) Theory	34
	1.3.6. Classical Trajectory Monte Carlo Method	35
	References	39

## CHAPTER-2

### **STATE-SELECTIVE CHARGE TRANSFER IN ION-ION INTERACTION AT INTERMEDIATE AND HIGH ENERGIES**

2.1.	Introduction	45
2.2.	Theory	46
2.3.	Results and discussion	49
	A. Non-resonant reactions	49
	B. Resonant reactions	50
2.4.	Conclusions	50
	References	58

## CHAPTER-3

### **SINGLE- ELECTRON CAPTURE PROCESSES IN COLLISIONS OF $\text{He}^{2+}$ , $\text{Li}^{q+}$ ( $q=1,2,3$ ), $\text{C}^{6+}$ AND $\text{O}^{8+}$ IONS WITH HELIUM**

3.1.	Introduction	61
3.2.	Theory	63
3.3.	Results and discussion	69
	A. Symmetric collision	69
	B. Asymmetric collision	70
3.4.	Conclusions	71
	References	78

## CHAPTER- 4

### **ELECTRON CAPTURE BY FAST PROTONS FROM HELIUM LIKE IONS**

4.1.	Introduction	82
4.2.	Theory	83
4.3.	Results and discussion	88
4.4.	Conclusions	90

	References	95
--	------------	----

## CHAPTER- 5

### SINGLE-ELECTRON CAPTURE FROM HELIUM BY FAST PROTONS

5.1.	Introduction	98
5.2.	Theory	100
5.3.	Results and discussion	102
5.4.	Conclusions	105
	References	117

## CHAPTER- 6

### ELECTRON CAPTURE CROSS SECTION IN COLLISION OF MULTI-CHARGED NEON IONS WITH GROUND STATE HYDROGEN AND HELIUM

6.1.	Introduction	121
6.2.	Theory	123
	6.2.1. Classical formulation	123
	6.2.2. Quantum mechanical formulation	124
	6.2.2.1. Single charge transfer	124
	6.2.2.2. Double charge transfer	126
6.3.	Results and discussion	127
	6.3.1. Single charge transfer and ionization	128
	6.3.2. Double charge transfer	129

6.4.	Conclusions	130
	References	147

## **CHAPTER- 7**

### **SINGLE-ELECTRON CAPTURE FROM HYDROGEN LIKE ATOMIC SYSTEMS**

7.1.	Introduction	151
7.2.	Theory	153
7.3.	Results and discussion	162
7.4.	Conclusions	165
	References	170

## SUMMARY

Theoretical investigation on ion-ion and ion-atom collision in intermediate and high energies has been reported in the present thesis. The thesis is submitted to the Jadavpur University for fulfillment of requirement for the degree of Doctor of Philosophy (Science).

Part I of the thesis contains the general introduction mentioning the basic definition and necessity of the cross section data in the diverse field of Physics. The author has reviewed up-to-date investigations in the framework of different approximation in ion-atom and ion-ion collision which are also the contents of this part. Part II of this thesis contains quantum and classical studies of ion-atom interaction. This part is subdivided into six chapters.

In Chapter II, total and state-selective cross sections for charge transfer in  $H^+ + He^+$ ,  $He^{2+} + Li^{2+}$ ,  $He^{2+} + He^+$  and  $Li^{3+} + Li^{2+}$  collisions have been calculated using the three body boundary corrected continuum intermediate state (BCCIS-3B) approximation at energy range 30-2000 keV/amu. In this model, distortions in the final channel related to the Coulomb continuum states of the projectile ion and the electron in the field of the residual target are included. Sub-shell distribution of total charge transfer cross section has been reported in tabular form. The comparison of the results is made with those of other recent theoretical methods and with experimental measurements. Results so obtained are in very good agreement with the available experimental findings.

In Chapter III, cross sections for single-electron capture in collisions of  $He^{2+}$ ,  $Li^{q+}$  ( $q=1,2,3$ ),  $C^{6+}$  and  $O^{8+}$  ions with helium atom at incident energy ranging from 50 to 5000 keV/amu have been calculated in the framework of four-body boundary corrected continuum intermediate state (BCCIS-4B) approximation in both prior and post forms. In this formalism, distortion in the final channel related to the Coulomb continuum states of the projectile ion and the active electron in the field of residual target ion are included. In all cases, total single-electron capture cross sections have been calculated by summing over all contributions upto  $n=3$  shells and sub-shells respectively. It has been observed that the contribution of the capture cross section into the excited states is significant for asymmetric collision ( $Z_P > Z_T$ ) and is insignificant for symmetric

collision. Numerical results for the total cross sections show good agreement with the available experimental findings particularly in the post-form. Post-prior discrepancy has been found to be within 30% except for  $\text{Li}^+ + \text{He}$  interaction below 150 keV/amu.

In Chapter IV, four-body formalism of boundary corrected continuum intermediate state (BCCIS-4B) approximation have been applied to calculate the single-electron capture cross sections by fast protons through some helium like ions in a large energy range from 30-1000 keV. In this model, distortion has been taken into account in the entrance channel. In the final channel, the passive electron plays the role of screening of the target ion. However, continuum states of the projectile and the electron in the field of the residual target ion are included. The comparison of the results is made with those of other theoretical investigations and experimental findings. The present calculated results are found to be in good agreement with the available experimental findings.

In Chapter V, single-electron capture in p-He collisions have been calculated at incident projectile energies ranging from 30 keV to 1 MeV by means of the four-body boundary corrected continuum intermediate state approximation. The effect of the dynamic electron correlations is explicitly taken into account through the complete perturbation potentials. Total single-electron capture cross sections have been calculated by summing over the contributions upto  $n=2$  shells and sub-shells respectively. The differential cross sections are calculated at impact energies in the range from 30 to 293 keV. Overall, the calculated cross sections are in good agreement with the recent experimental findings. Post-prior discrepancy for total cross sections is negligible below 200 keV.

In Chapter VI, the Classical Trajectory Monte Carlo (CTMC) method and the post form of three-body boundary corrected continuum intermediate state (BCCIS-3B) approximation are employed to calculate the cross sections for total and state-selective electron capture in collision of highly charged  $\text{Ne}^{q+}$  ions with ground state hydrogen atom in the intermediate to high energy region. In both these methods, the active electron interactions with the partially stripped neon ions are described by a model potential containing both a long-range part and a short-range part. We have also calculated the double electron- capture cross sections in collision of fully stripped neon ion

with helium atom in the energy range 80-2000 keV/amu using the post-form of four-body BCCIS approximation (BCCIS-4B). In BCCIS formalism, the intermediate continuum state of the active electrons with the projectile ion has been taken into account as the projectile charge is greater than the target charge. In addition, state-selective charge transfer cross sections are given in tabular and graphical form.

In Chapter VII, the total cross sections for single-charge transfer in  $H + H$ ,  $He^+ + H$ ,  $He^+ + He^+$  and  $Li^{2+} + H$  collisions have been calculated in the framework of four-body formalism of boundary corrected continuum intermediate state approximation in the energy range 20 – 5000 keV/amu. The dynamic electron correlation is explicitly taken into account through the complete perturbation potentials. In the initial channel, the passive electron plays the role of screening of the projectile ion. However, continuum states of the target ion and the electron in the field of the residual projectile ion are included. In all cases, total single- electron capture cross sections have been calculated by summing over all contributions up to  $n = 2$  shells and sub shells, respectively except H-H collision. The present computed results, both in prior and post forms of BCCIS - 4B method for symmetric and asymmetric cases have been compared with the available theoretical and experimental results. We found that our computed results particularly in the prior form are in better agreement with the experimental observations in comparison to other theoretical findings. Post-prior discrepancy has been found to be within 20% above 70 keV/amu for all interactions.

## LIST OF PUBLICATIONS

1. State-selective charge transfer in ion-ion interaction at intermediate and high energies→ **R. Samanta**, M. Purkait and C.R.Mandal→ *Phys. Scr.* **82**, 065303 (2010).
2. Single-electron capture processes in collisions of  $\text{He}^{2+}$ ,  $\text{Li}^{q+}$  ( $q=1,2,3$ ),  $\text{C}^{6+}$  and  $\text{O}^{8+}$  ions with helium→ **R. Samanta**, M. Purkait and C.R.Mandal→ *Phys. Rev. A* **83**, 032706 (2011).
3. Electron capture by fast protons from helium like ions→ **R. Samanta** and M.Purkait→ *Eur. Phys. J. D* **64**, 311 (2011).
4. Single-electron capture from helium by fast protons→ **R. Samanta** and M. Purkait→ *Phys. Scr.* **84**, 065301 (2011).
5. Single-electron capture from hydrogen like atomic systems→ **R. Samanta**, S. Jana, C. R. Mandal and M. Purkait→ *Phys. Rev. A* **85**, 032714 (2012).
6. Electron capture and ionization in collisions of multi-charged neon ions with ground state hydrogen and helium → **R. Samanta**, S. Jana, S. Ghosh, M. Purkait and C. R. Mandal→ *Indian J. Phys.* **86**, 503 (2012).
7. Electron capture by hydrogen like projectile ions from ground state atomic hydrogen→ S. Jana, **R. Samanta** and M. Purkait→ *Nucl. Instr. And Meth. In Phys. Res. B.* **285**, 37 (2012).
8. Angular distribution of electron emission from atomic hydrogen by bare ion impact → S. Jana, **R. Samanta** and M. Purkait→ *Eur. Phys. J. D.* **66**, 243 (2012).
9. Classical simulation of single-electron capture and ionization in ion-atom interaction at intermediate energies→ S. Jana, **R. Samanta** and M. Purkait→ *Indian J. Phys.* **87**(10), 963 (2013).
10. Double-differential cross sections for single ionization of helium by bare ion impact→ S. Jana, **R. Samanta**, C. R. Mandal, and M. Purkait→ *Phys. Scr.* **88**, 055301 (2013).

**GENERAL INTRODUCTION**

*N.B.: Atomic units are used throughout the work unless otherwise stated.*

# 1. INTRODUCTION

Research in theoretical atomic, molecular, and optical physics (TAMOP) is characterized by two intertwined strands, *understanding* and *utility*. AMO physics seeks to investigate and understand the fundamental behaviour of matter and fields as Nature presents them to us, at the energy and length scales set by electrons, atoms, molecules, and photons and their interactions. Building on this understanding, TAMOP researchers seek also to formulate and develop techniques for manipulating and controlling AMO systems to perform tasks that Nature never contemplated, tasks that lie at the heart of present and future technology development. That AMO physics is planted so firmly at the intersection of understanding and utility is the field's greatest strength—and makes it unique among the sub disciplines of physics. At this intersection theoretical and experimental research efforts are often very tightly coupled.

In last few decades, AMO physics has undergone a renaissance. As some evidence of this, 5 of the last 16 Nobel prizes have been awarded in AMO physics: 1997, 2001, 2005, 2009, and 2012. As one of the areas leading to the development of quantum mechanics, atomic/molecular collisions have been core components of AMO research since the beginning of modern physics. These traditional fields continue to be of tremendous importance, both for fundamental research and for practical applications.

Recently, charge transfer in ion-atom/ion collisions is being able to make a remarkable place in the study of atomic and molecular physics. But these studies are not only confined to intrinsic science they also find their applications in diverse branches of physics, viz. astrophysics, atmospheric physics, plasma physics, in fusion researches, in the development of the production of soft x-ray lasers etc. All these physical aspects are described in brief as follows.

The cross-sectional data of charge transfer between partially or fully stripped ions and heavy atoms are of paramount importance in atmospheric physics as well as in astrophysics. The emission strengths of lines arising from transitions in neutral and ionized atomic systems such as CI, NI, NII, NeII, OI, OII, SI and SII in gaseous nebulae are considerably stronger than the strengths in theoretical models calculated (particularly for OII doublets) for quasars, planetary nebulae, Seyfert galaxies and diffuse HII regions. The two-phase model of the interstellar

medium has become successful to a great extent in explaining many of the characteristics of the interstellar gas. This model is based upon the postulate of an ionizing source uniform throughout the galaxy with suitable frequencies ( $10^{-15} \text{ sec}^{-1}$ ) which is attributed either to low energy cosmic rays or soft x-rays neither of which can be detected in the solar neighbourhood. Steigman has pointed out that charge transfer in collisions between highly charged ions of C,N,O,Ne,Mg,Si,P,S,etc. and neutral atoms of hydrogen or helium may be rapid at thermal energies, which is consistent with the work of Bates and Moiseiwitsch. If these reactions are rapid, they will suppress highly charged ions in the HI region. This feature guarantees that the observed absorption features from such ions can not originate in the interstellar gas. The possible implications of this reaction are consistent with the observations of interstellar medium, HII regions and planetary nebulae. Thus the discrepancies in this field of astrophysics are removed. Observations by x-ray satellites such as ROSAT, INTEGRAL, RXTE etc. indicate that X-rays are produced by almost all comets and many other objects in the solar system. Such X-ray observations of comets and other objects of the solar system may be used to determine the structure and dynamics of the solar wind. Minor ions in the solar wind exist in highly charged states, including the species such as  $\text{O}^{7+}$ ,  $\text{O}^{6+}$ ,  $\text{C}^{6+}$ ,  $\text{C}^{5+}$ ,  $\text{N}^{6+}$ ,  $\text{Ne}^{8+}$ ,  $\text{Si}^{9+}$  and  $\text{Fe}^{12+}$ . Such ions readily undergo charge transfer reactions in which an incident ion removes an electron from a target neutral atom or molecule. The product ion remains highly charged and is almost always left in an excited state. The energy required to power X-ray or EUV emission originates in the hot solar corona and is temporarily stored as potential energy in highly stripped solar wind ions until this energy is released by charge transfer collisions. The X-ray emission line intensities of the comets C/2002 T7 (LINEAR), C/2001 Q4 (NEAT) etc. are consistent with the model emission lines of C,N,O,Mg,Fe,Si and Ne solar wind ions. In a recent report, a group of scientist from USA has claimed that they have recorded the X-ray emission of highly charged ions of carbon, nitrogen and oxygen which simulates charge exchange reactions between heavy ions in the solar wind and neutral gases in cometarycomae. However, extraction of useful information on solar wind properties from such observations will require further improvement in our understanding of the SWCX (Solar Wind Charge Exchange) mechanism. The SWCX mechanism operates whenever the solar wind interacts with neutral gas and has also been suggested as a source of X-ray emission from Venus and Mars, the terrestrial hydrogen geo-corona and interstellar neutral gas.

The X-ray line spectra of highly charged oxygen ions and the Ultraviolet emission-line spectra of precipitating oxygen atoms and ions in the auroral atmosphere of Jupiter have been calculated using cross sectional data of state-selective charge transfer. In both the above cases the oxygen atoms or ions excited by charge transfer interaction with molecular hydrogen. With these studies people come to know that the UV emissions from the precipitating oxygen atoms and ions are far from being discernible in the Jovian auroral spectra. And this finding also provides a straightforward explanation of the negative search for any direct UV signature of heavy ion precipitation in the Jovian aurora, putting an end to the decade-long controversy on the auroral mechanism of Jupiter.

Neutral beam of atoms may be used for probing plasmas in Tokmak devices. Kislyakov and Petrov have used 4-14 keV beams of hydrogen as a probe. Attenuation of such type of beams occurs due to ionization of the injected beams by the process of charge transfer and ionization by the plasma protons or ionization by plasma electrons. Thus the proton density in plasma can be determined by the knowledge of the cross sections of such processes. The multiple electron transfer between an ion and an atom plays an important role as an energy loss mechanism in high temperature and astrophysical plasmas. The X-ray spectra obtained from electron capture will be powerful diagnostic probes of the capture mechanism and of the diverse range of laboratory and astrophysical plasma. Shaikh et al have constructed a model which describes a partially ionized magneto-fluid ISM (interstellar medium) that couples a neutral hydrogen fluid with plasma primarily through charge exchange interactions. In double electron capture by alpha particles from lithium atoms, a neutral lithium beam may be used as a probe to find the alpha particle distribution in Tokmak fusion reactors. After double electron capture, the resulting helium atom can escape from the plasma field and can be analyzed by conventional means. Electron capture by plasma protons from the injected beam results in the formation of hydrogen atom in excited states. An emission of radiation is followed due to subsequent decay of these excited atoms. Studies of Doppler shift of such radiation help to assess the temperature of the plasma.

In fusion devices based on magnetic confinement of high temperature plasma, one of the most promising forms of supplementary heating is by the injection of fast neutral beams of an

appropriate isotope of hydrogen. In practice, the effectiveness of this form of heating is complicated by the presence of small fractions of partially or fully ionized impurities such as carbon, nitrogen, oxygen etc. as well as partially ionized metal atoms of high atomic number  $z$  arising from interactions at the walls of the confining vessel. The injection of fast neutral beams (beams of  $^3\text{He}$  are also possible) is being considered for the supply of fuel to the plasma in a fusion reactor. When an intense fast neutral beam of an appropriate isotope of hydrogen (e.g. deuterium) injects through the magnetic confining field and into the plasma it undergoes electron loss by both charge transfer ( $\text{H}^+ + \text{H} \rightarrow \text{H} + \text{H}^+$ ) and ionization ( $\text{H}^+ + \text{H} \rightarrow \text{H}^+ + \text{H}^+ + \text{e}$ ) in collisions with the plasma protons. The resulting fast protons are trapped in the confining field and give up their energy in collisions with the plasma constituents. Since electron capture takes place into highly excited states, the population inversion of the parent ions occur. The subsequent radiative decay of such short-lived excited states can result in very substantial energy loss.

The studies of radiation effects on biological bodies, nuclear workers demand the knowledge of collision processes. Therapeutic treatments are being done to treat the cancer and other foreign bodies. Several years' proton therapy found greater advantages over other conventional radiation. Proton beam causes less damage to the live tissues surrounding the affected part of the patient. The three dimensional hologram of energy spectrum of proton beam are readily obtainable and proper dose level may be ascertained to the patient.

These many fold applications of cross-sectional data in diverse field of physics and astrophysics play an important role behind our motivation for collision studies on charge transfer and ionization in ion-atom/ion collisions.

## **1.1. BASIC DEFINITIONS:**

Collision is short duration interaction between two bodies or more than two bodies simultaneously causing change in motion of bodies involved due to internal forces acted between them during this. The range of scale of collision may be microscopic of subatomic particle to the astronomic scale of colliding stars and colliding galaxies. Although, the most common colloquial use of the word "collision" refers to accidents in which two or more objects collide, in scientific use, it is an isolated event in which two or more moving bodies exert forces on each other for a

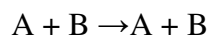
relatively short time. In collision, the momentum and kinetic energy are transferred from one object to another, but the total momentum of both objects before and after collision is the same. A collision does not have to be a force of contact. In scattering processes the strength of interactions among atomic particles could be viewed through observables called cross sections.

➤ **Scattering:**

Scattering occurs when we fire a projectile at a target. The projectile will be 'scattered' from it or could remain unscattered, i.e. its direction of motion is altered by the target. By measuring the numbers of particles which scatter by different amounts we can work out much about the structure of the target. There are two kinds of scattering elastic and inelastic. For scattering it is easiest if the projectile is a fundamental particle (so can be considered as a point without any structure, such as the electron) so that the effects of any size is not there to complicate results and we are only observing the target (say a proton).

➤ **Elastic scattering:**

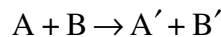
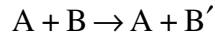
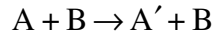
In an elastic collision the incident and target particles remain intact (like billiard balls). No energy is lost (to other processes) and the projectile's kinetic energy is shared between itself and the target after the collision, momentum is of course always conserved. If the target is point-like then elastic scattering is the only possibility. If the target has size then the scattering may still be an elastic process, however the formula for it will be altered slightly, depending on the momentum imparted to the target particle (by a factor called the form factor). Let us assume a typical collision between a system A of the incident beam and a scattered B of the target, then in elastic scattering, two bodies A and B are simply scattered without any change in their internal structure,



➤ **Inelastic scattering:**

In inelastic scattering part of the kinetic energy of the incident particle is lost inside the target giving rise to some internal processes and only a fraction of it goes into moving the whole target. For example if you take a spherical container and then fire a small ball onto it the collision could be considered to be elastic (in an ideal world). If you were then to fill it with some marbles and

then fire another ball at it some of the kinetic energy would go into moving the ball, but a fraction would also move around the marbles inside. In this sense we can say that inelastic scattering will occur if the target consists of smaller components. One other difference between inelastic and elastic scattering is that with elastic scattering the target will not change form, whereas with inelastic scattering the target can break up into new forms. A proton may make hadrons (particles built from quarks) by inelastic collisions. We now see that if we can show that the target (say a proton) scatters inelastically then we can presume that there must be some internal process occurring, which should not happen if the particle is fundamental, because this suggests there is something smaller inside to cause this process. In this scattering, the two particles A and (or) B undergo a change in their internal quantum state after collision.

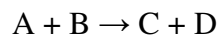


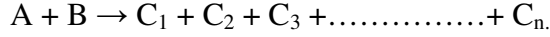
where  $A'$  and  $B'$  are the new internal states after inelastic collision.

These interaction (scattering) processes are in general mediated by the electromagnetic force, meaning that it is really an exchange process between the incident electron and the target. This is an electromagnetic interaction and the mediator (the particle which is exchanged between the two interacting ones and produces the force, in this case for electromagnetic it's the photon).

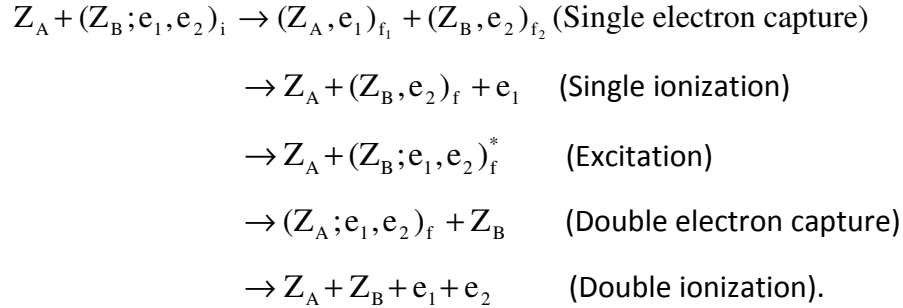
Take for example a particle of initial momentum  $p$  which interacts and scatters from the target with a new momentum  $p'$ . The difference is  $q = p - p'$  which is the momentum transferred to the target. It is found that in elastic scattering the cross-section of scattering falls as  $q^2$  increases. If we are able to work out what the form factor is (by seeing how the scattering is reduced from its value for a point particle), then we can get an idea of how the charge is distributed inside the target (in fact the form factor is the fourier transform of the charge distribution).

➤ **Reactions:** It can also possible that a composite system (A+B) splits into two systems C and D, different from A and B, or into  $n \geq 2$  systems i.e.





In elastic collisions the two colliding particles A and B remain in the initial channel, while inelastic collisions or reactions processes leading from a given initial channel to a different final channel in scattering between a bare nucleus of charge (projectile)  $Z_A$  and  $Z_B$ . Let us consider, the target nucleus of charge  $Z_B$  has two electrons ( $e_1$  and  $e_2$ ) bound to the nucleus (helium-like atomic system). Then the following rearrangement collision may be possible,



Other than the above mentioned process there are also some processes like transfer ionization, transfer excitation, multiple ionization etc.

The most important thing is the energy range of collision according to the value of  $W$ , which is defined as the ratio between the relative velocity of the projectile and the orbital velocity ( $v_0$ ) of the active electron in the target.

- $W \ll 1$  indicates adiabatic or low energy region.
- $W \approx 1$  indicates intermediate energy region.
- $W \gg 1$  indicates high energy region.

The unit of cross section is that of area. Since the order of atomic radius is of the order of  $10^{-8}$  cm, the atomic cross section will be in the order of  $10^{-16}$  cm<sup>2</sup>. But, in atomic and molecular physics cross sections are generally expressed in unit of  $\pi a_0^2$ , where  $a_0$  is the radius of the first Bohr orbit of hydrogen atom.

## 1.2. APPLICATION AREAS

Elastic collisions are of paramount importance for Ohmic heating and energy dissipation into the plasma; inelastic collisions are responsible for all the electronic excitation processes. For both processes, the deductive approach is chosen. By electronic and ionic impact, electrons can be

released from surfaces; this process is required for the carrier avalanche in DC discharges, but has regained interest for stabilizing processes in production reactors whose inner surface is subject to various (mostly unintended) coating reactions. In addition we can describe the application areas of atomic collisions with the following points.

### **1.2.1. RADIATION THERAPY**

When radiations (particles or photons) from an outside source impinge on and penetrate into a material, various observable phenomena occur that are a direct result of a chain of events referred to as a radiation cascade. The change of the structure of a material can possibly be subjected to fast heavy particle radiation, like, alpha particles, protons, or neutrons. It can be understood as a series of collision events of the incident particles with the atoms of the target material. The fast moving incident particles in the collisions transfer kinetic energy to a number of target atoms and may ionize or excite these atoms and even initiate nuclear reaction. Very high energy photons, x-rays and  $\gamma$ -rays are often produced in materials when the tightly bonded, inner-shell electrons of heavy atoms are removed or when nuclear reactions are initiated. These high energy photons may also produce additional ionization and hence electrons. The damage to biological materials is mostly due to the cascade of ionization events set up by the secondary electrons and high-energy photons. Radiation cascades are also used to modify the nature of a material, by implanting incident atoms, and to remove layers of a material, by “knocking off” the surface atoms.

The biological case is worth pursuing as a means of understanding the relationship between initial radiation events and final macroscopic effects. The effect of high-energy radiation may be used on cells or the biological constituents of the cell, i.e., DNA, RNA and various enzymes. The energized charged particles such as proton and other forms of radiation pass near the orbiting electrons of the atoms, positively charged of proton attracts negatively charged electrons pulling them out from the orbits. Hence ionization occurs and it changes the characteristics of the atom and consequently the characteristics of the molecules within which the atom resides. Because of ionization, the radiation damages the molecules within the cell especially the DNA or genetic material. The damaged DNA destroys the specific cell functions, particularly the ability to divide or proliferate. Hence enzymes fail to adequately repair the injury caused to the cells.

The radiation effect can be used in therapeutic applications. Proton therapy can be used for cancer treatment. Recently, it is found very useful over conventional radiation. The major advantage is that proton beam causes less harm to the live tissues surrounding the affected cells. The capability provides greater control and precision and therefore, superior management of treatment.

### **1.2.2. ELECTRON COLLISION CROSS SECTION DATA IN PLASMA PHYSICS**

Charge transfer research has a great importance in astrophysics to understand the processes involved inside the nebulae, supernova remnants and other astrophysical phenomena. The cross sectional data of charge transfer between partially or fully stripped ions and atoms are used for investigating the emission strengths of lines arising from transitions in neutral and ionized atomic systems such as C I, N I, N II, N E II, O I, O II, S I and S II in gaseous nebulae. They are considerably stronger than the strengths in theoretical models calculated for quasars [1], planetary nebulae [2], Seyfert galaxies [3] and diffuse H II regions [4].

The needs for electron cross section data depend on the subfield of plasma physics and parameters and characteristics of plasma [5]. Generally, one can observe diverse conditions of plasmas i.e. densities, temperatures, energy distributions of atomic particles, particle compositions, etc. Depending on what is the major subject of the study, whether it is astrophysical or fusion plasmas, plasmas in gas discharge lasers or plasma etching processes in semiconductor manufacturing, or just optical plasma diagnostics, one should consider appropriate set of elementary atomic particle processes and accordingly adequate cross sections.

Numerous atomic and molecular species are present in plasmas and are used in applications such as etching and deposition. Very often rare gas atoms are present and considered as plasma constituents together with di-, tri- and poly-atomic molecules as well as radicals and other fragments. These species could be in their ground state or excited (and metastable) states. In the study of electron interaction with these atomic particles, the variety of processes is possible and each of them is characterized by cross section that is energy and angular dependent value.

### 1.2.3. NEEDS FOR CROSS SECTIONS IN DIFFERENT TYPES OF PLASMAS

Regarding the needs for atomic and molecular data in *astrophysical plasmas*, Jorissen [6] identified two major purposes where data are used: (i) in computing opacity of the stellar matter and (ii) in determining abundances for specific chemical elements. He had recognized several current problems where atomic data are important for appropriate solutions: iron problem and the question of estimating stellar metallicity, oxygen problem, the importance of accurate knowledge of energies, transitions, and oscillator strengths for heavy elements, problem of dating the oldest galactic stars, etc. In *fusion plasmas* accurate atomic and molecular data sets are used to model conditions in tokamak edge radiation and particle behaviour in cold divertor regions (Kubo [7]). For controlling the impurity particle transport and edge plasma radiation losses, data for effective ionization and recombination rate coefficients are required. Currently Ar atoms are injected for radiation loss power enhancement but the role of Kr atoms is envisaged in this process. Also study of other heavy atoms is a priority due to their use as divertor plates. Collisions of hydrogen molecule, hydrocarbon molecules and He atoms have been extensively studied in cold divertor plasmas. Regarding the electron collision processes major investigations are directed toward the understanding of the role of vibrationally excited H<sub>2</sub> molecules [8]. Plasma processes in *gas discharge lasers* [9] are well understood and described in detail. Electron collisions play an important role in creating population inversion. They can easily populate metastable states as the scattering process could be viewed as an interaction of a multipole with the atomic field and electron cloud. Determining the electron excitation cross sections of optically forbidden states could serve as a test for lasing properties of the particular element. By the development of ultrafast laser technology, when the sub-femtosecond pulses are achieved, the study of the re-scattering processes of electrons emitted under strong laser field with their parent ions becomes possible with high precision [10]. Challenge in today's semiconductor manufacturing industry is using the *plasma etching* processes for producing nanometric patterns. For optical *plasma diagnostics* the knowledge of electron cross sections for rare gas atoms is crucial. Boffard and collaborators [11] have demonstrated that by knowing these cross sections and combining them with plasma emission measurements it is possible to extract many plasma parameters. Cross section data are needed for both ground state and metastable states atoms. The role of cross

sections for metastable atoms had been emphasized in the recent review on *plasma electronics* by Makabe and Petrović [12].

#### **1.2.4. CROSS SECTIONS FOR ELECTRON INTERACTIONS WITH RADICAL SPECIES**

Radicals, as atomic and molecular species with unpaired electrons, are common constituents in plasma media and are seen as a key chemical component in many plasma applications in semiconductor manufacturing. Although of great practical importance, data sets of electron collisional cross sections with radical species is rather scarce in scientific literature. It is partly due to the difficulties in experimental handling of radicals as unstable and highly reactive species. That is why the available literature is mainly consisting of theoretical data.

The main feed gases used in the plasma etching processes are perfluorocarbons but these are also strong greenhouse gases [13]. CF radicals have been studied by several authors. Lee *et al* [14] used a complex optical potential method to calculate elastic differential, integral and momentum transfer cross sections as well as total and absorption cross sections in the energy range from 1 to 500 eV. After comparison they found that DCS data are larger for CF than NO molecule especially in the domain of smaller scattering angles (below  $60^\circ$ ). Rozumet *al* [15] exploited R-matrix theory to obtain elastic and excitation cross sections at the low energy region (below 10 eV). They also found three shape resonances of different symmetries. Most recently Trevisanet *al* [16] investigated resonant electron – CF collision processes which could lead to production of negative ions. They studied the vibrational excitation and electron attachment processes and found several low lying negative ion states which are expected to dominate the scattering process.

Rozumet *al* [17] and Lee *et al* [18] have used R-matrix method to investigate electron - CF<sub>2</sub> radical cross sections at low-energy electron collisions (less than 10 eV) and calculated elastic and excitation cross sections of the six lowest-lying electronically excited states. Lee *et al* [18] have used an iterative Schwinger variational method combined with the distorted-wave approximation to solve the scattering equations. Cross sections are deduced in the energy range from 1 to 500 eV.

The need for comprehensive data bases of electron interactions with atomic particles has been identified long ago. International Conference on Atomic and Molecular Data and Their Applications [19] (a continuing series of the conferences) has been devoted to this aspect of research activities. Recent development in the field has been summarised also by Mason [20] who had examined new developments in electron induced processing, reviewed the current status of databases and identified the most important needs in the future electron/molecule research [21].

### **1.2.5. X-RAY LASER DEVELOPMENT**

Electron captures by partly or fully stripped heavy ions from ground state atomic hydrogen or helium takes place mainly into excited states due to energy resonance. The charge transfer into excited state by emission of radiation [22]. The radiation generally belongs to the soft x-ray region. This phenomenon may attribute as x-ray source in the interstellar medium [23]. This property of interest may also lead to the possibility of production of an x-ray laser [24-26].

### **1.3. FORMAL THEORY OF QUANTUM SCATTERING**

Quantum mechanical formalism is classified into two categories i.e., time dependent and time independent formalism. Here we shall mainly discuss the time independent formalism. However, these two formalism have been shown to be equivalent [27]. In low energy region, molecular state expansion method in the framework of close-coupling approximation is best suited. In this method, the electronic states are determined by the states of the quasi molecules so formed during the slow counter. All features and development of this theory are explained in the review articles of Greentand [28] and Delos [29] and also Basu et al [30]. A lot of progress has been achieved by many authors [31-38] to investigate the fully/ partially stripped ion-atom collisions in the low energy region by the use of molecular state expansion method. Kimura and Olson [39] have studied the single and double electron capture cross section from helium by  $C^{4+}$  and the single electron capture cross section by  $C^{6+}$  in the low energy region using molecular orbital method.

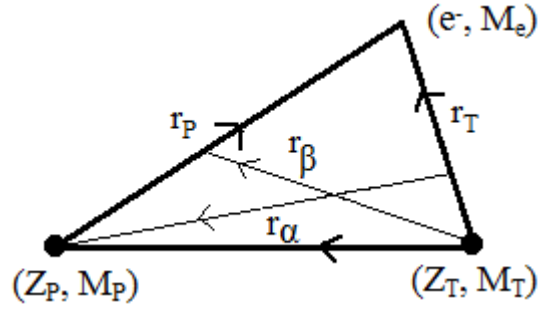


**Fig.1.1. Collision Diagram**

In order to discuss different high energy methods, we shall now start from the origin of these methods in the framework of formal theory of scattering.

We are dealing with the rearrangement process of the type

$$\alpha + (\beta, \gamma) \rightarrow (\alpha, \gamma) + \beta \quad (1)$$

where  $\alpha$  and  $\beta$  are two colliding objects (may be structureless or not) and  $\gamma$  is the active electron to be transferred.  $\alpha$ ,  $\beta$  and  $\gamma$  interact via two-body potential  $V_i$  ( $i = \alpha, \beta, \gamma$ ). For the reaction (1), the particle labeled by  $\alpha$  is free in the initial channel, so the initial channel is described by  $\alpha$ - channel and the final channel by  $\beta$ - channel. Interaction between any two particles will be represented by the third particle i.e.  $V_\alpha$  represents the interaction between the particles labeled by  $\beta, \gamma$  and so on. The Schrodinger equation for the whole system may be written as,

$$H\psi = E\psi \quad (2)$$

Here  $H$ , the hamiltonian for the whole system may be written as,

$$H = -\frac{1}{2\mu_\alpha} \nabla_{r_\alpha}^2 - \frac{1}{2a} \nabla_x^2 + v_\alpha + v_\beta + v_\gamma, \quad (3a)$$

$$\leftarrow \quad H_0 \quad \rightarrow \quad \leftarrow \quad V_i \quad \rightarrow$$

$$\begin{aligned}
&= -\frac{1}{2\mu_\beta} \nabla_{\vec{r}_\beta}^2 - \frac{1}{2b} \nabla_s^2 + v_\alpha + v_\beta + v_\gamma, \\
&\leftarrow \quad H_0 \quad \rightarrow \quad \leftarrow \quad V_f \quad \rightarrow
\end{aligned} \tag{3b}$$

where  $H_0$  is the kinetic energy operator in the center of mass frame.

Co-ordinates and reduced masses are defined as

$$\vec{x} = \vec{r}_e - \vec{r}_T \tag{4a}$$

$$\vec{s} = \vec{r}_e - \vec{r}_p, \tag{4b}$$

$$\vec{R} = \vec{r}_p - \vec{r}_T, \tag{4c}$$

$$\vec{r}_\alpha = \vec{r}_p - \frac{M_T \vec{r}_T + \vec{r}_e}{M_T + 1}, \tag{4d}$$

$$\vec{r}_\beta = \vec{r}_T - \frac{M_p \vec{r}_p + \vec{r}_e}{M_p + 1}, \tag{4e}$$

where  $\vec{r}_T$ ,  $\vec{r}_e$ ,  $\vec{r}_p$  are respectively the co-ordinates of the particles labeled by  $\beta, \gamma$  and  $\alpha$  with respect to an arbitrary frame of reference. The reduced masses are defined as

$$\mu_\alpha = \frac{M_p (M_T + 1)}{M_p + M_T + 1}, \tag{5a}$$

$$\mu_\beta = \frac{M_T (M_p + 1)}{M_p + M_T + 1}, \tag{5b}$$

$$a = \frac{M_T}{M_T + 1}, \tag{5c}$$

$$b = \frac{M_p}{M_p + 1}, \tag{5d}$$

where 1,  $M_T$  and  $M_p$  are respectively the mass of the particles labeled by  $\gamma$ ,  $\beta$  and  $\alpha$ . The total hamiltonian of the whole system may be split in terms of channel Hamiltonian as,

$$H = H_\alpha + V_\alpha \tag{6a}$$

$$= H_\beta + V_\beta \tag{6b}$$

where  $H_\alpha$ ,  $H_\beta$  are the hamiltonian for the channels,  $\alpha + (\beta, \gamma)$  and  $(\alpha, \gamma) + \beta$  respectively. Let the complete set of eigen states of  $H_\alpha$  and  $H_\beta$  are given by

$$(E_\alpha - H_\alpha)\varphi_i^\alpha = 0 \quad (7a)$$

$$(E_\beta - H_\beta)\varphi_i^\beta = 0 \quad (7b)$$

where,

$$E_\alpha = \frac{k_\alpha^2}{2\mu_\alpha} + \varepsilon_\alpha, \quad (8a)$$

$$E_\beta = \frac{k_\beta^2}{2\mu_\beta} + \varepsilon_\beta, \quad (8b)$$

Here,  $\varepsilon_\alpha$  ( $\varepsilon_\beta$ ) is the bound state energy and  $k_\alpha$  ( $k_\beta$ ) is the momentum vector in the entrance (exit) channel respectively. Any subscript i or j represents the corresponding states of the system in either channel. With ‘On shell energy’ consideration, we may write

$$E = E_\alpha = E_\beta.$$

The transition amplitude from the i-th state in the  $\alpha$ - channel to the j-th state in the  $\beta$ - channel may be written as

$$T_{ij}^{\alpha\beta+} = \langle \psi_j^\beta | V_\beta | \psi_{i,\alpha}^+ \rangle \quad (\text{post form}) \quad (9a)$$

$$T_{ij}^{\alpha\beta-} = \langle \psi_{j,\beta}^- | V_\alpha | \psi_i^\alpha \rangle \quad (\text{prior form}) \quad (9b)$$

where,

$$\psi_{i,\alpha}^+ = \varphi_i^\alpha + G_\alpha^+ V_\alpha \psi_{i,\alpha}^+ = \varphi_i^\alpha + G^+ V_\alpha \varphi_i^\alpha = \Omega_\alpha^+ \varphi_i^\alpha \quad (10a)$$

and

$$\psi_{j,\beta}^- = \varphi_j^\beta + G_\beta^- V_\beta \psi_{j,\beta}^- = \varphi_j^\beta + G^- V_\beta \varphi_j^\beta = \Omega_\beta^- \varphi_j^\beta \quad (10b)$$

Here  $\Omega_\alpha^+$  and  $\Omega_\beta^-$  are the Moller operators.  $G^+$ ,  $G^-$  and  $G_\beta^-$  are respectively the total  $\alpha$ -channel and  $\beta$ -channel Green’s operators.

Hence the transition matrix elements given by equations (9a) and (9b) may be written as

$$T_{ij}^{\alpha\beta+} = \langle \varphi_j^\beta | V_\beta (1 + G^+ V_\alpha) | \varphi_i^\alpha \rangle = \langle \varphi_j^\beta | V_\beta \Omega_\alpha^+ | \varphi_i^\alpha \rangle, \quad (11a)$$

$$T_{ij}^{\alpha\beta-} = \langle \varphi_j^\beta | V_\beta (1 + G^+ V_\alpha) | \varphi_i^\alpha \rangle = \langle \varphi_j^\beta | \Omega_\beta^{-*} | \varphi_i^\alpha \rangle. \quad (11b)$$

Here any asterisk (\*) represents the complex conjugate of the corresponding quantity.

The differential cross section may be written as

$$\frac{d\sigma_{ij}^{\alpha\beta\pm}}{d\Omega} = \frac{\mu_\alpha \mu_\beta}{4\pi^2} \frac{k_\beta}{k_\alpha} \left| T_{ij}^{\alpha\beta\pm} \right|^2, \quad (12)$$

where  $\Omega$  is the solid angle around  $k_\alpha$ . The total cross section may be written as

$$\sigma_{ij}^{\alpha\beta\pm} = \int \frac{d\sigma_{ij}^{\alpha\beta}}{d\Omega} d\Omega. \quad (13)$$

### 1.3.1. PERTURBATION SERIES WITH THE CORRECT BOUNDARY CONDITIONS

The dynamics of the entire four-body system are described by means of the Schrodinger equation

$$(H - E)\psi^\pm = 0 \quad (14)$$

where  $\psi^\pm$  are the full scattering states with the outgoing and incoming boundary conditions, respectively

$$\psi^+ \rightarrow \varphi_i^+ \quad (R_i \rightarrow \infty) \quad \psi^- \rightarrow \varphi_f^- \quad (R_f \rightarrow \infty) \quad (15)$$

The exact transition amplitude with the correct boundary conditions can be written in the post (+) and prior (-) forms as

$$T_{if}^+ = \langle \varphi_f^- | V_f^d | \psi_i^+ \rangle, \quad T_{if}^- = \langle \psi_f^- | V_i^d | \varphi_i^+ \rangle. \quad (16)$$

Both the forms are equivalent to each other on the energy shell i.e. the exact on-shell expressions are equal,  $T_{if}^+ = T_{if}^-$ , for the transitions for which the total energy is conserved.

Solving a scattering problem in which four bodies take part (two nuclei and two electrons) is extremely difficult. As usual, at intermediate and high impact energies, the powerful and versatile procedure of perturbation series expansion is frequently employed. To, this end it is convenient to convert the schrodinger equation for a four-body problem into the corresponding integral equation such as Lippmann- Schwinger or Faddeev equations or their corresponding perturbation expansion series, the correct boundary conditions must always be imposed to the entrance and exit channels [40-43]. Despite the widely accepted importance of such initial

conditions [44-49], confusion and debates persisted in the literature for a long time on this very point.

### 1.3.2. THE LIPPMANN-SCHWINGER EQUATIONS

The total scattering function is  $\psi_i^+ = i\epsilon G^+ \phi_i^+$  (17)

where  $G^+$  is the full Green's operator and  $\phi_i^+$  is the wave function. Here,  $\epsilon$  is an infinitesimally small positive number. In addition to the total Green operators  $G^\pm$ , we also define the initial  $G_i^\pm$ , the final  $G_f^\pm$  and the free Green resolvent propagators  $G_0^\pm$  as

$$G^\pm = (E - H \pm i\epsilon)^{-1} \quad (18)$$

$$G_i^\pm = (E - H_i^d \pm i\epsilon)^{-1} \quad (19)$$

$$G_f^\pm = (E - H_f^d \pm i\epsilon)^{-1} \quad (20)$$

$$G_0^\pm = (E - H_0 \pm i\epsilon)^{-1} \quad (21)$$

These propagators are inter-related by the following Lippmann-Schwinger integral equations for the total Green functions

$$\begin{aligned} G^\pm &= G_i^\pm + G_i^\pm V_i^d G^\pm \\ G^\pm &= G_f^\pm + G_f^\pm V_f^d G^\pm \\ G^\pm &= G_0^\pm + G_0^\pm V G^\pm. \end{aligned} \quad (22)$$

Applying the iteration process to equation (6), we obtain the following explanations for the total Green resolvent  $G^+$  in terms of  $G_0^+$ ,  $G_i^+$  and  $G_f^+$

$$G^+ = G_0^+ + G_0^+ V G_0^+ + G_0^+ V G_0^+ V G_0^+ + G_0^+ V G_0^+ V G_0^+ V G_0^+ + \dots \quad (23)$$

$$G^+ = G_i^+ + G_i^+ V_i^d G_i^+ + G_i^+ V_i^d G_i^+ V_i^d G_i^+ + G_i^+ V_i^d G_i^+ V_i^d G_i^+ V_i^d G_i^+ \dots \quad (24)$$

$$G^+ = G_f^+ + G_f^+ V_f^d G_f^+ + G_f^+ V_f^d G_f^+ V_f^d G_f^+ + G_f^+ V_f^d G_f^+ V_f^d G_f^+ V_f^d G_f^+ \dots \quad (25)$$

Hence, the formal solution of the four-body Lippmann-Schwinger equation in terms of the total Green operator  $G^+$  is

$$\psi_i^+ = \phi_i^+ + G^+ V_i^d \phi_i^+ = (1 + G^+ V_i^d) \phi_i^+. \quad (26)$$

### 1.3.3. THE BORN EXPANSIONS WITH THE CORRECT BOUNDARY CONDITIONS

Inserting the formal solution equation (26) into equation (16) for the post form of the transition amplitude, it follows that

$$T_{if}^+ = \langle \varphi_f^- | V_f^d | \psi_i^+ \rangle = \langle \varphi_f^- | V_f^d (1 + G^+ V_i^d) | \varphi_i^+ \rangle. \quad (27)$$

This implies that by substituting  $G^+$  from equation (23)-(25) into equation (27), we can write several different versions of the Born expansions with the correct boundary conditions

$$T_{if}^+ = T_{if}^{(CB1)+} + \langle \varphi_f^- | V_f^d G_o^+ V_i^d | \varphi_i^+ \rangle + \langle \varphi_f^- | V_f^d G_o^+ V G_o^+ V_i^d | \varphi_i^+ \rangle + \dots \quad (28)$$

$$T_{if}^+ = T_{if}^{(CB1)+} + \langle \varphi_f^- | V_f^d G_i^+ V_i^d | \varphi_i^+ \rangle + \langle \varphi_f^- | V_f^d G_i^+ V_i^d G_i^+ V_i^d | \varphi_i^+ \rangle + \dots \quad (29)$$

$$T_{if}^+ = T_{if}^{(CB1)+} + \langle \varphi_f^- | V_f^d G_f^+ V_i^d | \varphi_i^+ \rangle + \langle \varphi_f^- | V_f^d G_f^+ V_f^d G_f^+ V_i^d | \varphi_i^+ \rangle + \dots \quad (30)$$

$$T_{if}^{(CB1)+} = \langle \varphi_f^- | V_f^d | \varphi_i^+ \rangle. \quad (31)$$

Here  $T_{if}^{(CB1)+}$  is the post form of the first Born method with the correct boundary conditions for the four body collisions i.e. the CB1-4B method [50,51]. Likewise, the  $n$  th Born method with the correct boundary conditions (CBn-4B) may be obtained by keeping the first  $n$  terms in the perturbation expansions. For example, the four body second Born method with the correct boundary condition (CB2-4B) can be obtained in this way in the forms

$$T_{if;0}^{(CB2)+} = T_{if}^{(CB1)+} + \langle \varphi_f^- | V_f^d G_o^+ V_i^d | \varphi_i^+ \rangle \quad (32)$$

$$T_{if;i}^{(CB2)+} = T_{if}^{(CB1)+} + \langle \varphi_f^- | V_f^d G_i^+ V_i^d | \varphi_i^+ \rangle \quad (33)$$

$$T_{if;f}^{(CB2)+} = T_{if}^{(CB1)+} + \langle \varphi_f^- | V_f^d G_f^+ V_i^d | \varphi_i^+ \rangle \quad (34)$$

Here, equation (32) in terms of  $G_o^+$  is recognized as a direct extension of the corresponding CB2-3B method of Belkic [52-54]. Many other versions of Born expansion can be formulated by

utilizing various possible iterative solutions for  $G^+$ . In other words, a unique Born series of the transition amplitude  $T_{if}^+$  does not exist.

### 1.3.4. BOUNDARY CORRECTED CONTINUUM INTERMEDIATE STATE (BCCIS) APPROXIMATION

Belkic [55] have proposed the new theory CDW and CIS approximation in which the distorting potential in either channel is chosen to be internuclear two-body coulomb potential. But, the conventional CIS approximation does not satisfy the correct boundary condition. To overcome the difficulties of conventional CIS approximation Mandal et al [56] have proposed the boundary corrected continuum intermediate state (BCCIS) approximation in which the distorting potential in the entrance channel has been chosen in such a way that proper boundary conditions for the scattering wave functions are satisfied. Another useful feature of this method lies in fact that the perturbing potential at which the transition amplitude is calculated, decreases faster than the Coulomb potential. The formula used here may be extended easily to non-Coulombic interaction.

The prior form of the transition amplitude for single capture in the framework of the BCCIS approximation may be written as,

$$T_{if}^{(-)} = \langle \Psi_f^{\text{BCCIS}(-)} \left| \frac{1}{R_T} - \frac{1}{r_p} \right| \Psi_i \rangle. \quad (35)$$

The initial non-perturbed wave function is given by

$$\Psi_i = \varphi_i(\vec{r}_T) \chi_i^+(\vec{R}_T), \quad (36)$$

where  $\varphi_i(\vec{r}_T)$  is the initial bound state wave function. The function  $\chi_i^+(\vec{R}_T)$  is an outgoing Coulomb continuum wave function representing the projectile ion moving in the field of an effective ion of charge  $(Z_T-1)$ , so the Schrodinger equation is

$$(E - H_i') \chi_i^+ = 0$$

$$\text{where } \chi_i^+(\vec{R}_T) = e^{-\frac{\pi}{2}\alpha_3} \Gamma(1+i\alpha_3) e^{i\vec{k}_i \cdot \vec{R}_T} {}_1F_1\left\{-i\alpha_3; 1; i(k_i R_T - \vec{k}_i \cdot \vec{R}_T)\right\}, \quad \alpha_3 = \frac{Z_P(Z_T-1)}{v_i}.$$

Here  $\vec{k}_i$  is the initial wave vector.

The prior form of the transition matrix element,

$$T_{if}^{(-)} = \langle \Psi_f^- | V_i | \Psi_i \rangle \quad (37)$$

$$\approx \langle \Psi_f^{\text{BCCIS-3B}} | V_i | \Psi_i \rangle.$$

We write the final wave function,

$$\Psi_f^{\text{BCCIS(-)}} = e^{\frac{\pi}{2}(\alpha_1 - \alpha_2)} \Gamma(1 + i\alpha_1) \Gamma(1 - i\alpha_2) e^{i\vec{k}_f \cdot \vec{R}_P} \varphi_f(\vec{r}_P) {}_1F_1\{-i\alpha_1; 1; -ia(\vec{v}_f \cdot \vec{r}_T + \vec{v}_f \cdot \vec{r}_T)\} \times {}_1F_1\{i\alpha_2; 1; -ib(\vec{k}_f \cdot \vec{R}_T + \vec{k}_f \cdot \vec{R}_T)\}, \quad (38)$$

where  $\alpha_1 = \frac{Z_T}{v_f}, \quad \alpha_2 = \frac{Z_P Z_T}{v_f}.$

The transition amplitude can be written as

$$T_{if}^{(-)} = N \iint d\vec{r}_T d\vec{R}_T e^{i\vec{k}_i \cdot \vec{R}_T - i\vec{k}_f \cdot \vec{R}_P} \varphi_f^*(\vec{r}_P) \left( \frac{Z_P}{R_T} - \frac{Z_P}{r_P} \right) {}_1F_1\{i\alpha_1; 1; ia(\vec{v}_f \cdot \vec{r}_T + \vec{v}_f \cdot \vec{r}_T)\} \times {}_1F_1\{-i\alpha_2; 1; ib(\vec{k}_f \cdot \vec{R}_T + \vec{k}_f \cdot \vec{R}_T)\} \varphi_i(\vec{r}_T) {}_1F_1\{-i\alpha_3; 1; i(\vec{k}_i \cdot \vec{R}_T - \vec{k}_i \cdot \vec{R}_T)\}, \quad (39)$$

where  $N = e^{\frac{\pi}{2}(\alpha_1 - \alpha_2 - \alpha_3)} \Gamma(1 - i\alpha_1) \Gamma(1 + i\alpha_2) \Gamma(1 + i\alpha_3).$

Using integral representation  ${}_1F_1(i\alpha; 1; z) = \frac{1}{2\pi i} \oint d\tau \tau^{i\alpha-1} (\tau-1)^{-i\alpha} e^{tz}$ . The transition amplitude of equation (39) may be written as

$$T_{if} = \frac{AN}{(2\pi i)^3} \ell \lim_{\varepsilon_1 \rightarrow 0} D(\varepsilon_1, \lambda, \beta) \oint dt_1 t_1^{i\alpha_1-1} (t_1-1)^{-i\alpha_1} \oint dt_2 t_2^{-i\alpha_2-1} (t_2-1)^{i\alpha_2} \oint dt_3 t_3^{-i\alpha_3-1} (t_3-1)^{i\alpha_3} J \quad (40)$$

where  $J = \iint d\vec{r}_T d\vec{R}_T e^{i\vec{k}_i \cdot \vec{R}_T - i\vec{k}_f \cdot \vec{R}_P + ia\vec{v}_f \cdot \vec{r}_T + ib\vec{k}_f \cdot \vec{R}_T - i\vec{k}_i \cdot \vec{R}_T} \frac{e^{-\beta_1 r_T}}{r_T} \frac{e^{-\lambda r_P}}{r_P} \frac{e^{-\varepsilon R_T}}{R_T}, \quad (40a)$

$$\beta_1 = \beta - ia v_f t_1 \quad \text{and} \quad \varepsilon = \varepsilon_1 - ib k_f t_2 - i k_i t_3.$$

Here the constant A is originating from the initial and final bound state wave functions.  $D(\varepsilon_1, \lambda, \beta_1)$  is a parametric differential operator used to generate higher excited state wave functions.  $\beta$  and  $\lambda$  are the orbital exponent of the initial and the final bound state wave functions.

Taking the Fourier transform of equation (40a) and using integral representation of general three denominator integration of Lewis [59], Sinha and Sil [60],

$$J = \frac{16\pi^2}{a^2} \int_0^\infty \frac{dx}{a'x^2 + 2b'x + c'}. \quad (41)$$

Using equation (7), the transition matrix element now becomes

$$T_{if} = \frac{NA}{(2\pi i)} \frac{16\pi^2}{a^2} \ell \lim_{\varepsilon_1 \rightarrow 0} D(\varepsilon_1, \lambda, \beta) \int dt_2 t_2^{-i\alpha_2-1} (t_2-1)^{i\alpha_2} \int_0^\infty K dx \quad (42)$$

$$\text{where } K = \frac{1}{A} \left( \frac{A}{A+B} \right)^{i\alpha_1} \left( \frac{A}{A+C} \right)^{-i\alpha_3} {}_2F_1\{i\alpha_1; -i\alpha_3; 1; z\}, \quad z = \frac{BC-AD}{(A+B)(A+C)}.$$

Now the complex integration of  $t_2$  is converted to real integral which has been subdivided into a number of sub-intervals and each sub-interval is integrated numerically using Gauss Laguerre quadrature method. Finally a single electron capture cross sections is obtained numerically over scattering angles with the Gauss Legendre quadrature method. The orders of two dimensional integral are varied until convergence to three decimal places is obtained for the total charge transfer cross sections.

### 1.3.5. CONTINUUM DISTORTED WAVE (CDW) THEORY

Cheshire [61] has been formulated the continuum distorted-wave approximation (CDW) to include the continuum intermediate states in impact parameter treatments of rearrangement collisions. Originally a continuum distorted wave (CDW) was a quantummechanical Coulomb wave associated with the motion of an electron attached to an ion/atom relative to, and, while simultaneously in, the continuum of another ion [61]. The context was charge transfer. Subsequently this was generalized to the continuum of an electron [62], but not before it was generalized to ionization in an ion-atom collision [63]. Based on these latter two papers, Crothers and McCann [64] invented CDW-EIS (eikonal initial state) which guarantees unitarity of the propagating initial state. Other later *notations* for the electron projectile case [62] are C3 and BBK. CDW is appropriate for high impact energies and small and medium impact parameters. CDW-EIS is appropriate for large impact parameters and lower energies. One of the principal advantages of CDW theory lies in its Coulomb phases which guarantee the correct

asymptotic/boundary behaviour [65–67]. Of course CDW-EIS is intended to describe ionization in intermediate and high-energy collisions. At lower energies charge transfer is an important intermediate event. The wave version of the post form of charge transfer amplitude of Cheshire may be obtained with the following choices

$$w_\alpha = 0, v_x = -\frac{1}{x} \text{ and } w_\beta = \frac{1}{x} - \frac{1}{R} - u_\beta, \quad (43)$$

where  $u_\beta$  is a short range potential. In CDW approximation, the intermediate continuum states are taken into account by the choice of some potential in the form of differential operators. These differential operators find their applications onto the continuous spectrum and operate only on the subspace where the total scattering wavefunctions may be factorised into two parts, which satisfy the proper boundary conditions both in the entrance and exit channels. Cheshire [61] has found the asymptotic form of the cross sections in the CDW approximation as

$$Q_{\text{CDW}} \underset{v \rightarrow \infty}{\approx} \left(0.2946 + \frac{5\pi v}{2^{12}}\right) Q_{\text{OBK}} \quad (44)$$

which is of the same form as that of the second Born approximation (B2). This approximation has been applied by several authors [68-70]. Belkic et al [71], Crothers [72], Datta et al [73], Mandal et al [74] have applied this method to calculate the charge transfer cross section between heavy stripped ions with atomic hydrogen in ground state and also with multi-electron target. Their results fit well with the existing experimental results [75,76]. Crothers and McCann [77] have also examined theoretically the symmetric resonance charge exchange in proton hydrogen collision using CDW theory within variational framework.

### 1.3.6. CLASSICAL TRAJECTORY MONTE CARLO (CTMC) METHOD

In 1966, Abrines and Percival [78] was first introduced the classical trajectory Monte Carlo Method to study ion-atom collisions. Previous classical theory was based on two assumptions: (i) during the collision the particle obeys Newtonian laws of motion (ii) The many-particle collision is assumed by two-body collision for each atomic electron. The model can be understood in terms of classical mechanics including statistical aspects. CTMC is a numerical method used to

calculate the time evolution of a classical distribution  $f(x,p,t)$  in phase space. We consider a collision system composed by two frozen cores (projectile and target cores) of masses  $M_p$  and  $M_T$  and on active electron of unit mass initially bound to the target.

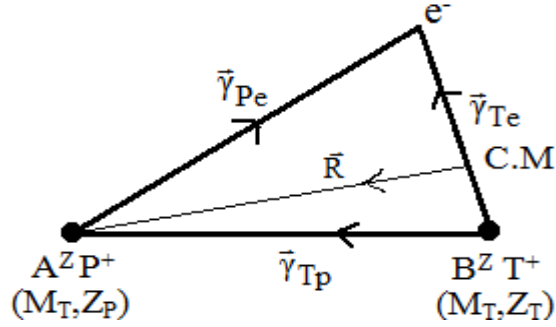


**Fig.1.2. Collision diagram (symbols have the usual meanings)**

Let the cartesian co-ordinates of the active electron with respect to the target ion (T) are  $q_1$ ,  $q_2$  and  $q_3$  respectively. Let the same quantities are  $q_4$ ,  $q_5$  and  $q_6$  respectively for the incoming projectile ion (P) with respect to the centre of mass of the target system. So  $\vec{r}_{ij}$  ( $i, j = e, T, P$ ), the distance between any pair of two particles may easily be expressed in terms of  $q_i$  ( $i = 1, 6$ ) provided mass ( $M_T$ ) of the residual target ion, mass ( $M_P$ ) of the projectile ion and electron mass are known. Let  $p_i$  ( $i=1, 6$ ) are the canonical momenta conjugate to the rectangular co-ordinate  $q_i$  ( $i=1, 6$ ).

$$r_{pe}^2 = (\mu\mu_1 - q_4)^2 + (\mu\mu_2 - q_5)^2 + (\mu\mu_3 - q_6)^2, \quad (45)$$

$$r_{Te}^2 = q_1^2 + q_2^2 + q_3^2, \quad (46)$$

$$r_{PT}^2 = \left(\frac{\mu}{M_T} q_1 + q_4\right)^2 + \left(\frac{\mu}{M_T} q_2 + q_5\right)^2 + \left(\frac{\mu}{M_T} q_3 + q_6\right)^2. \quad (47)$$

So the classical hamiltonian of the three system may be written as

$$H = \sum_{i=1}^3 \frac{p_i^2}{2\mu} + \sum_{j=4}^6 \frac{p_j^2}{2M} + V_{Te}(\vec{r}_{Te}) + V_{Pe}(\vec{r}_{Pe}) + V_{TP}(\vec{r}_{TP}), \quad (48)$$

$$\text{where } \mu = \frac{M_T}{M_T + 1}, \quad M = \frac{M_P(M_T + 1)}{M_P + M_T + 1},$$

and  $V_{ij}$  ( $i, j = e, T, P$ ) is the two body pair interaction between  $i$ -th and  $j$ -th particle. So the Hamilton's equations of motion may be written as

$$p_i = \mu \dot{q}_i, \quad i=1,2,3, \quad (49)$$

$$p_i = M \dot{q}_i, \quad i=4,5,6, \quad (50)$$

$$\dot{p}_i = -\frac{1}{r_{Pe}} \frac{\partial V}{\partial r_{Pe}} \mu(\mu q_i - q_{i+3}) - \frac{1}{r_{Te}} \frac{\partial V}{\partial r_{Te}} q_i - \frac{1}{r_{TP}} \frac{\partial V}{\partial r_{TP}} \frac{\mu}{M_T} \left( \frac{\mu}{M_T} q_i + q_{i+3} \right), \quad i=1,2,3, \quad (51)$$

$$\dot{p}_i = -\frac{1}{r_{Pe}} \frac{\partial V}{\partial r_{Pe}} (q_i - \mu q_{i-3}) - \frac{1}{r_{TP}} \frac{\partial V}{\partial r_{TP}} \left( q_i + \frac{\mu}{M_T} q_{i-3} \right), \quad i=4,5,6, \quad (52)$$

where  $V = V_{Te}(\vec{r}_{Te}) + V_{Pe}(\vec{r}_{Pe}) + V_{TP}(\vec{r}_{TP})$ .

This set of twelve equations given by (49) - (52) describes the motion of the whole system in center of mass frame of the active electron and residual target ion. The interaction of the active electron with the target is uniquely determined by the coulomb potential. The twelve coupled equations are integrated numerically from  $t = -\infty$  to  $+\infty$  with the initial conditions determined from a microcanonical ensemble in terms of six random numbers. Such calculations are repeated for several thousand trajectories. If  $N_T$  is the total number of trajectories calculated and  $N_R$  is the number of trajectories which satisfy the criteria of a particular final channel, the cross section for the corresponding final channel may be given by,

$$\sigma_R = \frac{N_R}{N_T} \pi b_{\max}^2 \quad (53)$$

where  $b_{\max}$  is the maximum impact parameter beyond which no interaction takes place. The standard error is calculated as either

$$s^2 = \sigma_R \left( \frac{\pi b_{\max}^2 - \sigma_R}{N_T - 1} \right)$$

or

$$s^2 = \sigma_R \left( \frac{N_T - N_R}{N_T N_R} \right)^{1/2} \quad (54)$$

The classical trajectory Monte Carlo (CTMC) method originated with Hirschfelder, who studied the  $H + D_2$  exchange reaction using a mechanical calculator [79]. With the availability of computers, the CTMC method was actively applied to a large number of chemical systems to determine reaction rates, and final state vibrational and rotational populations (see, e.g., Karplus *et al.* [80]). For atomic physics problems, a major step was introduced by Abrines and Percival [78] who employed Kepler's equations and the Bohr-Sommerfeld model for atomic hydrogen to investigate electron capture and ionization for intermediate velocity collisions of  $H^+ + H$ . An excellent description is given by Percival and Richards [81]. Peach et al [82] applied the CTMC method to obtain charge transfer and ionization. Later Wills et al [83] followed the same technique for different system. Purkait et al [84] have employed the CTMC simulation method to study the sub-shell distributions of total charge transfer cross sections and total ionization cross sections in collisions of partially stripped ions of carbon, nitrogen and oxygen in different charge states with ground state atomic hydrogen in the energy range of 10-200 keV/amu. They have also taken into account the interaction of the active electron with the partially stripped projectile ion by non-coulomb model potential. Later Ichihiro [85] studied electron transfer cross sections for slow, highly charged ion-atomic hydrogen collision with CTMC method. Perez and Olson [86] investigated the state selective electron capture cross sections for low energy collisions between highly charged bare ions and neutral atoms using this method. Wang et al [87] also studied the charge transfer and ionization in collisions of ground state  $Si^{3+}$  ions with atomic hydrogen. The CTMC method has a wide range of applicability to strongly-coupled systems, such as collisions by multiply-charged ions [88]. In such systems, perturbation methods fail, and basis set limitations of coupled channel molecular- and atomic-orbital techniques have difficulty in representing the multitude of active excitation, electron capture, and ionization channels.

Vector and parallel-processors now allow increasingly detailed study of the dynamics of the heavy projectile and target, along with the active electrons.

In many ways it is surprising that a classical model can be successful in a quantum mechanical world, since the classical radial distribution for the hydrogen atom is described so poorly. However, hydrogen's classical momentum distribution is exactly equivalent to the quantum one, and since collision processes are primarily determined by velocity matching between projectile and electron, reasonable results can be expected. Moreover, the CTMC method preserves conservation of flux, energy, and momentum; and Coulomb scattering is the same in both quantum and classical frameworks.

## **REFERENCES**

- [1] K. Davidson, *Astrophysics. J.***171**, 213 (1972).
- [2] J. S. Miller, *Ann. Rev. Astron, Astrophysics.***12**, 331, (1974).
- [3] G. Shields and J. B. Oke, *Astrophysics. J.***197**, 5 (1975).
- [4] J. S. Mathis, *Astrophysics. J.* **125**, 318 (1976).
- [5] B. P. Marinković, V. Pejčev, D. M. Filipović, D. Šević, A. R. Milosavljević, S. Milisavljević, M. S. Rabasović, D. Pavlović and J. B. Maljković, *Journal of Physics: Conference Series***86**, 012006 (2007).
- [6] A. Jorissen, *Physica Scripta***T112**, 73, (2004).
- [7] H. Kubo, Proc. 3rd International Conference on Atomic and Molecular Data and Their Applications, Eds. D. R. Schulz, P. S. Krstić and F. Ownby, *AIP Conference Proceedings***636**, 161 (2002).
- [8] K. Sawada and T. Fujimoto, *Contrib. Plasma Phys.* **42**,603 (2002).
- [9] I. Čadež, R. I. Hall, M. Landau, F. Pichou and C Schermann, *J. Chem. Phys.* **106**,4745 (1997).
- [10] M. Kitzler and M. Lezius, *Phys. Rev. Lett.* **95**,253001 (2005).

- [11] J. B. Boffard, C. C. Lin, C. A. DeJosephJr, *J.Phys.D: Appl.Phys.* **37**,R143 (2004).
- [12] T. Makabe and Z. Petrović, in *Plasma Electronics: Applications in Microelectronic Device Fabrication*, Teylor& Francis, New York, London (2006) pp.75 – 105.
- [13] N.J. Masona, P. Limão Vieira, S. Eden, P. Kendall, S. Pathak, A. Dawes, J. Tennyson, P.Tegeder, M. Kitajima, M. Okamoto, K. Sunohara, H. Tanaka, H. Cho, S. Samukawa, S.V.Hoffmann, D. Newnham and S.M. Spyrou, *Int. J. Mass Spectrom* **223**,647 (2003).
- [14] M.T. Lee, I. Iga, L. M. Brescansin, L. E. Machado, and F. B. C. Machado, *Phys. Rev. A* **66**, 012720 (2002).
- [15] I. Rozum, N. J. Mason and J. Tennyson, *J. Phys. B: At. Mol. Opt. Phys.* **36**, 2419(2003).
- [16] C. S. Trevisan, A. E. Orel and T. N. Rescigno, *Phys. Rev. A* **72**, 062720 (2005).
- [17] I. Rozum, N. J. Mason and J. Tennyson, *J. Phys. B: At. Mol. Opt. Phys.* **35**,1583 (2002).
- [18] M.-T. Lee, I. Iga, L. E. Machado, L. M. Brescansin, E. A. y Castro and G. L. C. de Souza, *Phys.Rev. A* **74**, 052716 (2006).
- [19] <http://physics.nist.gov/Divisions/Div842/Icamdata/Homepage/icamdata.html>
- [20] N. J. Mason, in *Atomic and Molecular Data and Their Applications* Ed. E. Roueff, AIPConference Proceedings Volume 901, Melville, New York, 2006. Invited Lecture, pp. 74 – 84.
- [21] T. A. Field, A. E. Slattery, D. J. Adams, and D. D. Morrison, *J. Phys. B: At. Mol. Opt. Phys.* **38**,255 – 264 (2005).
- [22] R. C. Isler and E. C. Crume, *Phys. Rev. Lett.* **41**, 1296 (1978).
- [23] D. W. Rule andK. Omidvar, *Astrophys. J* **229**, 1198 (1979).
- [24] A. V.Vinogradov and I. I. Sobelman, *Sov. Phys. JETP* **36**, 115 (1973).
- [25] R. H. Dixon, J. F. Seely and R. C. Eltron,*Phys. Rev. Lett.* **40**, 122 (1978).
- [26] W. H. Louisell, M. O. Scully and W. B. McKnight, *Phys. Rev. Lett.* **11**, 989 (1975).
- [27] R. Shakeshaff, *J. Phys. B* **6**, 1357 (1973).
- [28] P. T. Greenland, *Phys. Rep.* **81**, 133 (1982).
- [29] J. B. Delos, *Rev. Mod. Phys.* **53**, 287 (1981).
- [30] D. Basu, S. C. Mukherjee and D. P. Sural, *Physics Reports* **42C**, 145 (1978).
- [31] J. Vabeen and J. S. Briggs, *J. Phys. B* **10**, L521 (1977).
- [32] A. Salop and R. E. Olson, *Phys. Rev. A* **16**, 1811 (1977).

- [33] T. G. Winter, G. J. Hatton and N. F. Lane, Phys. Rev. A **22**, 930 (1980).
- [34] T. A. Green, Phys. Rev. A **23**, 519 (1981).
- [35] R. J. Allan, J. Phys. B **19**, 321 (1986).
- [36] H. C. Tseng and C. D. Lin, Phys. Rev. A **61**, 034701 (2000).
- [37] S. Suzuki, L. Gulyas, N. Shimakura, P. D. Fainstein and T. S. Shirai, J. Phys. B **33**, 3307 (2000).
- [38] N. Shimakura, Mi.Itoh and M. Kimura, Phys. Rev. A **45**, 267 (1992).
- [39] M. Kimura and R.E. Olson, J. Phys. B **17**, L713 (1984).
- [40] J. D. Dollard, Asymptotic convergence and the Coulomb interaction, J. Math. Phys., **5**, 729-738, 1964.
- [41] I. M. Cheshire, Continuum distorted wave approximation; resonant charge transfer by fast protons in atomic hydrogen, Proc. Phys. Soc., **84**, 89-98, 1964.
- [42] R. Gayet, Charge exchange scattering amplitude to first order of a three body expansion, J. Phys. B, **5**, 483-491, 1972.
- [43] Dz. Belkic, R. Gayet and A. Salin, Electron capture in high-energy ion-atom collisions, Phys. Rep., **56**, 279-369, 1979.
- [44] B. H. Bransden and D. P. Dewangan, High energy charge transfer, Adv. At. Mol. Opt. Phys., **25**, 343-374, 1988.
- [45] B. H. Bransden and M. R. C. McDowell, *Charge exchange and the Theory of Ion-Atom Collisions*, The international series of monographs in physics, Clarendon, Oxford, 1992.
- [46] D. S. F. Clothers and L. J. Dube, Continuum distorted wave methods in ion-atom collisions, Adv. At. Mol. Opt. Phys., **30**, 287-337, 1993.
- [47] D. P. Dewangan and J. Eichler, Charge exchange in energetic ion-atom collisions, Phys. Rep., **247**, 59-219, 1994.
- [48] Dz. Belkic, Leading distorted wave theories and computational methods for fast ion-atom collisions, J. Comput. Meth. Sci. Eng., **1**, 1-74(2001).
- [49] B. H. Bransden and C. J. Joachain, *Physics of Atoms and Molecules*, 2<sup>nd</sup> Ede. Prentice Hall, New York, 2003.
- [50] Dz. Belkic, Phys. Rev. A **47**, 189 (1993).
- [51] Dz. Belkic, J. Phys. B **26**, 497 (1993).

- [52] Dz. Belkic, *Principles of Quantum Scattering Theory*, Institute of Physics Publishing, Bristol, 2004.
- [53] Dz. Belkic, *Europhys. Lett.*, **7**, 323 (1988).
- [54] Dz. Belkic, *Phys. Rev. A* **43**, 4751 (1991).
- [55] Dz. Belkic, *J. Phys. B: At. Mol. Opt. Phys.* **10**, 3491 (1977).
- [56] C. R. Mandal, Mita Mandal and S. C. Mukherjee, *Phys. Rev. A.* **44**, 2962 (1991).
- [57] S. C. Mukherjee, K. Roy and N. C. Sil, *Phys.Rev. A* **12**, 1719 (1975).
- [58] C. Sinha and S. Tripathi, *J.Phys.B: At.Mol.Opt.Phys.* **24**, 3659 (1991).
- [59] R. R. Lewis , *Phys.Rev.* **102**, 537 (1956).
- [60] C. Sinha and N. C. Sil, *J.Phys.B:At.Mol.Phys.* **11**, L333 (1978).
- [61] I. M. Cheshire, “Continuum distorted wave approximation;resonant charge transfer by fast protons in atomic hydrogen,”*Proceedings of the Physical Society*, vol. **84**, no. 1, pp. 89–98,1964.
- [62] D. S. F. Crothers, “Refined orthogonal variational treatment ofcontinuum distorted waves,”*Journal of Physics B*, vol. **15**, no.13, pp. 2061–2074, 1982.
- [63] Dz. Belkic, “A quantum theory of ionisation in fast collisionsbetween ions and atomic systems,” *Journal of Physics B*, vol. **11**,no. 20, pp. 3529–3552, 1978.
- [64] D. S. F. Crothers and J. F.McCann, “Ionisation of atoms by ionimpact,” *Journal of Physics B*, vol. **16**, no. 17, pp. 3229–3242,1983.
- [65] L. Rosenberg, “Variational methods in charged-particle collisiontheory,” *Physical Review D*, vol. **8**, no. 6, pp. 1833–1843,1973, P. J. Redmond, unpublished.
- [66] D. S. F. Crothers and L. J. Dub´e, “Continuum distortedwave methods in ion—atom collisions,” *Advances in Atomic,Molecular, and Optical Physics*, vol. **30**, pp. 287–337, 1992.
- [67] J. D. Dollard, “Asymptotic convergence and the Coulombinteraction,” *Journal of Mathematical Physics*, vol. **5**, no. 6, pp.729–738, 1964.
- [68] R. Gayet, *J. Phys. B* **5**, 483 (1972).
- [69] Dz. Belkic and R. Janev, *J. Phys. B* **6**, 1020 (1979).
- [70] Dz. Belkic and R. Gayet, *J. Phys. B* **10**, 1923 (1977).
- [71] Dz. Belkic and A. Salin, *J. Phys. B* **11**, 3905 (1978).
- [72] D.S.F. Crothers, *J. Phys. B* **14**, 1035 (1981).
- [73] S. Datta, C. R. Mandal, S. C. Mukherjee and N. C. Sil, *Phys. Rev. A* **26**, 2551 (1982).

- [74] C. R. Mandal, S. Datta and S. C. Mukherjee, Phys. Rev. A **28**, 1141 (1983).
- [75] M. B. Saha, T. V. Goffe and H. B. Gilbody, J. Phys. B **11**, L233 (1978).
- [76] T. V. Goffe, M. B. Saha and H. B. Gilbody, J. Phys. B **12**, 3763 (1979).
- [77] D. S. F. Crothers and J. F. McCann, J. Phys. B **18**, 2907 (1985).
- [78] R. Abrines and I. C. Percival, Proc. Phys. Soc. **88**, 861 (1966).
- [79] J. Hirschfelder, H. Eyring, and B. Topley, J. Chem. Phys. **4**, 170 (1936).
- [80] M. Karplus, R. N. Porter, and R. D. Sharma, J. Chem. Phys. **43**, 3259 (1965).
- [81] I. C. Percival and D. Richards, Adv. At. Mol. Phys. **11**, 1 (1975).
- [82] G. Peach, S. L. Wills and M. R. McDowell, J. Phys. B: At. Mol. Opt. Phys. **16**, 2851 (1985).
- [83] S. L. Wills, G. Peach, M. R. McDowell and J. Banerji, J. Phys. B: At. Mol. Opt. Phys. **18**, 3939 (1985).
- [84] M. Purkait, A. Dhara, S. Sounda and C. R. Mandal, J. Phys. B: At. Mol. Opt. Phys. **34**, 755 (2001).
- [85] Y. Ichihiro, J. Plasma Fusion Res. **6**, 442 (2004).
- [86] J. A. Perez and R. E. Olson, Nucl. Instrum. Methods Phys. Res. B **241**, 134 (2005).
- [87] J. G. Wang, B. He, Y. Ning, C. L. Liu, J. Yan, P. C. Stancil and D. R. Schultz, Phys. Rev. A **74**, 052709 (2006).
- [88] R. E. Olson and A. Salop, Phys. Rev. A **16**, 531 (1977).

## **CHAPTER- 2**

# **STATE-SELECTIVE CHARGE TRANSFER IN ION-ION INTERACTION AT INTERMEDIATE AND HIGH ENERGIES**

## 2.1. INTRODUCTION

Atomic data for single charge transfer between different combinations of ion-atom/ion are on very much demand to study the behaviors of impurity ions in all types of plasma [1]. As a consequence, both theoretical [2-11] and experimental studies [12-17] of such processes have made substantial progress. In this theoretical paper, we are mainly concerned with the charge transfer of hydrogen like ions by the impact of  $H^+$ ,  $He^{2+}$  and  $Li^{3+}$  ions in the wide range of energies.

The electron capture by protons from hydrogenic ions such as  $He^+$  and  $Li^{2+}$  has been investigated using the Coulomb-Born (CB) approximation [2]. The calculated capture cross sections in the ground state have been shown a significant difference from the corresponding Born cross sections in the intermediate energy region. Mukherjee and Sil [5] have calculated the one electron capture from the hydrogen like target ions by protons and the alpha particles impact into the ground state and the excited 2s state only using the continuum distorted wave (CDW) approximation in the energy range 100-2000 keV. They have shown that the major contribution to the cross sections for the system  $He^{2+}-He^+$  comes from ground to ground state. Fojon et al [3,4] studied the formation of positronium atoms through electron capture in collision of positrons with hydrogen like target ions such as  $He^+$ ,  $Li^{2+}$  and  $Be^{3+}$  using Coulomb Born Approximation (CBA) and CDW-final state approximation (CDW-FS). They have also reproduced the differential cross sections and given a scaling law, which is very good for high nuclear target charge ( $Z_T$ ). The recent experiment on ion-ion collisions was performed by Brauning et al [16] and this data are compared to other theoretical calculations using a two centre extension of the basis generator method (BGM) [9-11]. They have also calculated the cross sections of such reactions using BGM. The experimental data are in reasonably good agreement with BGM calculation. In this paper [16] we have found that the BGM calculations show excellent agreement with the iso-electronic resonant collision system  $He^+ + He^{2+}$  as well as the non-resonant collision system  $Li^{2+} + He^{2+}$ ,  $He^+ + H^+$ . Recently, Minami et al [8] have calculated the charge transfer cross section for  $H^+ + He^+$  and  $He^{2+} + Li^{2+}$  collisions using the lattice time-dependent Schrodinger equation (LTDSE) and atomic orbital close coupling (AOCC) method in the velocity range of 0.5 to 4 amu. They have only given the state-selective contribution of

charge transfer cross sections in different principal quantum numbers ( $n$ ) for  $H^+ + He^+$  collision in tabular form using AOCC, finite-differences LTDSE (LTDSE-FD) and Fourier collection LTDSE (LTDSE-FC) methods in the whole energy range. We found that their results are slightly overestimate the BGM results of Brauning et al [16] for  $He^{2+} + Li^{2+}$  collision. They have given a scaling of the total charge transfer cross sections. However, to the best of our knowledge, no theoretical data of details sub-shell results for the collision system are available. Under the context, we are motivated to study the sub-shell distribution of charge transfer cross sections for  $H^+ + He^+$ ,  $He^{2+} + He^+$ ,  $He^{2+} + Li^{2+}$  and  $Li^{3+} + Li^{2+}$  collisions in the 30-2000 keV/amu impact energy range. Here we have employed the three body formalism of the boundary corrected continuum intermediate state (BCCIS-3B) approximations.

The plan of this paper is as follows. Presenting the details of our calculations in Section 2, we discuss our computed results in Sec. 3. Finally in Sec. 4 we make our concluding remarks. Atomic units have been used throughout.

## 2.2. Theory

The total Hamiltonian for the collision system may be written as

$$H = H_i + V_i = H_f + V_f \quad (1)$$

$$\text{where, } H_i = -\frac{1}{2\mu_i} \nabla_{R_T}^2 + \frac{Z_P(Z_T-1)}{R_T} - \frac{1}{2a} \nabla_{r_T}^2 - \frac{Z_T}{r_T}, \quad V_i = \frac{Z_P}{R_T} - \frac{Z_P}{r_P}$$

$$\text{and } H_f = -\frac{1}{2\mu_f} \nabla_{R_P}^2 - \frac{1}{2b} \nabla_{r_P}^2 - \frac{Z_P}{r_P},$$

$$V_f = \frac{Z_P Z_T}{R_T} - \frac{Z_T}{r_T}, \quad \mu_i = \frac{M_P(1+M_T)}{1+M_P+M_T}, \quad \mu_f = \frac{M_T(1+M_P)}{1+M_P+M_T}, \quad a = \frac{M_T}{1+M_T}, \quad b = \frac{M_P}{1+M_P}.$$

Here e, T and P present active electron, target ion and projectile ion respectively.  $\vec{R}_T$  and  $\vec{R}_P$  be the position vector of P and T relative to the centre of mass of (T, e) and (P, e) respectively. The initial non-perturbed wave function is given by

$$\Psi_i = \varphi_i(\vec{r}_T) \chi_i^+(\vec{R}_T) \quad (2)$$

where  $\varphi_i(\vec{r}_T)$  is the initial bound state wave function. The function  $\chi_i^+(\vec{R}_T)$  is an outgoing Coulomb continuum wave function representing the projectile ion moving in the field of an effective ion of charge  $(Z_T-1)$ , so the Schrodinger equation is

$$(E - H'_i) \chi_i^+ = 0$$

$$\text{where } \chi_i^+(\vec{R}_T) = e^{-\frac{\pi}{2}\alpha_3} \Gamma(1 + i\alpha_3) e^{i\vec{k}_i \cdot \vec{R}_T} {}_1F_1\left\{-i\alpha_3; 1; i(k_i R_T - \vec{k}_i \cdot \vec{R}_T)\right\}, \quad \alpha_3 = \frac{Z_P(Z_T-1)}{v_i}.$$

Here  $\vec{k}_i$  is the initial wave vector.

The prior form of the transition matrix element,

$$T_{if}^{(-)} = \langle \Psi_f^- | V_i | \Psi_i \rangle \approx \langle \Psi_f^{\text{BCCIS-3B}} | V_i | \Psi_i \rangle. \quad (3)$$

We write the final wave function,

$$\Psi_f^{\text{BCCIS-3B}} = e^{\frac{\pi}{2}(\alpha_1 - \alpha_2)} \Gamma(1 + i\alpha_1) \Gamma(1 - i\alpha_2) e^{i\vec{k}_f \cdot \vec{R}_P} \varphi_f(\vec{r}_P) {}_1F_1\left\{-i\alpha_1; 1; -ia(v_f r_T + \vec{v}_f \cdot \vec{r}_T)\right\} \times {}_1F_1\left\{i\alpha_2; 1; -ib(k_f R_T + \vec{k}_f \cdot \vec{R}_T)\right\} \quad (4)$$

$$\text{where } \alpha_1 = \frac{Z_T}{v_f}, \quad \alpha_2 = \frac{Z_P Z_T}{v_f}.$$

The transition amplitude can be written as

$$T_{if}^{(-)} = N \iint d\vec{r}_T d\vec{R}_T e^{i\vec{k}_i \cdot \vec{R}_T - i\vec{k}_f \cdot \vec{R}_P} \varphi_f^*(\vec{r}_P) \left( \frac{Z_P}{R_T} - \frac{Z_P}{r_P} \right) {}_1F_1\left\{i\alpha_1; 1; ia(v_f r_T + \vec{v}_f \cdot \vec{r}_T)\right\} \times {}_1F_1\left\{-i\alpha_2; 1; ib(k_f R_T + \vec{k}_f \cdot \vec{R}_T)\right\} \varphi_i(\vec{r}_T) {}_1F_1\left\{-i\alpha_3; 1; i(k_i R_T - \vec{k}_i \cdot \vec{R}_T)\right\} \quad (5)$$

where  $N = e^{\frac{\pi}{2}(\alpha_1 - \alpha_2 - \alpha_3)} \Gamma(1 - i\alpha_1) \Gamma(1 + i\alpha_2) \Gamma(1 + i\alpha_3)$ .

Using integral representation  ${}_1F_1(i\alpha; 1; z) = \frac{1}{2\pi i} \oint d\tau \tau^{i\alpha-1} (\tau-1)^{-i\alpha} e^{z\tau}$ . The transition amplitude of equation (5) may be written as

$$T_{if} = \frac{AN}{(2\pi i)^3} \ell \lim_{\varepsilon_1 \rightarrow 0} D(\varepsilon_1, \lambda, \beta) \oint dt_1 t_1^{i\alpha_1-1} (t_1-1)^{-i\alpha_1} \oint dt_2 t_2^{-i\alpha_2-1} (t_2-1)^{i\alpha_2} \oint dt_3 t_3^{-i\alpha_3-1} (t_3-1)^{i\alpha_3} J \quad (6)$$

$$\text{where } J = \iint d\vec{r}_T d\vec{R}_T e^{i\vec{k}_i \cdot \vec{R}_T - i\vec{k}_p \cdot \vec{R}_p + i a \vec{v}_f \cdot \vec{r}_T t_1 + i b \vec{k}_f \cdot \vec{R}_T t_2 - i \vec{k}_i \cdot \vec{R}_p t_3} \frac{e^{-\beta_1 r_T}}{r_T} \frac{e^{-\lambda r_p}}{r_p} \frac{e^{-\varepsilon R_T}}{R_T}, \quad (6a)$$

$$\beta_1 = \beta - i a v_f t_1 \quad \text{and} \quad \varepsilon = \varepsilon_1 - i b k_f t_2 - i k_i t_3.$$

Here the constant A is originating from the initial and final bound state wave functions.

$D(\varepsilon_1, \lambda, \beta_1)$  is a parametric differential operator used to generate higher state wave functions.  $\beta$  and  $\lambda$  are the orbital exponent of the initial and the final bound state wave functions.

Taking the Fourier transform of equation (6a) and using integral representation of general three denominator integration of Lewis [18], Sinha and Sil [19],

$$J = \frac{16\pi^2}{a^2} \int_0^\infty \frac{dx}{a'x^2 + 2b'x + c'}. \quad (7)$$

Using equation (7), the transition matrix element now becomes

$$T_{if} = \frac{NA}{(2\pi i)} \frac{16\pi^2}{a^2} \ell \lim_{\varepsilon_1 \rightarrow 0} D(\varepsilon_1, \lambda, \beta) \oint dt_2 t_2^{-i\alpha_2-1} (t_2-1)^{i\alpha_2} \int_0^\infty K dx \quad (8)$$

$$\text{where } K = \frac{1}{A} \left( \frac{A}{A+B} \right)^{i\alpha_1} \left( \frac{A}{A+C} \right)^{-i\alpha_3} {}_2F_1\{i\alpha_1; -i\alpha_3; 1; z\}, \quad z = \frac{BC-AD}{(A+B)(A+C)}.$$

Now the complex integration of  $t_2$  is converted to real integral [20, 21] which has been subdivided into a number of sub-intervals and each sub-interval is integrated numerically using Gauss Laguerre quadrature method. Finally a single electron capture cross sections is obtained numerically over scattering angles with the Gauss Legendre quadrature method. The orders of two dimensional integral are varied until convergence to three decimal places is obtained for the total charge transfer cross sections.

## 2.3. Results and discussion

Total charge transfer cross sections have been obtained by summing over all contributions into each shell up to  $n=3$ . Variation of total charge transfer cross sections with the incident energy of the projectile ion are reported in graphical form for resonant and non resonant collision systems in Figures 1-4. Sub-shell distribution of total charge transfer cross sections have been displayed in Table I-IV.

### A. Non-resonant reactions

In figure 1 we display the present BCCIS-3B results along with available experimental and theoretical data for the iso-electronic collision system  $H^+ + He^+$  and shows good overall agreement with the experimental results [12-15] and other theoretical results [2,5,8]. Looking in more details reveals that in comparison with the experiments our results are slightly smaller than the measurements below 50 keV/amu. We find that the CDW results is about 84% larger at 400 keV and about 50% lower at 1000 keV. But our results are in good agreement with the results obtained by LTDSE-FD [8] method. The results of this reaction are given in Table I. From Table I, we see that the 1s cross sections are more significant than the other states. The cross section shows the typical dependence on the collision energy with a maximum around 50 keV. For the non-resonant collision system  $He^{2+} + Li^{2+}$ , our theoretical data given in Table II are compared with only the recent experimental data [16] and the theoretical results [5,8] in figure 2. Here the agreement between our results and experiment is very good in the low energy range (less than 60 keV/amu). Due to the higher charge state of the target, the peak positions of cross sections shift towards the higher projectile energies (near almost 80 keV/amu). From this figure 2, we have

seen that our results are underestimated compared to the other theoretical results. This may be due to the contribution of higher excited states, but the nature of the curve remains same. Here the ground state capture cross sections are maximum but less with respect to iso-electronic collision system  $H^+ + He^+$ . We note, regarding the importance of various angular momenta, the inclusion of  $\ell = 1$  state accounts for the majority of the resulting cross sections at low energies and  $\ell = 0$  state at high energies.

## B. Resonant reactions

In figure 3 our measured cross sections for  $He^{2+} + He^+$  collisions are plotted against the projectile energy together with previous theoretical results [5,6] and measurements [17]. Our results are in good agreement with CDW results but not so good with CTMC results [6]. At low collision energies, the agreements between the experimental results of Melchart et al [17] with our BCCIS-3B results are poor at 50 keV/amu energy. The computed results are given in Table-III. We find from the table that the major contribution to the cross sections comes from ground state as it is a resonating state. Since it is a resonant and charge symmetric system, large cross sections would be expected at intermediate collision energies. Here also we find that the contributions from  $n=2$  state may not be ignored. Due to non-availability of any experimental data, the variation of single electron capture cross sections with projectile energy are only compared with the results of Brauning et al [16] which is shown in figure 4. The computed results have been displayed in Table IV. From this graph, it is evident that the present computed results agree well with the results of Brauning et al [16] above 30 keV/amu energy. The Table IV shows the same feature as like  $He^{2+} + He^+$  collision but gives the higher value of cross sections.

## 2.4. Conclusions

By applying the three body boundary corrected continuum intermediate state (BCCIS-3B) approximation to ion-ion collision system, the results obtained are reasonably good in the whole energy range 50-2000 keV/amu. The distortions in the final channel related to the Coulomb continuum states of the residual target are included. The charged target ion introduces additional complications through the inclusion of a continuum state. At intermediate collision energies,

large cross sections can be obtained from a resonant and symmetric charge system than non-resonant and a symmetric charge system. For resonant collision systems differ simply by just one greater unit of charge on both the projectile and the target, it is found that the magnitude of cross sections will increase.

**TABLE-I. State selective cross sections  $\sigma_{n\ell}$  (in  $10^{-16} \text{ cm}^2$ ) for charge transfer in  $\text{H}^+\text{-He}^+$  collisions. The integer in parenthesis indicates the power of ten by which the number has to be multiplied.**

Energy (keV/amu)	1s	2s	2p	n=2	3s	3p	3d
30	1.58(-1)	3.37(-3)	7.20(-3)	1.06(-2)	1.56(-4)	9.28(-4)	7.04(-5)
40	1.81(-1)	3.07(-3)	7.80(-3)	1.09(-2)	1.52(-4)	8.96(-4)	4.83(-5)
50	2.03(-1)	2.73(-3)	7.31(-3)	1.00(-2)	1.42(-4)	7.98(-4)	3.08(-5)
60	1.87(-1)	1.55(-3)	6.98(-3)	8.53(-3)	1.10(-4)	3.41(-4)	2.17(-5)
80	1.50(-1)	1.21(-3)	4.54(-3)	5.75(-3)	8.52(-5)	1.51(-4)	1.45(-5)
100	1.14(-1)	9.21(-4)	3.30(-3)	4.22(-3)	4.43(-5)	1.00(-4)	1.17(-5)
200	1.79(-2)	2.71(-4)	5.06(-4)	7.77(-4)	2.00(-5)	7.85(-5)	3.23(-6)
400	1.87(-3)	5.63(-5)	4.89(-5)	1.05(-4)	1.00(-5)	3.98(-5)	2.08(-7)
500	8.04(-4)	3.15(-5)	1.04(-5)	4.19(-5)	4.43(-6)	1.27(-5)	6.37(-8)
800	1.03(-4)	5.00(-6)	9.38(-7)	5.93(-6)	3.39(-7)	4.34(-6)	3.91(-9)
1000	3.73(-5)	2.14(-6)	2.74(-7)	2.41(-6)	9.91(-8)	1.52(-6)	9.49(-10)

**Continue to Table-I**

Energy (keV/amu)	n=3	Total
30	1.15(-3)	1.70(-1)
40	1.10(-3)	1.93(-1)
50	9.70(-4)	2.14(-1)

60	4.70(-4)	1.96(-1)
80	2.50(-4)	1.56(-1)
100	1.56(-4)	1.18(-1)
200	1.00(-4)	1.87(-2)
400	5.00(-5)	2.02(-3)
500	1.72(-5)	8.63(-4)
800	4.68(-6)	1.14(-4)
1000	1.62(-6)	4.13(-5)

**TABLE-II. State selective cross sections  $\sigma_{n\ell}$  (in  $10^{-16}$  cm<sup>2</sup>) for charge transfer in He<sup>2+</sup> -Li<sup>2+</sup> collisions. The integer in parenthesis indicates the power of ten by which the number has to be multiplied.**

Energy (keV/amu)	1s	2s	2p	n=2	3s	3p	3d
30	6.40(-2)	9.20(-3)	1.23(-2)	2.15(-2)	8.13(-3)	1.25(-2)	9.61(-4)
40	7.56(-2)	1.15(-2)	1.25(-2)	2.40(-2)	1.03(-2)	1.42(-2)	1.22(-3)
50	1.02(-1)	5.15(-3)	2.80(-2)	3.31(-2)	2.79(-3)	3.79(-3)	3.44(-4)
60	1.07(-1)	9.96(-3)	1.85(-2)	2.84(-2)	7.41(-3)	9.19(-3)	1.05(-3)
80	1.46(-1)	1.68(-3)	1.30(-2)	1.46(-2)	7.07(-4)	1.55(-3)	9.61(-5)
100	1.22(-1)	5.14(-3)	8.21(-3)	1.33(-2)	1.99(-3)	3.11(-3)	1.83(-4)
200	4.67(-2)	1.73(-3)	1.46(-2)	1.63(-2)	9.95(-4)	6.15(-4)	1.05(-4)
400	1.29(-2)	9.32(-4)	2.01(-3)	2.94(-3)	8.19(-4)	3.51(-4)	2.06(-5)
500	8.38(-3)	6.88(-4)	4.39(-4)	1.12(-3)	4.08(-4)	1.64(-4)	3.60(-6)
800	2.94(-3)	1.34(-4)	9.89(-5)	2.32(-4)	1.36(-4)	5.08(-5)	2.51(-6)
1000	1.66(-3)	6.23(-5)	3.13(-5)	9.36(-5)	7.69(-5)	2.34(-5)	1.01(-6)
2000	1.97(-4)	4.76(-6)	3.76(-6)	8.52(-6)	8.98(-6)	1.40(-6)	3.10(-8)

Continue to Table-II

Energy (keV/amu)	n=3	Total
30	2.15(-2)	1.07(-1)
40	2.54(-2)	1.25(-1)
50	6.92(-3)	1.41(-1)
60	1.76(-2)	1.53(-1)
80	2.35(-3)	1.63(-1)
100	5.28(-3)	1.40(-1)
200	1.71(-3)	6.47(-2)
400	1.19(-3)	1.70(-2)
500	5.75(-4)	1.00(-2)
800	1.89(-4)	3.36(-3)
1000	1.01(- 4)	1.85(-3)
2000	1.04(-5)	2.15(-4)

**TABLE-III.** State selective cross sections  $\sigma_{n\ell}$  (in  $10^{-16} \text{ cm}^2$ ) for charge transfer in  $\text{He}^{2+} - \text{He}^+$  collisions. The integer in parenthesis indicates the power of ten by which the number has to be multiplied.

Energy (keV/amu)	1s	2s	2p	n=2	3s	3p	3d
30	9.35(-1)	8.40(-2)	3.33(-1)	4.17(-1)	5.83(-2)	1.02(-1)	3.27(-2)
40	1.11(+0)	6.84(-2)	3.12(-1)	3.80(-1)	1.80(-2)	2.03(-2)	2.44(-3)
50	1.00(+0)	8.00(-2)	3.30(-1)	4.10(-1)	1.52(-2)	2.00(-2)	4.64(-3)

60	9.70(-1)	3.83(-2)	2.72(-1)	3.10(-1)	8.56(-3)	1.23(-2)	1.38(-3)
80	6.84(-1)	4.36(-2)	2.46(-1)	2.89(-1)	1.04(-2)	1.38(-2)	3.73(-3)
100	4.93(-1)	4.65(-2)	2.03(-1)	2.49(-1)	1.31(-2)	1.39(-2)	3.28(-3)
200	1.05(-1)	1.13(-2)	2.71(-2)	3.84(-2)	5.40(-3)	4.20(-3)	4.25(-4)
400	2.36(-2)	4.67(-3)	2.22(-3)	6.89(-3)	1.23(-3)	8.44(-4)	7.80(-5)
500	1.26(-2)	1.47(-3)	9.85(-4)	2.45(-3)	6.67(-4)	3.75(-4)	2.89(-5)
800	2.82(-3)	1.44(-4)	6.73(-5)	2.11(-4)	1.47(-4)	5.51(-5)	2.77(-6)
1000	1.21(-3)	5.05(-5)	1.69(-5)	6.74(-5)	6.26(-5)	1.92(-5)	7.94(-7)
2000	5.24(-5)	1.89(-6)	1.02(-6)	2.91(-6)	2.46(-6)	3.82(-7)	8.16(-9)

Continue to Table-III

<b>Energy (keV/amu)</b>	<b>n=3</b>	<b>Total</b>
30	1.93(-1)	1.54(+0)
40	4.07(-2)	1.53(+0)
50	3.98(-2)	1.45(+0)
60	2.22(-2)	1.30(+0)
80	2.79(-2)	1.00(+0)
100	3.02(-2)	7.72(-1)
200	1.00(-2)	1.53(-1)
400	2.15(-3)	3.26(-2)
500	1.07(-3)	1.61(-2)
800	2.05(-4)	3.23(-3)
1000	8.25(-5)	1.35(-3)
2000	2.85(-6)	5.81(-5)

**TABLE-IV** State selective cross sections  $\sigma_{n\ell}$  (in  $10^{-16} \text{ cm}^2$ ) for charge transfer in  $\text{Li}^{3+} - \text{Li}^{2+}$  collisions. The integer in parenthesis indicates the power of ten by which the number has to be multiplied.

Energy (keV/amu)	1s	2s	2p	n=2	3s	3p	3d
30	1.35(+0)	1.35(-1)	1.46(-1)	2.81(-1)	3.09(-1)	3.80(-1)	8.02(-2)
40	1.28(+0)	7.44(-2)	9.36(-2)	1.68(-1)	2.47(-1)	2.39(-1)	5.04(-2)
50	1.00(+0)	5.30(-2)	1.17(-1)	1.70(-1)	1.34(-1)	1.65(-1)	3.08(-2)
60	7.94(-1)	4.70(-2)	1.27(-1)	1.74(-1)	8.12(-2)	1.17(-1)	2.21(-2)
80	4.86(-1)	2.17(-2)	2.02(-1)	2.23(-1)	4.93(-2)	3.51(-2)	9.47(-3)
100	2.97(-1)	2.40(-2)	2.14(-1)	2.38(-1)	3.85(-2)	4.11(-2)	1.21(-2)
200	1.22(-1)	1.88(-2)	6.08(-2)	7.96(-2)	5.46(-3)	7.55(-3)	6.92(-4)
400	4.15(-2)	5.68(-3)	2.29(-2)	2.85(-2)	2.41(-3)	2.24(-3)	3.50(-4)
500	2.71(-2)	5.48(-3)	1.38(-2)	1.92(-2)	1.99(-3)	1.86(-3)	3.17(-4)
800	1.03(-2)	3.50(-3)	2.14(-3)	5.64(-3)	8.67(-4)	7.62(-4)	1.15(-4)
1000	7.21(-3)	1.15(-3)	7.28(-4)	1.87(-3)	3.28(-4)	2.94(-4)	3.18(-5)
2000	8.68(-4)	2.39(-5)	4.61(-5)	7.00(-5)	3.92(-5)	1.78(-5)	1.06(-6)

Continue to Table-IV

Energy (keV/amu)	n=3	Total
30	7.69(-1)	2.40(+0)
40	5.36(-1)	1.98(+0)
50	3.29(-1)	1.50(+0)
60	2.20(-1)	1.18(+0)

80	9.38(-2)	8.02(-1)
100	9.17(-2)	6.26(-1)
200	1.37(-2)	2.15(-1)
400	5.00(-3)	7.50(-2)
500	4.16(-3)	5.04(-2)
800	1.74(-3)	1.76(-2)
1000	6.53(-4)	9.73(-3)
2000	5.80(-5)	9.96(-4)

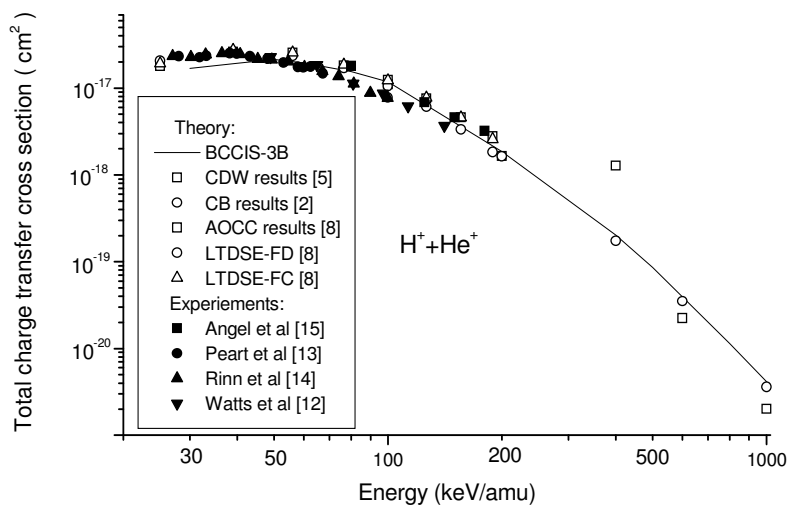


**Figure 1.** Comparison of the total charge transfer cross sections in  $H^+ + He^+$  by various theories and experiments. Correspondence between each symbol and methods / authors is given in the figure.

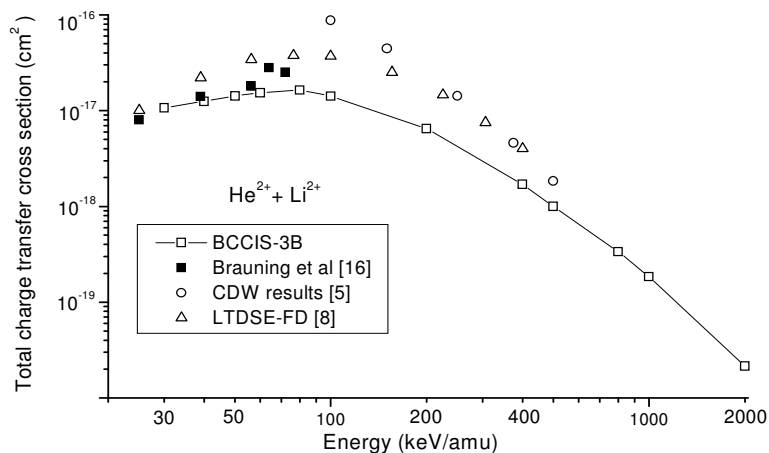


**Figure 2.** The total charge transfer cross sections in  $\text{He}^{2+} + \text{Li}^{2+}$  by various theories and experiments.

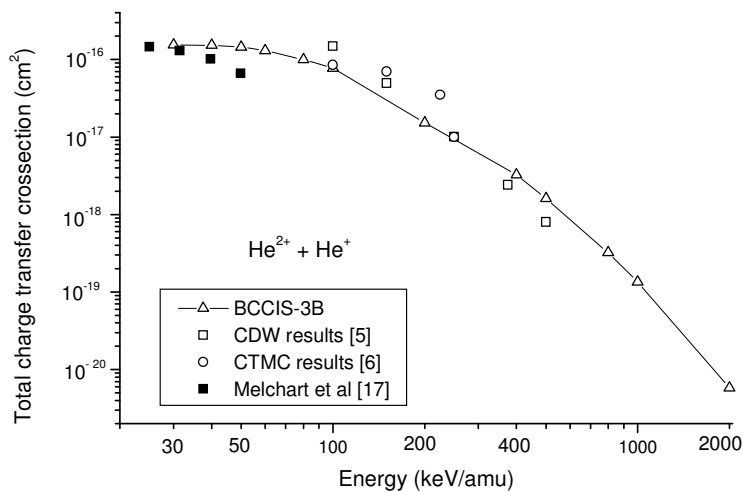


**Figure 3.** The total charge transfer cross sections in  $\text{He}^{2+} + \text{He}^+$  by various theories and experiments.

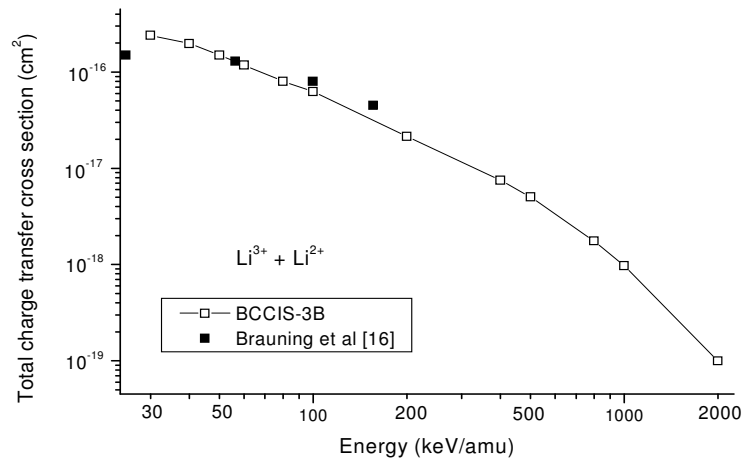


**Figure 4.** The total charge transfer cross sections in  $\text{Li}^{3+} + \text{Li}^{2+}$  by various theories and experiments.

## References

- [1] Janev R K, Atomic and Molecular processes in Fusion Edge Plasmas (New York: Plenum) (1995).
- [2] Mukherjee S, Sil N C and Basu D, J.Phys.B: Atom.Molec.Phys. **12**, 1259 (1979).
- [3] Fojon O A and Rivarola R D, Phys.Rev. A **54**, 4923 (1996).
- [4] Fojon O A, Rivarola R D, Gayet R, Hanssen J and Hervieux P A, J.Phys.B:At.Mol.Opt.Phys. **30**, 2199 (1997).
- [5] Mukherjee S and Sil N C, J.Phys.B: At.Mol.Phys. **13**, 3421 (1980).
- [6] Olson R E, J.Phys.B: Atom.Molec.Phys. **11**, L227 (1978).
- [7] Belkic Dz and Janev R K, J.Phys.B:Atom.Molec.Phys. **6**, 1020 (1973).
- [8] Minami T, Pindzola M S, Lee T G and Schultz D R, J.Phys.B: At.Mol.Opt.Phys. **40**, 3629 (2007).
- [9] Ludde H J, Henne A, Kirchner T and Dreizler R M, J.Phys.B: At.Mol.Opt.Phys. **29**, 4423 (1996).
- [10] Kroneisen O J, Ludde H J and Dreizler R M, J.Phys.A: Math.Gen. **32**, 2141 (1999).

- [11] Zapukhlyak M, Kirchner T, Ludde H J, Knoop S, Morgenstern R and Hoekstra R, *J.Phys.B: At.Mol.Opt.Phys.* **38**, 2353 (2005).
- [12] Watts M F, Dunn K F and Gilbody H B, *J.Phys.B:At.Mol.Opt.Phys.* **19**,L355 (1986).
- [13] Peart B, Rinn K and Dolder K, *J.Phys.B:At.Mol.Phys.* **16**, 1461 (1983).
- [14] Rinn K, Melchert F and Salzborn E, *J.Phys.B: At.Mol.Phys.* **18**, 3783 (1985).
- [15] Angel G C, Sewell E C, Dunn K F and Gilbody H B, *J.Phys.B:Atom.Molec.Phys.* **11**, L297 (1978).
- [16] Brauning H, Trassl R, Theiß A, Diehl A, Salzborn E, Keim M, Achenbach A, Ludde H J and Kirchner T, *J.Phys.B: At.Mol.Opt.Phys.* **38**, 2311 (2005).
- [17] Melchert F, Krudener S, Schulze R, Petri S, Pfaff S and Salzborn E, *J.Phys.B:At.Mol.Opt.Phys.* **28**, L355 (1995).
- [18] Lewis R R, *Phys.Rev.* **102**, 537 (1956).
- [19] Sinha C and Sil N C, *J.Phys.B:At.Mol.Phys.* **11**, L333 (1978).
- [20] Mukherjee S C, Roy K and Sil N C, *Phys.Rev. A* **12**, 1719 (1975).
- [21] Sinha C and Tripathi S, *J.Phys.B: At.Mol.Opt.Phys.* **24**, 3659 (1991).

## CHAPTER- 3

# SINGLE- ELECTRON CAPTURE PROCESSES IN COLLISIONS OF $\text{He}^{2+}$ , $\text{Li}^{q+}$ ( $q=1, 2, 3$ ), $\text{C}^{6+}$ AND $\text{O}^{8+}$ IONS WITH HELIUM

### 3.1. INTRODUCTION

Single-electron capture by the multiply charged projectiles from multi-electron atoms has recently received considerable attention from theoretical [1-23] as well as experimental [24-35] points of view due to its fundamental importance and various possibilities of applications in plasma physics, astrophysics, and controlled thermo-nuclear fusion research. As to applications, single-electron capture from helium atom by partially stripped ions also plays an important role in tokamak fusion plasmas [1]. In the development of the theoretical formulation of charge transfer processes, Dewangan and Eichler [2] are premier to find that the boundary conditions for the transition potential and the scattering wavefunction have to be satisfied properly in first and higher order calculations. Any exception to it is sure to generate singular structure of the transition amplitude. These characteristic features have been critically analysed by their latter works [3,4] and by others [5-7] as well. If either or both of the collision partners are many electron systems, the influence of the electron-electron interaction is important on the dynamics in the collision phenomena [6]. Since the helium atom is the simplest of many electron target where one can assess the importance of electron correlations, its investigation has attracted most attention from both the theoretical and experimental works. The role of electron correlation during a high energy ion-atom collision was investigated [21-23] by the correlation in the initial and final states. There are two kinds of electronic correlations: static and dynamic. Static correlations are built into multi-electron bound state wavefunctions. The dynamic correlations describe interactions between two electrons in the exit channel. Such type of correlation is one of the causes of the transition from the initial to the final state of the four-body system. In the present theoretical investigation, we have focused our attention to determination of electron transfer from helium atom by the impact of  $\text{He}^{2+}$ ,  $\text{Li}^{q+}$  ( $q=1-3$ ),  $\text{C}^{6+}$ , and  $\text{O}^{8+}$  projectile ion in the energy range of 50 -5000 keV/amu.

Cross sections for single-electron capture to the ground state in collisions of protons, alpha particles and lithium nuclei with He atoms are calculated at incident energies from 0.025 to 4 MeV/amu in the independent-electron-approximation (IEA) [8]. The calculations show that below 500 keV/amu there are substantial differences with the experimental results. Jain et al [9] have studied the sub-shell capture cross sections from helium atoms in collisions with bare ions

in the framework of two-center atomic-orbital-(AO) expansion method at high energies and compared those findings with experimental results. The results are in good agreement with the existing experimental data in the high energy region. With the extension of previous work of Belkic et al [10] and Mancev [11] have calculated the single-electron capture cross sections by fully stripped projectile ions from helium like atom in the energy range of 50 keV to 10 MeV with in the framework of the four-body formalism of continuum distorted wave (CDW-4B) method. In this work both static and dynamic correlations have been included through the perturbation potentials and the bound state wave function. Computed results are not in satisfactory agreement over the whole energy range. Later, Mancev [12] have employed the same method to calculate the total cross sections for single electron capture and transfer ionization for  $\text{Li}^{3+} + \text{He}(1s^2)$  collision. In this work, state-selective single electron capture cross sections have been displayed in tabular form at a few selective projectile energies. Mancev [13] have also developed second order Born distorted wave approximation (BDW) to study the single charge transfer in fast symmetric collisions between alpha particles and helium. Recently Mancev and Milojevic [14] have applied the four-body boundary-corrected first Born approximation (CB1-4B) both in post and prior form to study the single-electron capture cross sections from He atom by  $\text{H}^+$  and  $\text{He}^{2+}$  ions respectively. The results so obtained have reasonable agreement with the experimental findings except in the low energy region. Under the context, we are motivated to study the single charge transfer cross sections from He atom by fully stripped ( $\text{He}^{2+}$ ,  $\text{Li}^{3+}$ ,  $\text{C}^{6+}$ ,  $\text{O}^{8+}$ ) ions and partially stripped projectile ions ( $\text{Li}^+$ ,  $\text{Li}^{2+}$ ) in the energy range 50 to 5000 keV/amu. Based on the success of the four-body formalism of the boundary corrected continuum intermediate state (BCCIS-4B) approximation [36,37], we are motivated to study the above mentioned processes in the framework of BCCIS-4B theory.

The organization of the paper is as follows. Sec.II contains the theoretical calculations of the problem. Results and discussion are presented in the Sec.III. Finally, conclusions are given in Sec.IV. Atomic units have been used throughout the work.

### 3.2. THEORY

Single-electron capture from a two-electron atom by the impact of projectile ions ( $\text{He}^{2+}$ ,  $\text{Li}^{q+}$  ( $q=1,2,3$ ),  $\text{C}^{6+}$ ,  $\text{O}^{8+}$ ) may be written as

$$Z_P + (Z_T, e_1, e_2)_i \rightarrow (Z_P, e_1)_{f_1} + (Z_T, e_2)_{f_2}, \quad (1)$$

where  $Z_P$  and  $Z_T$  are the nuclear charges of the projectile and the target respectively.  $e_1$  and  $e_2$  are two electrons initially bound to the target nucleus and finally one active electron is bound to the projectile. The total Hamiltonian of the whole collision system may be written as

$$H = H_i + V_i = H_f + V_f, \quad (2)$$

where  $H_{i,f}$  represents Hamiltonian in the entrance and exit channel respectively and  $V_{i,f}$  are the corresponding perturbation potentials. In the initial channel,

$$H_i = H_0 - \frac{Z_T}{x_1} - \frac{Z_T}{x_2} + \frac{1}{r_{12}}, \quad V_i = \frac{Z_P Z_T}{R} - \frac{Z_P}{s_1} - \frac{Z_P}{s_2}$$

and

$$H_0 = -\frac{1}{2\mu_i} \nabla_{R_T}^2 - \frac{1}{2a} \nabla_{x_1}^2 - \frac{1}{2a} \nabla_{x_2}^2.$$

In the final channel,

$$H_f = H_0 - \frac{Z_P}{s_1} - \frac{Z_T}{x_2} + \frac{(Z_P-1)(Z_T-1)}{R_P},$$

$$V_f = \frac{Z_P Z_T}{R} - \frac{Z_T}{x_1} - \frac{Z_P}{s_2} + \frac{1}{r_{12}} - \frac{(Z_P-1)(Z_T-1)}{R_P}.$$

Using  $R_P \approx R$ , we obtain the following approximate expression:

$$V_f = Z_T \left( \frac{1}{R} - \frac{1}{x_1} \right) + Z_P \left( \frac{1}{R} - \frac{1}{s_2} \right) + \left( \frac{1}{r_{12}} - \frac{1}{R} \right)$$

and 
$$H_0 = -\frac{1}{2\mu_f} \nabla_{\vec{R}_p}^2 - \frac{1}{2b} \nabla_{\vec{s}_1}^2 - \frac{1}{2a} \nabla_{\vec{x}_2}^2,$$

$$\mu_i = \frac{M_p(2+M_T)}{2+M_p+M_T}, \mu_f = \frac{(M_p+1)(M_T+1)}{2+M_p+M_T}, a = \frac{M_T}{1+M_T}, b = \frac{M_p}{1+M_p}.$$

Here e, T and P represent active electron, target atom and projectile ion respectively.  $\vec{R}$  denotes the position vector of the projectile (P) relative to the target (T) nucleus.  $\vec{x}_j$  and  $\vec{s}_j$  ( $j=1,2$ ) are the electron co-ordinates measured from the target and projectile nuclei respectively.  $\mu_i, \mu_f, a$  and  $b$  are the reduced masses associated with the relative coordinates  $\vec{R}_T, \vec{R}_p, \vec{x}_j$  ( $j=1,2$ ), and  $\vec{s}_j$  ( $j=1,2$ ), respectively. The interelectronic co-ordinate is denoted by  $\vec{r}_{12} = \vec{s}_1 - \vec{s}_2 = \vec{x}_1 - \vec{x}_2$ .

The prior form of the scattering amplitude may be written in the form

$$T_{if}^{(-)} = \langle \psi_f^- | V_i | \psi_i \rangle, \quad (3)$$

where  $\psi_i(\vec{x}_1, \vec{x}_2) = e^{i\vec{k} \cdot \vec{R}_T} \varphi_i(\vec{x}_1, \vec{x}_2)$ .  $\varphi_i(\vec{x}_1, \vec{x}_2)$  is the product of one-parameter orbitals for the initial bound state of helium atom with effective charge  $Z_{\text{eff}}=1.6875$ .  $\psi_f^{(-)}$  is the distorted wave in the final channel. Here one electron is active and other electron is passive. The passive electron plays the role to screen the target ion in the final channel. However the interaction of the active electron and the projectile ion with the screened target ion are described by the Coulomb continuum wave functions in the final channel. The final state wave function  $\psi_f^{(-)}$  is given by

$$\psi_f^{(-)} = e^{\frac{\pi}{2}(\alpha_1 - \alpha_2)} \Gamma(1+i\alpha_1) \Gamma(1-i\alpha_2) e^{i\vec{k}_f \cdot \vec{R}_p} {}_1F_1\{-i\alpha_1; 1; -i(\vec{v}_f \cdot \vec{x}_1 + \vec{v}_f \cdot \vec{x}_1)\} \times \quad (4)$$

$${}_1F_1\{i\alpha_2; 1; -ib(\vec{k}_f \cdot \vec{R}_T + \vec{k}_f \cdot \vec{R}_T)\} \varphi_f(\vec{x}_2, \vec{s}_1)$$

where  $\alpha_1 = \frac{Z_T - 1}{v_f}$ ,  $\alpha_2 = \frac{Z_p(Z_T - 1)}{v_f}$ .

In post form the scattering amplitude may be written as

$$T_{if}^{(+)} = \langle \psi_f | V_f | \psi_i^+ \rangle. \quad (5)$$

Here the wavefunction in the final channel is given by

$$\psi_f = \varphi_f(\vec{s}_1, \vec{x}_2) \chi_f^-(\vec{R}_p),$$

where  $\varphi_f(\vec{s}_1, \vec{x}_2)$  is the final bound state wavefunction which is the product of hydrogen like wavefunctions and  $\chi_f^-(\vec{R}_p)$  is the Coulomb distorted wave in the exit channel. Since both the target and the projectile are ionic in nature except for  $\text{Li}^+ + \text{He}$  collision, their relative motion should be described by Coulomb continuum function  $\chi_f^-(\vec{R}_p)$ , which satisfies the equation

$$\left( -\frac{1}{2\mu_f} \nabla_{R_p}^2 + \frac{(Z_p-1)(Z_T-1)}{R_p} - \frac{k_f^2}{2\mu_f} \right) \chi_f^-(\vec{R}_p) = 0.$$

However, in the construction of the above differential equation we have used the asymptotic form of the internuclear interaction to take account of the effect of core electron (s) in both the target and the projectile.

Solving this equation, we find

$$\chi_f^-(\vec{R}_p) = e^{-\frac{\pi}{2}\alpha_3} \Gamma(1-i\alpha_3) e^{i\vec{k}_i \cdot \vec{R}_p} {}_1F_1\left\{i\alpha_3; 1; -i(k_f R_p + \vec{k}_f \cdot \vec{R}_p)\right\}, \quad (6)$$

where  $\alpha_3 = \frac{(Z_p-1)(Z_T-1)}{v_f}$  and  $\vec{k}_f$  is the final wave vector.  $\psi_i^+$ , the Coulomb continuum wavefunction in the entrance channel, is given by

$$\psi_i^+ = e^{\frac{\pi}{2}(\alpha_1 - \alpha_2)} \Gamma(1-i\alpha_1) \Gamma(1+i\alpha_2) e^{i\vec{k}_i \cdot \vec{R}_T} {}_1F_1\left\{i\alpha_1; 1; i(v_i s_1 + \vec{v}_i \cdot \vec{s}_1)\right\} {}_1F_1\left\{-i\alpha_2; 1; i(k_i R_p + \vec{k}_i \cdot \vec{R}_p)\right\} \varphi_i(\vec{x}_1, \vec{x}_2), \quad (7)$$

where  $\alpha_1 = \frac{Z_p}{v_i}$ ,  $\alpha_2 = \frac{Z_T(Z_p-1)}{v_i}$ .

It is well known [36,37] that the post form of the BCCIS-4B method is suitable for asymmetric collision ( $Z_P > Z_T$ ) and for symmetric collisions, either form of the transition matrix element may be used.

The transition amplitude in the prior and post forms for single capture in the BCCIS-4B method may be written as

$$\begin{aligned} T_{if}^{(-)} = N \iiint d\vec{x}_1 d\vec{x}_2 d\vec{R} e^{-i\vec{k}_f \cdot \vec{R}_P + i\vec{k}_i \cdot \vec{R}_T} \varphi_f^*(\vec{x}_2, \vec{s}_1) {}_1F_1\{i\alpha_1; 1; i(v_f x_1 + \vec{v}_f \cdot \vec{x}_1)\} \times \\ {}_1F_1\{-i\alpha_2; 1; i(\vec{k}_f \cdot \vec{R}_T + \vec{k}_f \cdot \vec{R})\} \left( \frac{Z_P Z_T}{R} - \frac{Z_P}{s_1} - \frac{Z_P}{s_2} \right) \varphi_i(\vec{x}_1, \vec{x}_2), \end{aligned} \quad (8)$$

where  $N = e^{\frac{\pi}{2}(\alpha_1 - \alpha_2)} \Gamma(1 - i\alpha_1) \Gamma(1 + i\alpha_2)$ ,  $\alpha_1 = \frac{Z_T - 1}{v_f}$  and  $\alpha_2 = \frac{Z_P(Z_T - 1)}{v_f}$

$$\begin{aligned} \text{and } T_{if}^{(+)} = N \iiint d\vec{x}_1 d\vec{x}_2 d\vec{R} e^{-i\vec{k}_f \cdot \vec{R}_P + i\vec{k}_i \cdot \vec{R}_T} \varphi_f^*(\vec{x}_2, \vec{s}_1) {}_1F_1\{i\alpha_1; 1; i(v_i s_1 + \vec{v}_i \cdot \vec{s}_1)\} \times \\ {}_1F_1\{-i\alpha_2; 1; i(\vec{k}_i \cdot \vec{R} - \vec{k}_i \cdot \vec{R})\} \left\{ Z_T \left( \frac{1}{R} - \frac{1}{x_1} \right) + Z_P \left( \frac{1}{R} - \frac{1}{s_2} \right) + \left( \frac{1}{r_{12}} - \frac{1}{R} \right) \right\} \times \\ {}_1F_1\{-i\alpha_3; 1; i(\vec{k}_f \cdot \vec{R} + \vec{k}_f \cdot \vec{R})\} \varphi_i(\vec{x}_1, \vec{x}_2), \end{aligned} \quad (9)$$

where  $N = e^{\frac{\pi}{2}(\alpha_1 - \alpha_2 - \alpha_3)} \Gamma(1 - i\alpha_1) \Gamma(1 + i\alpha_2) \Gamma(1 + i\alpha_3)$ ,  $\alpha_1 = \frac{Z_P}{v_i}$ ,  $\alpha_2 = \frac{Z_T(Z_P - 1)}{v_i}$ ,

and  $\alpha_3 = \frac{(Z_P - 1)(Z_T - 1)}{R_P}$ .

Using integral representation  ${}_1F_1(i\alpha; 1; z) = \frac{1}{2\pi i} \oint dt (t-1)^{-i\alpha} t^{i\alpha-1} e^{zt}$ , the transition amplitude of

equations (8) and (9) may be written as

$$T_{if}^{(-)} = \frac{AN}{(2\pi i)^2} \ell \lim_{\varepsilon_1, \lambda_2 \rightarrow 0} D(\delta_1, \gamma_2, \lambda_1, \lambda_2, \varepsilon_1) \oint dt_1 t_1^{i\alpha_1-1} (t_1-1)^{-i\alpha_1} \oint dt_2 t_2^{-i\alpha_2-1} (t_2-1)^{i\alpha_2} J \quad (10)$$

$$\text{where } J = \iiint d\vec{x}_1 d\vec{x}_2 d\vec{R} e^{i\vec{k}_i \cdot \vec{R}_T - i\vec{k}_f \cdot \vec{R}_P + i\vec{v}_f \cdot \vec{x}_1 t_1 + i\vec{b}\vec{k}_f \cdot \vec{R} t_2} \frac{e^{-\beta_1 x_1}}{x_1} \cdot \frac{e^{-\beta_2 x_2}}{x_2} \cdot \frac{e^{-\lambda_1 s_1}}{s_1} \cdot \frac{e^{-\lambda_2 s_2}}{s_2} \cdot \frac{e^{-\varepsilon R}}{R}, \quad (11)$$

$$\beta_1 = \delta_1 - i v_f t_1, \beta_2 = \delta_1 + \gamma_2 \text{ and } \varepsilon = \varepsilon_1 - i \vec{b} \cdot \vec{k}_f t_2.$$

$$\text{and } T_{if}^{(+)} = \frac{NA}{(2\pi i)^3} \ell \lim_{\lambda_2, \varepsilon_1 \rightarrow 0} D(\delta_1, \gamma_2, \lambda_1, \lambda_2, \varepsilon_1) \oint dt_1 (t_1-1)^{-i\alpha_1} t_1^{i\alpha_1-1} \oint dt_2 (t_2-1)^{i\alpha_2} t_2^{-i\alpha_2-1} \times$$

$$\oint dt_3 (t_3-1)^{i\alpha_3} t_3^{-i\alpha_3-1}, \quad (12)$$

$$\text{where } J = \iiint d\vec{x}_1 d\vec{x}_2 d\vec{R} e^{i\vec{k}_i \cdot \vec{R}_T - i\vec{k}_f \cdot \vec{R}_P + i\vec{v}_f \cdot \vec{x}_1 t_1 + i\vec{b}\vec{k}_f \cdot \vec{R} t_2} \frac{e^{-\beta_1 x_1}}{x_1} \cdot \frac{e^{-\beta_2 x_2}}{x_2} \cdot \frac{e^{-\lambda_1 s_1}}{s_1} \cdot \frac{e^{-\lambda_2 r_{12}}}{r_{12}} \cdot \frac{e^{-\varepsilon R}}{R}, \quad (13)$$

$$\beta_1 = \delta_1, \beta_2 = \delta_1 + \gamma_2 \text{ and } \varepsilon = \varepsilon_1 - i \vec{k}_i t_2 - i \vec{k}_f t_3.$$

Here the constant A originates from the initial and final bound state wave functions.  $D(\delta_1, \gamma_2, \lambda_1, \lambda_2, \varepsilon_1)$  is a parametric differential operator used to generate the excited state wave functions.  $\delta_1, \gamma_2$  and  $\lambda_1$  are the orbital component of the initial and final bound state wave functions. To obtain the perturbation potential term  $\frac{1}{s_2}$  in the final channel, the term  $\frac{e^{-\lambda_2 r_{12}}}{r_{12}}$  in equation (13) is replaced by  $\frac{e^{-\lambda_2 s_2}}{s_2}$  and the parametric differential operator  $D(\delta_1, \gamma_2, \lambda_1, \lambda_2, \varepsilon_1)$  should be changed accordingly.

Using the techniques of Fourier transform, Feynman parametric integral and the integral representation of three denominator integral of Lewis [38], equation (11) or (13) may be reduced following Sinha and Sil [39] as

$$J = 32\pi^3 \int_0^1 \frac{dx}{\Delta} \int_0^\infty \frac{dy}{A + Bt_1 + Ct_2 + Dt_1t_2} \quad (14)$$

where  $\Delta^2 = \left\{ (1-a)\bar{k}_f - \frac{\bar{k}_i}{2 + M_T} \right\}^2 (1-x) + \beta_2^2 x + \lambda_2^2 (1-x)$  for post form

and  $\Delta^2 = \left\{ \frac{\bar{k}_i}{2 + M_T} \right\}^2 (1-x) + \beta_2^2 x + \lambda_2^2 (1-x)$  for prior form.

So the transition matrix element given by the equation (10) and (12) may be reduced as

$$T_{if}^{(-)} = 32\pi^3 A N \ell \lim_{\varepsilon_1, \lambda_2 \rightarrow 0} D(\delta_1, \gamma_2, \lambda_1, \lambda_2, \varepsilon_1) \int_0^1 \frac{dx}{\Delta} \int_0^\infty dy K \quad (15)$$

$$\text{and } T_{if}^{(+)} = 32\pi^3 \frac{AN}{(2\pi i)} \oint dt_3 t_3^{-i\alpha_3-1} (t_3-1)^{i\alpha_3} \ell \lim_{\varepsilon_1, \lambda_2 \rightarrow 0} D(\delta_1, \gamma_2, \lambda_1, \lambda_2, \varepsilon_1) \int_0^1 \frac{dx}{\Delta} \int_0^\infty dy K, \quad (16)$$

where  $K = A^{i\alpha_1-i\alpha_2-1} (A+B)^{-i\alpha_1} (A+C)^{-i\alpha_2} {}_2F_1(i\alpha_1; -i\alpha_2; 1; z)$  and  $z = \frac{BC-AD}{(A+B)(A+C)}$ .

The prior form of the transition amplitude contains two-dimensional integrals such as Lewis and Feynman, but the post form of the transition amplitude contains three-dimensional integrals such as Lewis, Feynman and a complex contour integration. The complex contour integration is changed into real integral from 0 to 1 which has been subdivided into several parts and each subdivision is integrated using Gauss-Laguerre quadrature method. The Lewis and Feynman integrals have been performed numerically by the Gauss-Legendre quadrature method. Finally single-electron capture cross sections are obtained numerically over scattering angles with the Gauss Legendre quadrature method. Convergence has been tested with an accuracy of 0.1%.

### 3.3. RESULTS AND DISCUSSION

Total single electron transfer cross sections have been obtained by summing over all contributions from individual shells and sub-shell upto  $n=3$  since the results have been found to converge within 8%. Variation of single-electron capture cross sections in collisions of different projectile ions with helium atoms in the energy range 50-5000 keV/amu are plotted in Figs. 1-6 respectively using both prior and post forms of BCCIS-4B approximation. Post-prior discrepancy has been found to be less than 30% except for  $\text{Li}^+ + \text{He}$  interaction below 150 keV/amu. However, numerical results for the sub-shell distribution of the total single charge transfer cross sections may be obtained on request.

#### A. Symmetric collision

In Fig.1, we have displayed the present results both in post and prior form for symmetric collisions of  $\text{He}^{2+} - \text{He}$  as a function of incident projectile energy from 100 to 5000 keV. Our computed results are compared with the measurements of Shah and Gilbody [24], Shah et al [25], de Castro et al [26], DuBois [27], and the theoretical results of Mancev [11,13,14], and Dunseath and Crothers [16]. The present results have good agreement with the experimental results of de Castro et al [26] below 2000 keV. It is also evident that the present computed results agree well with the experimental results of Shah and Gilbody [24] and DuBois [27] above 300 keV. CDW-4B results of Mancev [11] are in fair agreement with the experimental results at high energies but large variation is observed at low energies. This is expected because CDW approximation may not be accurate at lower energies. It is also observed that the present computed results agree well with the theoretical results of Dunseath and Crothers [16] using the prior form of CDW-IEM approximation using hydrogenic wavefunctions (HCDW), but agreement is not satisfactory with the same method using Pluvinage wavefunctions (PCDW) in the whole energy range. The BDW results of Mancev [13] underestimate the experimental results in the high energy region, which have almost similar energy variation of cross sections with the CDW-4B results. However, the results obtained in the CB1-4B method by Mancev and Milojevic [14] have good agreement with the experimental findings [24-27] between 150 and 5000 keV. However, they have calculated the total single electron capture cross section by

multiplying a scaling factor (1.202) with ground state capture cross section in order to include the contribution from higher excited states. We have observed that the ground state capture is dominant. This is expected because of the energy resonance and velocity matching of the active electron in the initial and final state. However, it is evident from Fig.1 that the present results obtained using post form has superiority over the results from prior form in connection with their comparison with experimental observations. This may be due to the fact that dynamic electron correlation with certain approximation has been included in the post form where static electron correlation has been highly simplified in prior form due to the use of helium wavefunction in the independent particle model with frozen core approximation.

## **B. Asymmetric collision**

In Fig. 2, we compare our theoretical results in both forms of transition amplitude for  $\text{Li}^{3+}$ - He collision together with a number of theoretical [8,12,17] and experimental results [24,28-30]. The present results are seen to be in good agreement with all the measurements above 150 keV/amu. However, the present results in post form have good agreement with the experimental findings of Shah and Gilbody [24] below 150 keV/amu as well. The reason may be due to inclusion of continuum interaction of the active electron with the projectile ion of higher charge together with the reasons mentioned earlier. It is also observed that the CDW-4B results of Mancev [12] underestimate the experimental results [24, 28-30] as well as present theoretical results in the whole energy region. The results of Belkic [17] in the prior and post form of the CB1 method using the independent particle model and the Roothan-Hartee-Fock target screening have very good agreement with the present results in the energy range 50 keV/amu to 1000 keV/amu. However the results of Sidorovich et al [8] overestimate the present findings at high energies. We have also found that ground state capture cross sections are competitive with those from the excited states due to the reasons cited above. Our results for  $\text{Li}^{2+}$ - He collision in the energy range from 50 to 5000 keV/amu are depicted in Fig.3. Present computed results in post form are in good agreement with the measurements of Voitke et al [30] and the theoretical results of Mancev [18] in the whole energy range. In this case the ground state capture cross sections dominate over other states. Here we have used the binding energy screening for the partially stripped projectile ions. Due to non-availability of any theoretical data for  $\text{Li}^{+}$ -

Hecollision, the present results in both forms have been compared with the experimental results of Voitke et al [30] shown in Fig.4. The present results in prior form are not satisfactory in the energy range below 500 keV/amu. Further the present results in post form have good agreement with the experimental results of Voitke et al [30] down to 200 keV/amu. However the post-prior discrepancy below 150 keV/amu is very high. This may be due to exclusion of many body effects in our formulation in such low energy region. Total cross sections for single-electron capture for  $C^{6+}$ -He collision is shown in Fig.5. The present data in both forms are compared with other available measurements [31,32] and theoretical data [9,19,20]. The agreement of the present cross sections with the results of Classical Trajectory Monte Carlo (CTMC) [19] and the two-center Atomic-orbital expansion [9] results are satisfactory in the whole energy range. However the results of Unitarized distorted-wave approximation (UDWA) [20] are higher than the present results at 400 keV/amu and 700 keV/amu respectively. Further the present results are in good agreement with the experimental results [31,32]. In such case the post-prior discrepancy is less than 10%. For  $O^{8+}$ -He collision, present computed results in both forms are presented in graphical form in Fig.6. We have compared our theoretical results with a number of experimental results [31-35] and theoretical results [9,19,20]. It is evident that the present results show good agreement with other theoretical results [19,20] below 3000 keV/amu. The present computed results are found to be in agreement with the available experimental findings [31,32]. However the experimental results of Afrosimov et al [33] underestimate the present results below 1000 keV/amu to a fair extent. In this case as well the post-prior discrepancy is less than 10%.

### 3.4. CONCLUSIONS

The four-body boundary corrected continuum intermediate state (BCCIS-4B) approximation previously employed for double electron capture has been extended to the case of single-electron capture at intermediate and high energy collision. The results so obtained are reasonably encouraging over the entire range of energy. This may be due to the fact that: (i) the continuum state of the active electron with the stronger charge has been taken into account; (ii) the scattering wavefunction satisfies the boundary condition; and (iii) the transition potential is faster falling than the coulomb potential. Electron correlation effect has been underestimated in our formalism. However, for single-electron capture process in an asymmetric collision ( $Z_P > Z_T$ )

in a multi-electron environment, the accurate study of correlation effect is important to test the validity of the BCCIS-4B approximation.

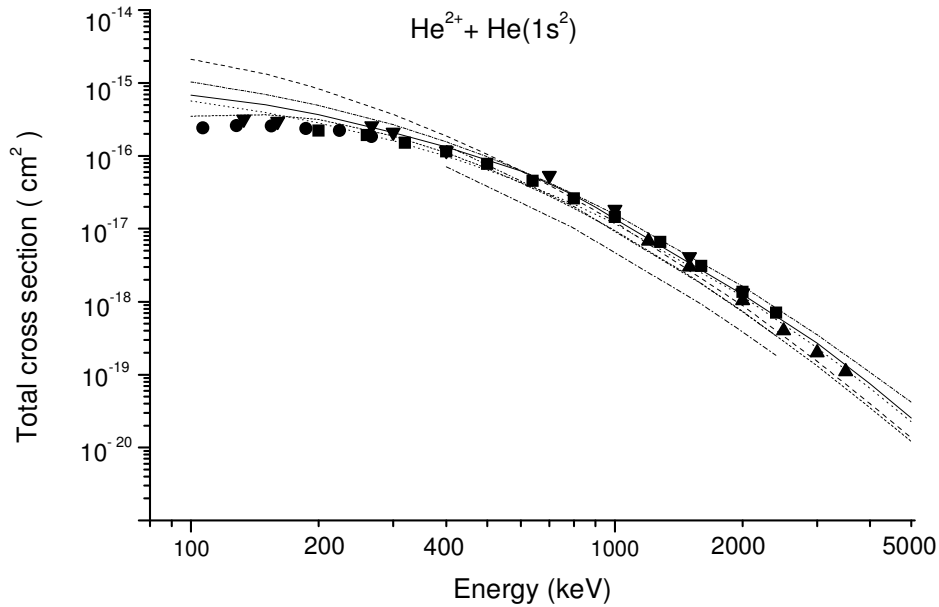


FIG. 1. Total cross sections (in  $\text{cm}^2$ ) as a function of the incident energy  $E$  (keV) for reaction  $\text{He}^{2+} + \text{He}(1s^2) \rightarrow \text{He}^+ + \text{He}^+$ .

Theory: solid line, present results (post form of BCCIS-4B); short dash-dotted line, present results (prior form of BCCIS-4B); dashed line, CDW-4B results of Mancev [11]; dotted line, CB1-4B results of Mancev and Milojevic [14]; dash-dotted line, PCDW results of Dunseath and Crothers [16]; dash-dot-dotted line, HCDW results of Dunseath and Crothers [16]; dense dotted line, BDW results of Mancev [13].

Experiments: ■, results of Shah and Gilbody [24]; ●, results of Shah et al [25]; ▲, results of de Castro et al [26]; ▼, results of DuBois [27]

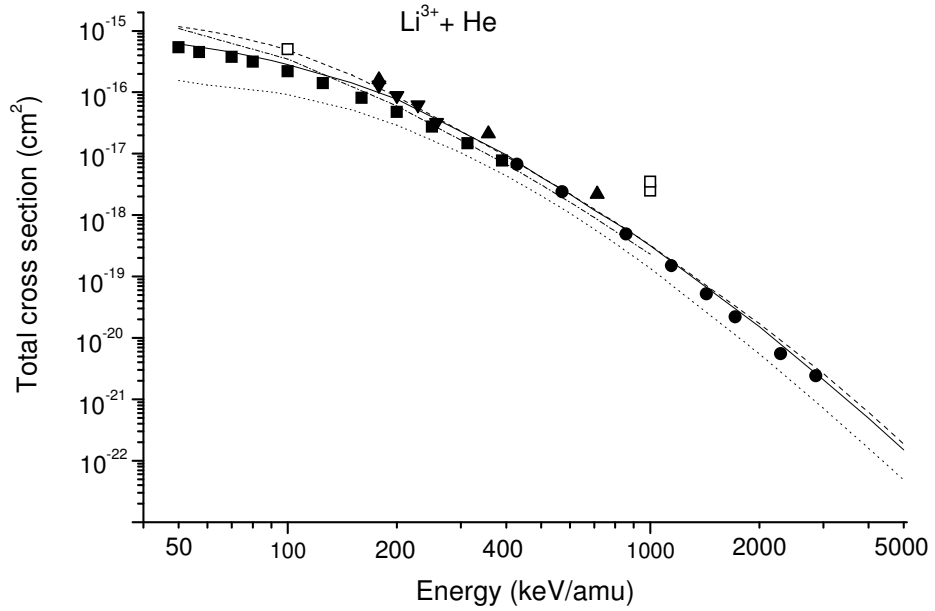


FIG. 2. Total cross sections (in  $\text{cm}^2$ ) as a function of the incident energy  $E$  (keV/amu) for reaction  $\text{Li}^{3+} + \text{He}(1s^2) \rightarrow \text{Li}^{2+} + \text{He}^+$ .

Theory: solid line, present results (post form of BCCIS-4B); dashed line, present results (prior form of BCCIS-4B); dotted line, CDW-4B results of Mancev [12]; dash-dotted line, CB1 results of Belkic [17];  $\square$ , IEA results of Sidorovich et al [8].

Experiments:  $\blacksquare$ , results of Shah and Gilbody [24];  $\bullet$ , results of Voitke et al [30];  $\blacktriangle$ , results of Nikolaev et al [28];  $\blacktriangledown$ , results of Pivovar et al [29].

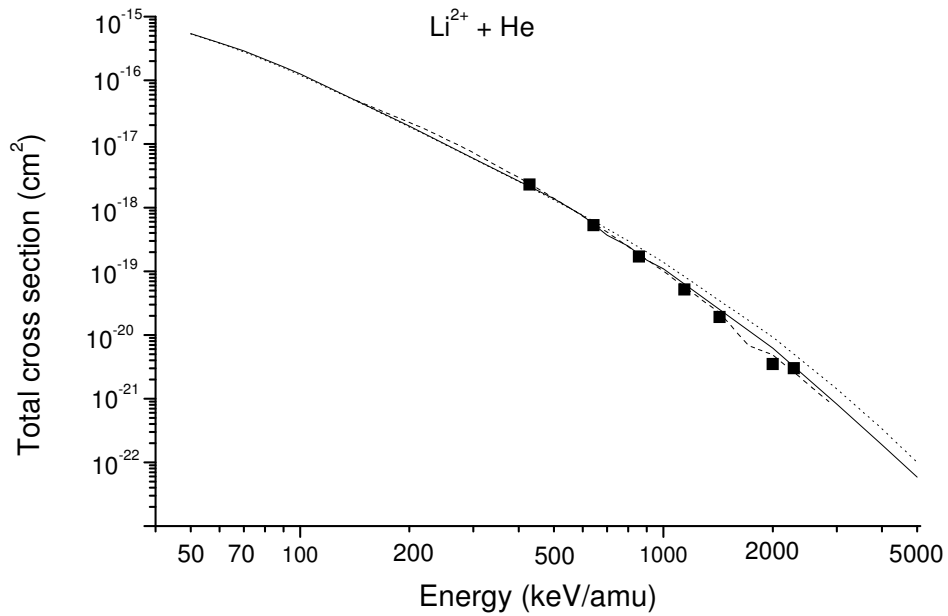


FIG. 3. Total cross sections (in  $\text{cm}^2$ ) as a function of the incident energy  $E$  (keV/amu) for reaction  $\text{Li}^{2+} + \text{He}(1s^2) \rightarrow \text{Li}^+ + \text{He}^+$ .

Theory: solid line, present results (post form of BCCIS-4B); dotted line, present results (prior form of BCCIS-4B); dashed line, CDW-4B results of Mancev [18].

Experiment: ■, results of Voitke et al [30].

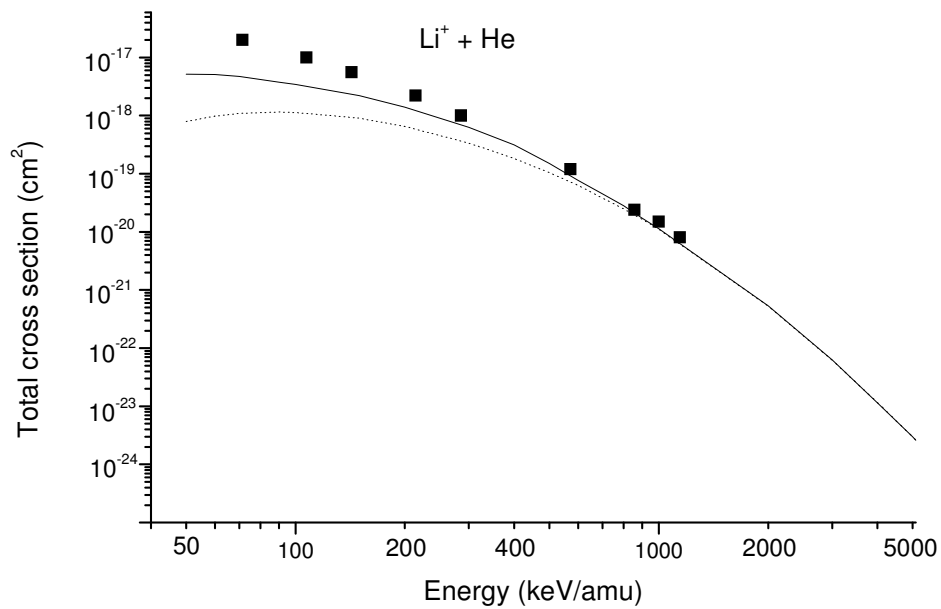


FIG. 4. Total cross sections (in  $\text{cm}^2$ ) as a function of the incident energy  $E$  (keV/amu) for reaction  $\text{Li}^+ + \text{He}(1s^2) \rightarrow \text{Li} + \text{He}^+$ .

Theory: solid line, present results (Post form of BCCIS-4B); dotted line, present results (Prior form of BCCIS-4B).

Experiment: ■, results of Voitke et al [30].

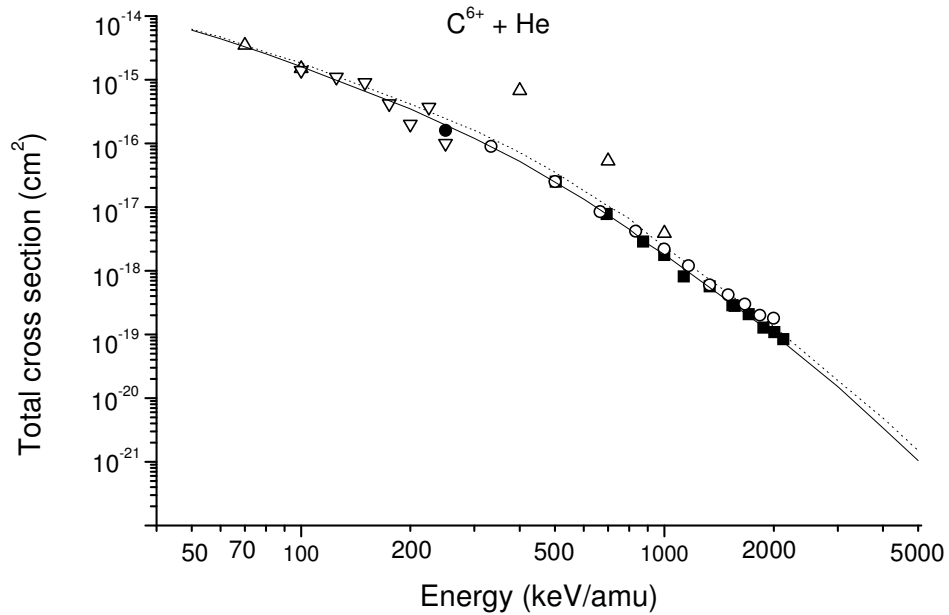


FIG. 5. Total cross sections (in  $cm^2$ ) as a function of the incident energy  $E$  (keV/amu) for reaction  $C^{6+} + He(1s^2) \rightarrow C^{5+} + He^+$ .

Theory: solid line, present results (post form of BCCIS-4B); dashed line, present results (prior form of BCCIS-4B);  $\circ$ , Atomic-orbital expansion results of Jain et al [9];  $\Delta$ , UDWA results of Suzuki et al [20];  $\nabla$ , CTMC results of Olson [19].

Experiments:  $\blacksquare$ , results of Dillingham et al [31];  $\bullet$ , results of Guffey et al [32].

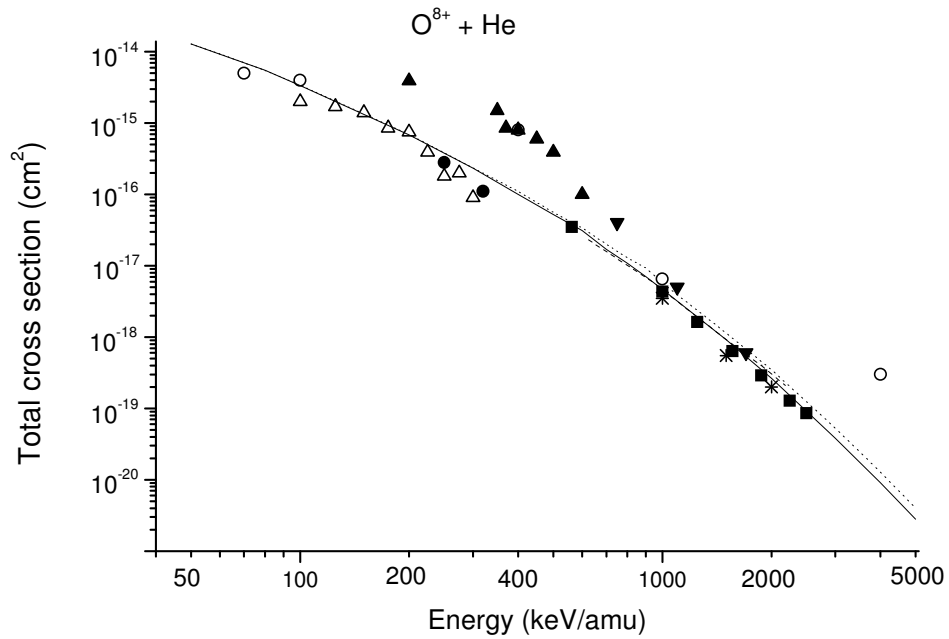


FIG. 6. Total cross sections (in  $cm^2$ ) as a function of the incident energy  $E$  (keV/amu) for reaction  $O^{8+} + He(1s^2) \rightarrow O^{7+} + He^+$ .

Theory: solid line, present results (post form of BCCIS-4B); dotted line, present results (prior form of BCCIS-4B); dashed line, atomic-orbital results of Jain et al [9];  $\circ$ , UDWA results of Suzuki et al [20];  $\Delta$ , CTMC results of Olson [19].

Experiments:  $\blacksquare$ , results of Dillingham et al [31];  $\bullet$ , results of Guffey et al [32];  $\blacktriangledown$ , results of Macdonald and Martin [34];  $\blacktriangle$ , results of Afrosimov et al [33];  $*$ , results of Hippler et al [35].

## REFERENCES

- [1] H. P. Summers, *Comm. At. Mol. Phys.* **21**, 277 (1988).
- [2] D. P. Dewangan and J. Eichler, *J. Phys. B* **19**, 2939 (1986).
- [3] D. P. Dewangan and J. Eichler, *Comm. At. Mol. Phys.* **21**, 1 (1987); **27**, 317 (1992).
- [4] D. P. Dewangan and J. Eichler, *Phys. Rep.* **247**, 59 (1994).
- [5] B. H. Bransden and M. R. C. McDowell, *Charge Exchange and the Theory of Ion-Atom Collisions* (Clarendon Press, Oxford, 1992).
- [6] J. McGuire, *Electron Correlation Dynamics in Atomic Collisions* (Cambridge University Press, Cambridge, 1997).
- [7] Dz. Belkic, *Quantum Theory of High Energy Ion-Atom Collisions* (Taylor & Francis, London, 2009).
- [8] V. A. Sidorovich, V. S. Nikolaev, and J. H. McGuire, *Phys. Rev. A* **31**, 2193 (1985).
- [9] A. Jain, C. D. Lin, and W. Fritsch, *Phys. Rev. A* **34**, 3676 (1986).
- [10] Dz. Belkic, R. Gayet, J. Hanssen, I. Mancev and A. Nunez, *Phys. Rev. A* **56**, 3675 (1997).
- [11] I. Mancev, *Phys. Rev. A* **60**, 351 (1999).
- [12] I. Mancev, *Phys. Rev. A* **64**, 012708 (2001).
- [13] I. Mancev, *J. Phys. B* **36**, 93 (2003).
- [14] I. Mancev and N. Milojevic, *Phys. Rev. A* **81**, 022710 (2010).
- [15] Dz. Belkic, I. Mancev, and J. Hanssen, *Rev. Mod. Phys.* **80**, 249 (2008).

- [16] K. M. Dunseath and D. S. F Crothers, *J. Phys. B* **24**, 5003 (1991).
- [17] Dz. Belkic, *Phys. Scr.* **40**, 610 (1989).
- [18] I. Mancev, *Phys. Rev. A* **75**, 052716 (2007).
- [19] R. E. Olson, *Phys. Rev. A* **18**, 2464 (1978).
- [20] H. Suzuki, Y. Kajikawa, N. Toshima, H. Ryufuku, and T. Watanabe, *Phys. Rev. A* **29**, 525 (1984).
- [21] F. Martin and A. Salin, *Phys. Rev. Lett.* **76**, 1437 (1996).
- [22] F. Martin and A. Salin, *Phys. Rev. A* **54**, 3990 (1996); **55**, 2004 (1997).
- [23] C. Diaz, F. Martin, and A. Salin, *J. Phys. B* **33**, 4373 (2000).
- [24] M. B. Shah and H. B. Gilbody, *J. Phys. B* **18**, 899 (1985).
- [25] M. B. Shah, P. McCallion, and H. B. Gilbody, *J. Phys. B* **22**, 3037 (1989).
- [26] N. V. de Castro Faria, F. L. Freire, Jr., and A. G. de Pinho, *Phys. Rev. A* **37**, 280 (1988).
- [27] R. D. DuBois, *Phys. Rev. A* **36**, 2585 (1987).
- [28] V. S. Nikolaev, I. S. Dmitriev, L. N. Fateeva, and Yu. A. Teplova, *Sov. Phys.-JETP* **13**, 695 (1961) [*Zh. Eksp. Teor. Fiz.* **40**, 989 (1961)].
- [29] L. I. Pivovarov, Yu. Z. Levchenko, and G. A. Krivonosov, *Sov. Phys.-JETP* **32**, 11 (1971) [*Zh. Eksp. Teor. Fiz.* **59**, 19 (1970)].
- [30] O. Voitke, P. A. Zavodszky, S. M. Ferguson, J. H. Houck, and J. A. Tanis, *Phys. Rev. A* **57**, 2692 (1998).
- [31] T. R. Dillingham, J. R. Macdonald, and Patrick Richard, *Phys. Rev. A* **24**, 1237 (1981).

- [32] J. A. Guffey, L. D. Ellsworth, and J. R. Macdonald, *Phys. Rev. A* **15**, 1963 (1977).
- [33] V. V. Afrosimov, A. A. Basalaev, E. D. Donets, K. O. Lozhkin, and M. N. Panov, *Abstracts of the Twelfth International Conference on the Physics of Electronic and atomic Collisions, Gatlinburg, Tennessee*, edited by S. Datz (North-Holland, Amsterdam), p. 690 (1981).
- [34] R. Macdonald and F. W. Martin *Phys. Rev. A* **4**, 1965 (1971).
- [35] R. Hippler, S. Datz, P. D. Miller, P. L. Pepmiller, and P. F. Dittner, *Phys. Rev. A* **35**, 585 (1987).
- [36] M. Purkait, S. Sounda, A. Dhara, and C. R. Mandal, *Phys. Rev. A* **74**, 042723 (2006).
- [37] S. Ghosh, A. Dhara, C. R. Mandal, and M. Purkait, *Phys. Rev. A* **78**, 042708 (2008).
- [38] R. R. Lewis, *Phys. Rev.* **102**, 537 (1956).
- [39] C. Sinha and N. C. Sil, *J. Phys. B* **11**, L333 (1978).

## CHAPTER- 4

# ELECTRON CAPTURE BY FAST PROTONS FROM HELIUM LIKE IONS

## 4.1. INTRODUCTION

Ion-atom/ion collisions and in particular electron transfer processes have been investigated intensely over many years. This research is not only motivated by the quest for a better understanding of the fundamental few-body dynamics, but also it has practical implications to applied fields, such as plasma physics and fusion research. For a long time, theoretical and experimental efforts have been concentrated on the energy dependence of total cross sections (TCSs). Charge transfer cross sections in collisions of fully stripped projectiles with hydrogen like ion have been studied in the framework of different three-body models viz the continuum distorted wave (CDW) approximation [1], Basic Generator method (BGM) [2-4], Lattice time-dependent Schrödinger equation (LTDSE) and the atomic orbital close coupling (AOCC) method [5] and the boundary corrected continuum intermediate state (BCCIS) approximation [6]. However, theoretical calculations based on four-body models are more detailed and exhaustive in nature. Such investigations in collisions of fully stripped projectile ions with helium-like ions include the Coulomb-Born (CB) and a modified Coulomb-Born (MCB) approximation of Sinha et al [7], the CDW approximation with independent-event model of Dunseath and Crothers [8], CDW-4B method of Belkic et al [9] and Mancev [10,11], second order Born distorted wave (BDW) method [12,13], continuum distorted wave-Born initial state (CDW-BIS) and Born final state (BFS) method of Mancev [14,15], continuum distorted-wave eikonal-initial state (CDW-EIS) method of Pedlow et al [16], the boundary-corrected first Born approximation (CB1-4B) of Mancev and Milojevic [17] and recently, the four-body formalism of boundary corrected continuum intermediate state (BCCIS-4B) approximation by Samanta et al [18]. In the present theoretical investigation, we have mainly focused our attention to determine the single-electron capture cross sections from helium like ion by the impact of proton in the incident energy range between 30 and 1000 keV.

Working within the framework of four-body distorted wave formalism, various approximations can be obtained by choosing different distortion potentials and distorted-wave functions in the entrance and exit channels. Sinha et al [7] calculated the electron-capture from the helium like ions ( $\text{Li}^+$ ,  $\text{Be}^{2+}$ ,  $\text{B}^{3+}$ ,  $\text{C}^{4+}$  and  $\text{O}^{6+}$ ) by the impact of protons using the four-body formalism of Coulomb-Born (CB) approximation in prior and post form in the energy range 20-

1000 keV. The calculations show that, there are substantial disagreement with the existing experimental results for p-Li<sup>+</sup>(1s) collision. Total cross sections for single-electron transfer from helium like atomic systems by bare projectiles have been studied by Mancev [10] in the framework of CDW-4B approximation in the energy range of 50 keV to 10,000 keV. Total cross sections are compared with the available experimental data. Computed results underestimate the available experimental findings for p-Li<sup>+</sup> collision. The problem of single charge transfer in collisions of H<sup>+</sup> ions with Li<sup>+</sup> target ions has been investigated by Mancev [14] in the framework of CDW-BIS and CDW-BFS approximations in the energy range of 50-2000 keV/amu. It has been found that the CDW-BIS approximation overestimates the available experimental results at low energy region whereas the CDW-BFS results underestimate the same. At higher impact energies both approximations have yielded nearly identical cross sections. In this context, we are motivated to study the single-charge transfer cross sections for p-Li<sup>+</sup> collision in the energy range of 30-1000 keV. Based on the success of BCCIS approximation in ion-atom collisions in the framework of 4-body [18-20] formalism and ion-ion collision in the framework of three-body formalism [6], we have studied the above mentioned process in the framework of BCCIS-4B theory.

The organization of this paper is as follows. Theoretical formulation has been described in Sec. II. Results and discussion are presented in Sec. III. Finally, in Sec. IV conclusions are given. Atomic units have been used throughout.

## 4.2. THEORY

Single-electron capture from helium like ions (Li<sup>+</sup>, Be<sup>2+</sup>, B<sup>3+</sup>) by the impact of proton may be written as  $Z_P + (Z_T, e_1, e_2)_i \rightarrow (Z_P, e_1)_{f_1} + (Z_T, e_2)_{f_2}$  ,

$$(1)$$

where  $Z_P$ ,  $Z_T$  are the projectile (P) and target (T) charges, respectively. The total Hamiltonian for the collision system may be written as

$$H = H_i + V_i = H_f + V_f ,$$

$$(2)$$

where  $H_i$  ( $H_f$ ) represents the entrance (exit) channel Hamiltonian and  $V_i$  ( $V_f$ ) is the corresponding perturbation potentials respectively. Here  $H_i$  ( $H_f$ ) and  $V_i$  ( $V_f$ ) may be written as

$$H_i = -\frac{1}{2\mu_i} \nabla_{R_T}^2 + \frac{Z_P(Z_T-2)}{R_T} - \frac{1}{2a} \nabla_{x_1}^2 - \frac{1}{2a} \nabla_{x_2}^2 - \frac{Z_T}{x_1} - \frac{Z_T}{x_2} + \frac{1}{r_{12}},$$

$$V_i = \frac{2Z_P}{R_T} - \frac{Z_P}{s_1} - \frac{Z_P}{s_2} \approx \frac{2Z_P}{R} - \frac{Z_P}{s_1} - \frac{Z_P}{s_2} \quad (3)$$

and

$$H_f = -\frac{1}{2\mu_f} \nabla_{R_p}^2 - \frac{1}{2a} \nabla_{x_2}^2 - \frac{Z_T}{x_2} - \frac{1}{2b} \nabla_{s_1}^2 - \frac{Z_P}{s_1},$$

$$V_f = \frac{Z_P Z_T}{R} - \frac{Z_T}{x_1} - \frac{Z_P}{s_2} + \frac{1}{r_{12}}, \quad (4)$$

$$\mu_i = \frac{M_P(2+M_T)}{(2+M_P+M_T)}, \quad \mu_f = \frac{(M_P+1)(M_T+1)}{(2+M_P+M_T)}, \quad a = \frac{M_T}{1+M_T}, \quad b = \frac{M_P}{1+M_P}.$$

Here e, T and P represent active electron, target ion and projectile ion respectively. Let  $\vec{R}$  be the position vector of the projectile ion (P) relative to the target (T) nucleus. In the entrance channel, it is convenient to introduce  $\vec{R}_T$  as the relative vector of the projectile with respect to the center of mass of  $(Z_T, e_1, e_2)_i$ . Symmetrically,  $\vec{R}_p$  be the position vector of the center of mass of  $(Z_P, e_1)_{f_1}$  relative to  $(Z_T, e_2)_{f_2}$  in the exit channel.  $\vec{s}_{1,2}$  and  $\vec{x}_{1,2}$  have been labeled as the position vectors of the electrons  $e_{1,2}$  relative to  $Z_P$  and  $Z_T$  respectively. Hence  $\vec{r}_{1,2}$  may be given by  $\vec{r}_{1,2} = |\vec{s}_1 - \vec{s}_2| = \vec{s}_{1,2} = |\vec{x}_1 - \vec{x}_2| = \vec{x}_{1,2}$ . The unperturbed channel state  $\psi_i$  may be defined by  $(H_i - E_i)\psi_i = 0$  with  $\psi_i = \varphi_i(\vec{x}_1, \vec{x}_2) e^{i\vec{k}_i \cdot \vec{R}_T}$ . Here  $\varphi_i(\vec{x}_1, \vec{x}_2)$  represents the two electron bound state wavefunction of the helium like atomic system  $(Z_T, e_1, e_2)_i$ . Here  $\vec{k}_i$  is the initial wave vector and  $E_i$  is the binding energy of the two electron target. Due to the presence of the asymptotic Coulomb repulsion, between the incoming projectile ion and the screened target

nucleus, the wavefunction in the initial channel  $\psi_i$  is distorted and the distorted wave function is given by

$$\psi_i = \varphi_i(\vec{x}_1, \vec{x}_2) \chi_i^+(\vec{R}_T) \quad (5)$$

where  $\chi_i^+(\vec{R}_T)$  is the Coulomb continuum function which satisfies the equation

$$\left( -\frac{1}{2\mu_i} \nabla_{R_T}^2 + \frac{Z_P(Z_T-2)}{R_T} - \frac{k_i^2}{2\mu_i} \right) \chi_i^+(\vec{R}_T) = 0. \quad (6)$$

The solution of the eigen value problem for  $\chi_i^+(\vec{R}_T)$  is given by

$$\chi_i^+(\vec{R}_T) = e^{-\frac{\pi}{2}a_3} \Gamma(1+i\alpha_3) e^{i\vec{k}_i \cdot \vec{R}_T} {}_1F_1\{-i\alpha_3; 1; i(\vec{k}_i R_T - \vec{k}_i \cdot \vec{R}_T)\}, \quad (7)$$

where 
$$\alpha_3 = \frac{Z_P(Z_T-2)}{v_i}.$$

It is well known [6,18-20] that the prior form of the BCCIS method is suitable for asymmetric collision ( $Z_T > Z_P$ ). However, for symmetric collisions, either form of the transition matrix element may be used. Here we have calculated the transition amplitude in prior form. The prior form of the transition amplitude in the BCCIS-4B approximation can be written as

$$T_{if}^{(-)} = \langle \psi_f^{(-)} | V_i | \psi_i \rangle \approx \langle \psi_f^{\text{BCCIS}} | V_i | \psi_i \rangle. \quad (8)$$

We write the final state wavefunction  $\psi_f^{\text{BCCIS}}$  in BCCIS-4B approximation as

$$\psi_f^{\text{BCCIS}} = e^{\frac{\pi}{2}(a_1 - a_2)} \Gamma(1+i\alpha_1) \Gamma(1-i\alpha_2) e^{i\vec{k}_f \cdot \vec{R}_P} {}_1F_1\{-i\alpha_1; 1; -i(v_f x_1 + \vec{v}_f \cdot \vec{x}_1)\} \times {}_1F_1\{i\alpha_2; 1; -ib(\vec{k}_f R_T + \vec{k}_f \cdot \vec{R}_T)\} \varphi_f(\vec{x}_2, \vec{s}_1), \quad (9)$$

where  $\alpha_1 = \frac{(Z_T - 1)}{v_f}$ ,  $\alpha_2 = \frac{Z_P(Z_T - 1)}{v_f}$ .

Here  $\varphi_f(\vec{x}_2, \vec{s}_1)$  is the final bound state wavefunction which is the product of hydrogen like wavefunctions and  $\vec{k}_f$  is the final wave vector.

The transition amplitude in the prior form for the single-electron capture in the BCCIS-4B method can be written as

$$\begin{aligned} T_{if}^{(-)} = N \iiint d\vec{x}_1 d\vec{x}_2 d\vec{R} e^{i\vec{k}_i \cdot \vec{R}_T - i\vec{k}_f \cdot \vec{R}_P} \varphi_f^*(\vec{s}_1, \vec{x}_2) {}_1F_1\{i\alpha_1; 1; i(v_f x_1 + \vec{v}_f \cdot \vec{x}_1)\} \times \\ {}_1F_1\{-i\alpha_2; 1; i\mathbf{b}(\mathbf{k}_f \mathbf{R}_T + \vec{k}_f \cdot \vec{R}_T)\} \left( \frac{2Z_P}{R} - \frac{Z_P}{s_1} - \frac{Z_P}{s_2} \right) {}_1F_1\{-i\alpha_3; 1; i(\mathbf{k}_i \mathbf{R}_T - \vec{k}_i \cdot \vec{R}_T)\} \varphi_i(\vec{x}_1, \vec{x}_2) \end{aligned} \quad (10)$$

where  $N = e^{\frac{\pi}{2}(\alpha_1 - \alpha_2 - \alpha_3)} \Gamma(1 - i\alpha_1) \Gamma(1 + i\alpha_2) \Gamma(1 + i\alpha_3)$ .

In the case of a heavy particle collision, it has been shown [21] that

$${}_1F_1\{-i\alpha_3; 1; i(\mathbf{k}_i \mathbf{R}_T - \vec{k}_i \cdot \vec{R}_T)\} \approx {}_1F_1\{-i\alpha_3; 1; i(\mathbf{k}_i \mathbf{R} - \vec{k}_i \cdot \vec{R})\}$$

and  ${}_1F_1\{-i\alpha_2; 1; i\mathbf{b}(\mathbf{k}_f \mathbf{R}_T + \vec{k}_f \cdot \vec{R}_T)\} \approx {}_1F_1\{-i\alpha_2; 1; i\mathbf{b}(\mathbf{k}_f \mathbf{R} + \vec{k}_f \cdot \vec{R})\}$ .

Using the integral representation of confluent hypergeometric function, the transition amplitude of equation (10) may be written as

$$\begin{aligned} T_{if}^{(-)} = \frac{C'N}{(2\pi i)^3} \ell \lim_{\varepsilon_1, \lambda_2 \rightarrow 0} D(\delta_1, \delta_2, \gamma_2, \varepsilon_1, \lambda_1, \lambda_2) \oint dt_1 t_1^{i\alpha_1 - 1} (t_1 - 1)^{-i\alpha_1} \oint dt_2 t_2^{-i\alpha_2 - 1} (t_2 - 1)^{i\alpha_2} \times \\ \oint dt_3 t_3^{-i\alpha_3 - 1} (t_3 - 1)^{i\alpha_3} J \end{aligned} \quad (11)$$

where J and  $D(\delta_1, \delta_2, \gamma_2, \varepsilon_1, \lambda_1, \lambda_2)$  may be written as

$$J = \iiint d\vec{x}_1 d\vec{x}_2 d\vec{R} e^{i\vec{k}_i \cdot \vec{R}_T - i\vec{k}_f \cdot \vec{R}_P + i\vec{v}_f \cdot \vec{x}_1 t_1 + i\vec{b}\vec{k}_f \cdot \vec{R} t_2 - i\vec{k}_i \cdot \vec{R} t_3} \frac{e^{-\beta_1 x_1}}{x_1} \frac{e^{-\beta_2 x_2}}{x_2} \frac{e^{-\lambda_1 s_1}}{s_1} \frac{e^{-\lambda_2 s_2}}{s_2} \frac{e^{-\varepsilon R}}{R} \quad (12)$$

$$\text{and } D(\delta_1, \delta_2, \gamma_2, \varepsilon_1, \lambda_1, \lambda_2) = \frac{\partial^4}{\partial \delta_1 \partial \delta_2 \partial \lambda_1 \partial \lambda_2} - \frac{\partial^4}{\partial \delta_1 \partial \delta_2 \partial \lambda_2 \partial \varepsilon_1} - \frac{\partial^4}{\partial \delta_1 \partial \delta_2 \partial \lambda_1 \partial \varepsilon_1}.$$

Here the constant  $C'$  originates from the initial and final bound state wavefunctions of helium like ion. The form of  $\beta_1, \beta_2, \varepsilon$  may be written respectively as,

$$\beta_1 = \delta_1 - i\vec{v}_f t_1, \beta_2 = \delta_2 + \gamma_2 \text{ and } \varepsilon = \varepsilon_1 - i\vec{b}\vec{k}_f t_2 - i\vec{k}_i t_3.$$

$D(\delta_1, \delta_2, \gamma_2, \varepsilon_1, \lambda_1, \lambda_2)$  is the appropriate parametric differential operator used to generate the wavefunctions of the excited state.  $\delta_1, \delta_2, \gamma_2$  and  $\lambda_1$  are the orbital components of the initial and final bound-state wavefunctions. Taking the Fourier transform of terms involving  $x_1, x_2, s_1, s_2$  and  $R$  and using the properties of delta function,  $J$  may be reduced to the following form

$$J = \frac{16}{\pi} \iint \frac{d\vec{Q}_1 d\vec{Q}_2}{(Q_1^2 + \lambda_1^2)(Q_2^2 + \lambda_2^2) \left\{ |\vec{Q}_1 - \vec{q}_1|^2 + \beta_1^2 \right\} \left\{ |\vec{Q}_2 - \vec{q}_2|^2 + \beta_2^2 \right\} \left\{ |\vec{Q}_1 + \vec{Q}_2 - \vec{q}|^2 + \varepsilon^2 \right\}} \quad (13)$$

$$\text{where } \vec{q}_1 = \frac{\vec{k}_i}{2 + M_T} + (1-b)\vec{k}_f - \vec{v}_f t_1, \vec{q}_2 = \frac{\vec{k}_i}{2 + M_T} + (1-a)\vec{k}_f,$$

$$\vec{q} = \vec{k}_i - \vec{b}\vec{k}_f + \vec{b}\vec{k}_f t_2 - \vec{k}_i t_3.$$

Using the Feynmann parametric integral such as  $\frac{1}{a'b'} = \int_0^1 \frac{dx}{[a'x + (1-x)b']^2}$  and applying the

Lewis integral [22], we can express the final form as

$$T_{if}^{(-)} = 32\pi^3 N C' \ell \lim_{\varepsilon_1, \lambda_2 \rightarrow 0} D(\delta_1, \delta_2, \gamma_2, \varepsilon_1, \lambda_1, \lambda_2) \cdot \frac{1}{(2\pi i)} \oint dt_1 t_1^{i a_1 - 1} (t_1 - 1)^{-i a_1} \int_0^1 \frac{dx}{\Delta} \int_0^\infty dy \cdot K, \quad (14)$$

where  $\Delta^2 = q_2^2 x(1-x) + \beta_2^2 x + \lambda_2^2 (1-x)$  and

$$K = \frac{1}{(2\pi i)^2} \oint dt_2 t_2^{-i\alpha_2-1} (t_2-1)^{i\alpha_2} \oint dt_3 t_3^{-i\alpha_3-1} (t_3-1)^{i\alpha_3} \cdot \frac{1}{A+Bt_2+Ct_3+Dt_2t_3}. \quad (15)$$

Applying Cauchy's residue theorem, the complex contour integration of equation (15) may be calculated to obtain a general term in the form

$$K = -\frac{1}{A} \left( \frac{A}{A+B} \right)^{-i\alpha_2} \left( \frac{A}{A+C} \right)^{-i\alpha_3} {}_2F_1(-i\alpha_2; -i\alpha_3; 1; z) \quad (16)$$

where 
$$z = \frac{BC-AD}{(A+B)(A+C)}.$$

Finally, the total cross section read 
$$\sigma = \frac{\mu_i \mu_f}{4\pi^2} \frac{k_f}{k_i} \left| T_{if}^{(-)} \right|^2 d\Omega \quad (17)$$

where  $d\Omega$  is the solid angle around  $\vec{k}_i$ .

The three-dimensional integral comprises Lewis, Feynman and one complex contour integration. Both the Lewis and the Feynman integrals have been evaluated numerically by the use of 64-point Gauss Legendre quadrature method. The complex contour integration is transformed into a real one dimensional integral [23] from 0 to 1 which has been sub-divided into several parts and each sub-division is integrated using 46-point Gauss-Laguerre quadrature method. Finally, integration over scattering angles has been performed with 54-point Gauss-Legendre quadrature method. Convergence has been tested with the accuracy of 0.1%.

### 4.3. RESULTS AND DISCUSSION

The variation of single-electron capture cross sections of ground state helium like ion by the impact of proton as a function of the incident projectile energy ranging from 30 to 1000 keV is shown in Figs.1-4, respectively.

In Fig.1, we have presented the calculated single-electron capture cross sections for p-Li<sup>+</sup> collision in the energy range 30-1000 keV. Our data has been compared with the measurements of Sewell et al [25] and the theoretical results of Mancev [10,14], Sinha et al [7], and Ermolaev et al [24]. The present results have excellent agreement with the experimental results of Sewell et al [25] in the whole energy range. The CDW-4B results of Mancev [10] are in fair agreement with the present results at high energies but agreement is not satisfactory in the low energy range. This is because CDW approximate may not be accurate at low energies. The results obtained in the CB method calculated by Sinha et al [7] underestimate the present findings above 40 keV. The calculated results obtained from the modified Coulomb Born (MCB) method [7] underestimate the present results in the whole energy range. The CDW-BFS results of Mancev [14] overestimate the experimental results [25] as well as present theoretical results below 150 keV, but the results of Mancev [14] in the form of the CDW-BIS method have discrepancies with the present results in the energy below 500 keV. However, the couple-state results of Ermolaev et al [24] have large variation with the present results in the whole energy range. Due to non-availability of any experimental data, the present calculated cross sections for p-Be<sup>2+</sup> collision is compared with other available theoretical results [7] in Fig.2. From this graph, it is evident that the present computed results agree favourably with the CB results of Sinha et al [7] above 200 keV energy. This is expected because the CB approximation is valid only in the high energy range. However, large variation of cross sections has been found between the present results and MCB results below 400 keV region. The cross sections for single-electron capture by fast protons from the target ions B<sup>3+</sup> and C<sup>4+</sup> are shown in Fig. 3 and Fig. 4 respectively. Both the figures have almost similar trend of energy variation of cross sections with the present BCCIS-4B results. From Figures 1-4, we observe that the peak position of cross sections shifts towards the higher projectile energies due to the higher charge state of the target ion. Same feature have been shown in our previous work of three body ion-ion collision [6]. The curves corresponding to the higher charged target ions tend to bend towards the lower energy side and this bending is more prominent for higher charge state of the target ions which was also observed in the work of Mukherjee and Sil [1]. We have found that ground-state capture is dominant for all such type of non-resonant reactions. This may be explained in terms of the near-resonance of energy and velocity matching of the active electron in the initial and final states.

#### 4.4. CONCLUSIONS

In the framework of four-body boundary corrected continuum intermediate state (BCCIS-4B) approximation, the single-electron capture cross sections in collision of proton with helium like ion ( $\text{Li}^+$ ) are well reproduced with the experimental findings in the collision energy range of 30-1000 keV. The energy dependence of the cross sections on the charge state of the target ion in four-body collision have the same trend of variation like those of ion-ion collision in three-body formalism. The reasons for such success are the following: (i) the continuum state of active electron has been taken into account properly; (ii) the boundary condition for the scattering wavefunction has also been satisfied; and (iii) the potential is faster falling than the Coulomb potential. It may be pointed out that in such a formulation, the dynamic correlation of the active electrons is absent. However more accurate experimental investigations are necessary for ion-ion interactions over a wide range of energies both for the development of refined theory and their applications in other branches of physics.

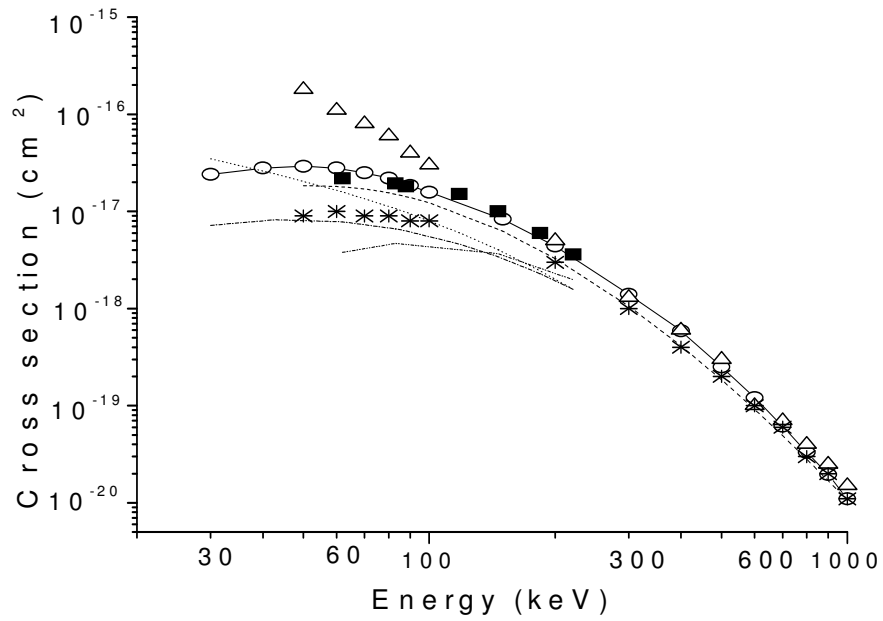


**Figure 1.** Cross sections (in  $\text{cm}^2$ ) as a function of the incident energy  $E$  (keV) for reaction  $\text{H}^+ + \text{Li}^+ \rightarrow \text{H} + \text{Li}^{2+}$ .

Theory: solid line with open circle, present results (prior form of BCCIS-4B); dashed line, CDW-4B results of Mancev [10]; dotted line, CB results (prior form) of Sinha et al [7]; dash-dotted line, MCB results of Sinha et al [7]; dash-dot-dotted line, couple-state results Ermolaev et al [24];  $\Delta$ , CDW-BFS results of Mancev [14]; \*, CDW-BIS results of Mancev [14].

Experiment:  $\blacksquare$ , results of Sewell et al [25].

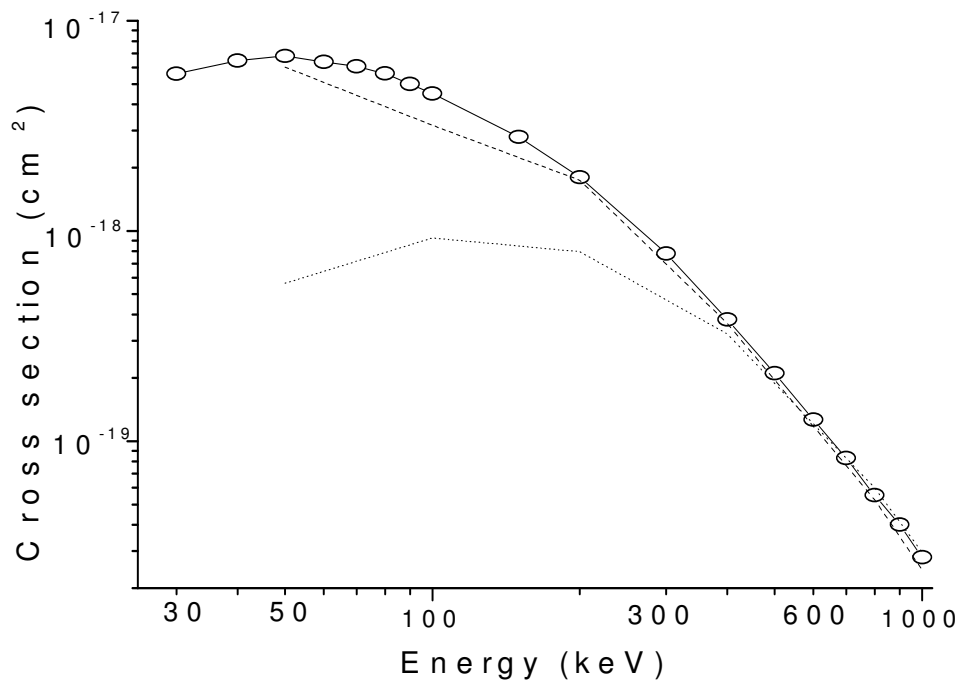


**Figure 2.** Cross sections (in  $\text{cm}^2$ ) as a function of the incident energy  $E$  (keV) for reaction  $\text{H}^+ + \text{Be}^{2+} \rightarrow \text{H} + \text{Be}^{3+}$ .

Theory: solid line with open circle, present results (prior form of BCCIS-4B); dashed line, CB results of Sinha et al [7]; dotted line, MCB results of Sinha et al [7].

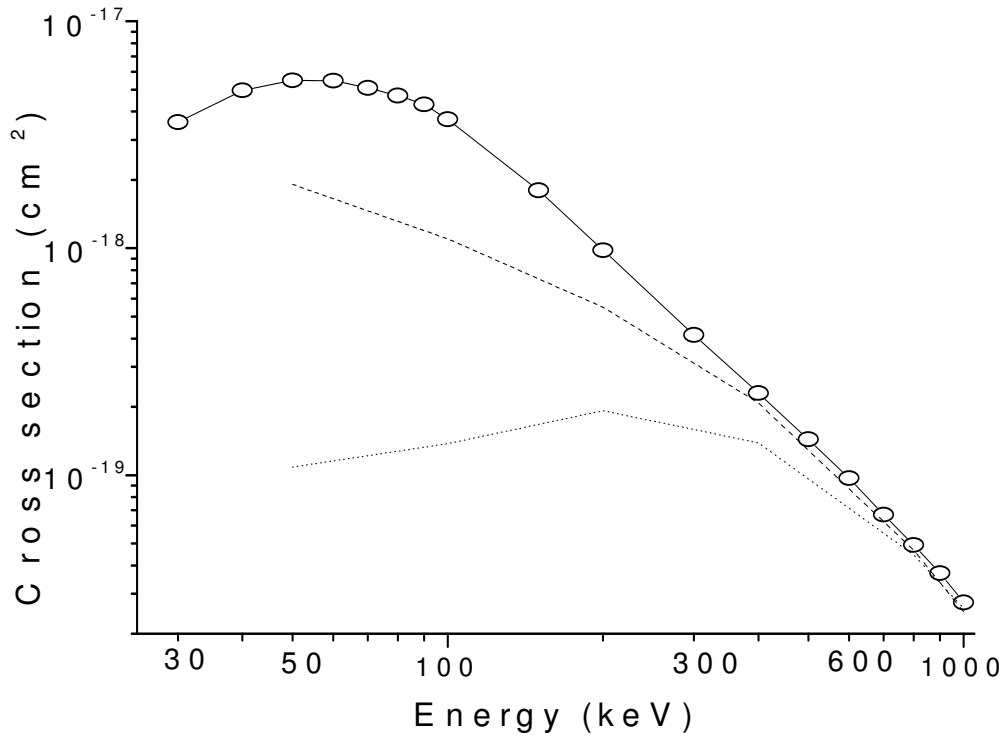


**Figure 3.** Cross sections (in  $\text{cm}^2$ ) as a function of the incident energy  $E$  (keV) for reaction  $\text{H}^+ + \text{B}^{3+} \rightarrow \text{H} + \text{B}^{4+}$ .

Theory: solid line with open circle, present results (prior form of BCCIS-4B); dashed line, CB results of Sinha et al [7]; dotted line, MCB results of Sinha et al [7].

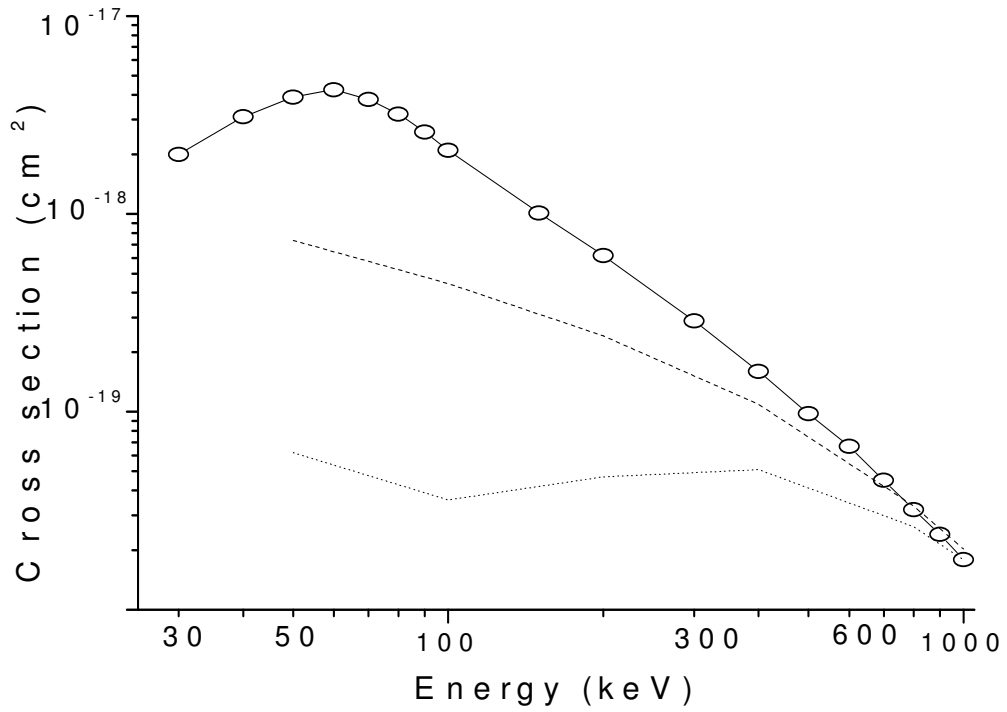


**Figure 4.** Cross sections (in  $\text{cm}^2$ ) as a function of the incident energy  $E$  (keV) for reaction  $\text{H}^+ + \text{C}^{4+} \rightarrow \text{H} + \text{C}^{5+}$ .

Theory: solid line with open circle, present results (prior form of BCCIS-4B); dashed line, CB results of Sinha et al [7]; dotted line, MCB results of Sinha et al [7].

## REFERENCES

1. S. Mukherjee and N. C. Sil, *J. Phys. B: At. Mol. Phys.* **13**, 3421 (1980).
2. T. Kirchner, M. Keim, A. Achenbach, H. J. Ludde, O. J. Kroneisen, and R. M. Dreizler, *Phys. Scr.* **T80**, 270 (1999).
3. D. Skiera, R. Trassel, K. Huber, H. Brauning, E. Salzborn, M. keim, A. Achenbach, T. Kirchner, H. J. Ludde, and R. M. Dreizler, *Phys. Scr.* **T92**, 423 (2001).
4. H. Brauning, R. Trassel, A. Theiß , A Diehl, E. Salzborn, M. Keim, A.Achenbach, H.J.Ludde, and T.Kirchner, *J. Phys. B: At. Mol. Opt. Phys.* **38**, 2311 (2005).
5. T. Minami, M. S. Pindzola, T. G. Lee, and D. R. Schultz, *J. Phys. B: At. Mol. Phys.* **40**, 3629 (2007).
6. R. Samanta, M. Purkait, and C. R. Mandal, *Phys. Scr.* **82**, 065303 (2010).
7. C. Sinha, S. Guha, P. K. Roy, and N. C. Sil, *Phys. Rev. A* **26**, 2586 (1982).
8. K. M. Dunseath and D. S. F. Crothers, *J. Phys. B* **24**, 5003 (1991).
9. Dz. Belkic, R. Gayet, J. Hanssel, I. Mancev, and A. Nunez, *Phys. Rev. A* **56**, 3675 (1997).
10. I. Mancev, *Phys. Rev. A* **60**, 351 (1999).
11. I. Mancev, *Phys. Rev. A* **64**, 012708 (2001).
12. I. Mancev, *J. Phys. B* **36**, 93 (2003).
13. I. Mancev, V. Mergel, and L. Schmidt, *J. Phys. B: At. Mol. Opt. Phys.* **36**, 2733 (2003).
14. I. Mancev, *Eur. Phys. Lett*, **69(2)**, 200 (2005).
15. I. Mancev, *J. Comp. Meth. Sci. Eng. (JCMSE)* **89**, 73 (2005).

16. R. T. Pedlow, S. F. C. O'Rourke, and D. S. F. Crothers, Phys. Rev. A **72**, 062719 (2005).
17. I. Mancev and N. Milojevic, Phys. Rev. A **81**, 022710 (2010).
18. R. Samanta, M. Purkait, and C. R. Mandal, Phys. Rev. A **83**, 032706 (2011).
19. S. Ghosh, A. Dhara, C. R. Mandal, and M. Purkait, Phys. Rev. A **78**, 042708 (2008).
20. M. Purkait, S. Sounda, A. Dhara, and C. R. Mandal, Phys. Rev. A **74**, 042723 (2006).
21. S. Datta, D. S. F. Crothers, and R. McCarroll, J. Phys. B **23**, 479 (1990).
22. R. R. Lewis, Phys. Rev. **102**, 537 (1956).
23. S. C. Mukherjee, K. Roy, and N. C. Sil, Phys. Rev. A **12**, 1719 (1975).
24. A. M. Ermolaev, C. J. Noble, and B. H. Bransden, Private Communication.
25. E. C. Sewell, G. C. Angel, K. F. Dunn, and H. B. Gilbody, J. Phys. B **13**, 2269 (1980).

## CHAPTER- 5

# SINGLE-ELECTRON CAPTURE FROM HELIUM BY FAST PROTONS

## 5.1. INTRODUCTION

The theoretical investigation of electron capture in collision between bare ions and two electron or multi-electron targets is a difficult task and in practice, application of many-body collision theory involves laborious calculations. Most of the calculations are simplified by a model where one captured electron is active and other non-captured electron(s) are being passive. This approximation is called frozen core approximation. The net result of such an approximation is a reduction of the many-body problem to a three-body problem. Such approximations have been developed. During the last few years, much attention has been given in developing the simple four-body collision problem of the basic single charge exchange between protons and helium atoms. The theoretical descriptions of these processes are very complicated in such reaction. The influence of electron-electron interaction is important to study the dynamics in the collision phenomena. Two types of correlations occur in such phenomena. One is static correlation and other is dynamic correlation. The static correlation arises from the Coulomb interaction between the two electrons in the heliumlike atomic system before the collision takes place. But the dynamic collision occurs during the collision. Such correlations are one of the causes of transition from the initial state to the final state. For a long time, theoretical [1-24] and experimental [25-40] efforts concentrated on the energy dependence of total cross sections (TCSs) as well as fully differential cross sections (DCSs). Different theories such as the Classical Trajectory Monte-Carlo (CTMC) method [9], the couple-state [12], the four-body formalism of continuum distorted wave (CDW-4B) [13,14], the Born distorted wave (BDW-4B) [15,16], the continuum distorted wave- eikonal initial state (CDW-EIS) [18], the continuum distorted wave Born final state (CDW-BFS) and the continuum distorted wave Born initial state (CDW-BIS) [19,20], the basic generator method (BGM) [21,22], the boundary-corrected first Born approximation (CB1-4B) [23] has been developed to study the single-electron capture by a fast bare ion in helium. In this paper, we have studied the single-electron capture from helium by fast protons in the energy range 20-11000 keV. We also report the state-selective differential cross sections for such collision at different projectile energies.

Cross sections for single-electron capture in collision of  $H^+$  and  $He^{2+}$  projectile ions with helium atoms are calculated by Dunseath and Crothers in the framework of CDW approximation

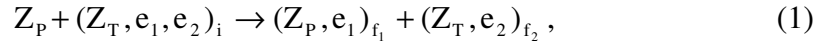
at incident energies from 100 to 1600 keV/amu [11]. In this calculation, the effects of electron correlation in the helium atom have been explicitly accounted by the use of correlated Pluvillage wavefunction. The calculation shows that above 100 keV/amu, the computed results are not in satisfactory agreement. Belkic et al [13] and Mancev [14] have calculated the cross sections for single-electron capture from helium like atom by the impact of projectile bare ions in the energy range of 20 keV to 20 MeV and 50 keV to 10 MeV respectively within the framework of CDW-4B method. In this calculation, the dynamic correlation has been taken into account through the perturbation potential. The computed results are in good agreement with all the available experimental results from energy range 70 keV to 11 MeV. Later, Mancev himself and separately with his collaborators [15,16] have employed successfully the BDW-4B approximation to study different properties of single-electron capture in  $H^+$ -He and  $He^{2+}$ -He collisions in the high energy region. They have also calculated the differential cross sections at different impact energies but there are substantial differences with the experimental results [16]. Generalization of the continuum distorted wave eikonal initial state (CDW-EIS) method has been developed by Abufager et al [18] to study the single-electron capture from the K-shell of He, Ne and Ar noble gases by the impact of bare ions. The computed results have reasonable agreement with the experimental results only for Ne target by the impact of  $H^+$ ,  $He^{2+}$  and  $Li^{3+}$  projectile ions but not satisfactory for He and Ar targets. Mancev [19,20] has applied the four-body formalism of CDW-BIS and CDW-BFS approximations to study the different properties of single-capture from helium-like atomic systems by bare projectiles in the wide range of energies, though all the calculations are confined to ground state capture only. However, the obtained total cross sections are larger than the measured values. The electron dynamics in  $H^+$ -He and  $He^{2+}$ -He collisions have been investigated using the two-centre basis generator method (BGM) [21,22]. The calculations are based on the independent-electron-model and the eikonal approximation. In this paper angular-differential cross sections for single and double transfer into ground state and singly excited state have also been shown. The computed differential cross section results are not in satisfactory agreement at large scattering angles for all projectile energies. Recently, Mancev and Milojevic [23] have investigated the single-electron capture cross sections from He atom by fast protons and  $\alpha$ -particles by means of the CB1-4B method both in post and prior form. The results so obtained have reasonable agreement with the experimental findings except in the low

energy range. Viewing on the success of four-body formalism of boundary corrected continuum intermediate state (BCCIS-4B) approximation [24], we are motivated to study the above mentioned process in the framework of BCCIS-4B theory at impact energies 20-11000 keV.

The organization of the paper is as follows. Section 2 contains the theoretical formulation of the problem. Results and discussion are presented in section 3. Finally in section 4 conclusions are given. Atomic units have been used throughout the work.

## 5.2. THEORY

The single-electron capture from helium atom by proton impact may be represented by



where  $Z_P$  and  $Z_T$  are, respectively, the nuclear charges of the projectile and the target.  $e_1$  and  $e_2$  are the two electrons initially bound to the target nucleus and finally one electron is captured to the projectile.  $\vec{s}_{1,2}$  and  $\vec{x}_{1,2}$  have been leveled as the position vectors of the electrons  $e_{1,2}$  relative to  $Z_P$  and  $Z_T$ , respectively. The inter-electronic coordinate is denoted by  $\vec{r}_{12} = \vec{s}_1 - \vec{s}_2 = \vec{x}_1 - \vec{x}_2$ .  $\mathbf{R}$  denotes the position vector of the projectile (P) relative to target (T) nucleus. The transition amplitude in the prior and post forms for single-electron capture in the BCCIS-4B method may be written as

$$\begin{aligned} T_{if}^{(-)} = N \iiint d\vec{x}_1 d\vec{x}_2 d\vec{R} e^{-i\vec{k}_f \cdot \vec{R}_P + i\vec{k}_i \cdot \vec{R}_T} \varphi_f^*(\vec{x}_2, \vec{s}_1) {}_1F_1\{i\alpha_1; 1; i(\mathbf{v}_f \cdot \mathbf{x}_1 + \mathbf{v}_f \cdot \vec{x}_1)\} \times \\ {}_1F_1\{-i\alpha_2; 1; i\mathbf{b}(\mathbf{k}_f \cdot \mathbf{R}_T + \vec{k}_f \cdot \vec{R}_T)\} \left( \frac{Z_P Z_T}{\mathbf{R}} - \frac{Z_P}{s_1} - \frac{Z_P}{s_2} \right) \varphi_i(\vec{x}_1, \vec{x}_2), \end{aligned} \quad (2)$$

$$\text{where } N = e^{\frac{\pi}{2}(\alpha_1 - \alpha_2)} \Gamma(1 - i\alpha_1) \Gamma(1 + i\alpha_2), \quad \alpha_1 = \frac{Z_T - 1}{v_f}, \quad \alpha_2 = \frac{Z_P(Z_T - 1)}{v_f}$$

and

$$T_{if}^{(+)} = N \iiint d\vec{x}_1 d\vec{x}_2 d\vec{R} e^{-i\vec{k}_f \cdot \vec{R}_P + i\vec{k}_i \cdot \vec{R}_T} \varphi_f^*(\vec{x}_2, \vec{s}_1) {}_1F_1\{i\alpha_1; 1; i(\mathbf{v}_i \cdot \mathbf{s}_1 + \mathbf{v}_i \cdot \vec{s}_1)\} \times$$

$${}_1F_1\left\{-i\alpha_2; 1; i\left(\vec{k}_i R - \vec{k}_i \cdot \vec{R}\right)\right\} \left\{Z_T\left(\frac{1}{R} - \frac{1}{x_1}\right) + Z_P\left(\frac{1}{R} - \frac{1}{s_2}\right) + \left(\frac{1}{r_{12}} - \frac{1}{R}\right)\right\} \times \quad (3)$$

$${}_1F_1\left\{-i\alpha_3; 1; i\left(\vec{k}_f R + \vec{k}_f \cdot \vec{R}\right)\right\} \varphi_i(\vec{x}_1, \vec{x}_2),$$

where  $N = e^{\frac{\pi}{2}(\alpha_1 - \alpha_2 - \alpha_3)} \Gamma(1 - i\alpha_1) \Gamma(1 + i\alpha_2) \Gamma(1 + i\alpha_3)$ ,  $\alpha_1 = \frac{Z_P}{v_i}$ ,  $\alpha_2 = \frac{Z_T(Z_P - 1)}{v_i}$  and

$$\alpha_3 = \frac{(Z_P - 1)(Z_T - 1)}{v_f}.$$

$\varphi_i(\vec{x}_1, \vec{x}_2)$  is the product of one-parameter orbitals for the initial bound state of helium atom with effective charge  $Z_{\text{eff}} = 1.6875$  and  $\varphi_f(\vec{s}_1, \vec{x}_2)$  is the final bound state wavefunction which is the product of hydrogen like wavefunctions.

Using integral representation of the hypergeometric function

$${}_1F_1(i\alpha; 1; z) = \frac{1}{2\pi i} \oint dt (t-1)^{-i\alpha} t^{i\alpha-1} e^{zt},$$

the technique of Fourier transform, Feynman parametric integral, and the integral representation of three denominator integral of Lewis [41] respectively, the equation (2) or (3) may be reduced as

$$T_{\text{if}}^{(-)} = 32\pi^3 C N \ell \lim_{\varepsilon_1, \lambda_2 \rightarrow 0} D(\delta_1, \lambda_1, \lambda_2, \varepsilon_1, \gamma_2) \int_0^1 \frac{dx}{\Delta} \int_0^\infty dy K \quad (4)$$

$$\text{and } T_{\text{if}}^{(+)} = 32\pi^3 \frac{CN}{(2\pi i)} \oint dt_3 t_3^{-i\alpha_3-1} (t_3-1)^{i\alpha_3} \ell \lim_{\varepsilon_1, \lambda_2 \rightarrow 0} D(\delta_1, \gamma_2, \lambda_1, \lambda_2, \varepsilon_1) \int_0^1 \frac{dx}{\Delta} \int_0^\infty dy K, \quad (5)$$

$$\text{where } K = \frac{1}{(2\pi i)^2} \oint dt_1 t_1^{i\alpha_1-1} (t_1-1)^{-i\alpha_1} \oint dt_2 t_2^{-i\alpha_2-1} (t_2-1)^{i\alpha_2} \cdot \frac{1}{A + Bt_1 + Ct_1 t_2 + Dt_2}, \quad (6)$$

$$\Delta^2 = \left\{ (1-a)\vec{k}_f - \frac{\vec{k}_i}{2 + M_T} \right\}^2 (1-x) + \beta_2^2 x \text{ for post form}$$

and 
$$\Delta^2 = \left\{ \frac{\vec{k}_i}{2 + M_T} \right\}^2 (1 - x) + \beta_2^2 x \quad \text{for prior form.}$$

Here the constant  $C$  originates from the initial and final bound state wavefunctions.  $D(\delta_1, \gamma_2, \lambda_1, \lambda_2, \epsilon_1)$  is the appropriate parametric differential operator used to generate the excited state wavefunctions.  $\delta_1$ ,  $\gamma_2$  and  $\lambda_1$  are the orbital component of the initial and final bound state wavefunctions. Now the complex integrations of equation (6) may be evaluated by applying Cauchy's residue theorem to obtain a general term in the form as

$$K = -A^{i\alpha_1 - i\alpha_2 - 1} (A + B)^{-i\alpha_1} (A + D)^{i\alpha_2} {}_2F_1 \left( i\alpha_1; -i\alpha_2; 1; \frac{P}{Q} \right), \quad (7)$$

where  $P = BD - AC$ ,  $Q = (A + B)(A + D)$ .

We see that the equation (4) contains two dimensional integrals such as Lewis and Feynman, but the equation (5) contains three dimensional integrals such as Lewis, Feynman and a complex contour integration of variable  $t_3$ . The Lewis integral with infinite upper limit and Feynman integral from 0 to 1 have been calculated numerically by the 40-point and 46-point Gauss-Legendre quadrature method, respectively with suitable transformations. The complex contour integration of variable  $t_3$  is converted into a real integral [42] from 0 to 1 which has been divided into a number of sub intervals and each of the sub intervals has been integrated numerically by the 42-point Gauss-Laguerre quadrature method. Finally single charge transfer cross section is obtained by numerical integration over scattering angles. However, it may be mentioned that cross sections have finally been evaluated with an accuracy of 0.1%.

### 5.3. RESULTS AND DISCUSSION

We have calculated the single-electron capture cross sections for collisions of protons with He atoms using both prior and post forms of BCCIS-4B approximation in the energy range 20-11000 keV. Total charge transfer cross sections have been obtained by summing over all contributions from individual shells and sub-shell upto  $n=2$ . Variation of total capture cross

sections (TCSs) with incident energy of the projectile ion are reported in graphical form in figure 1(a) and figure 1(b) and are also displayed in table 1. Theoretical results for differential cross sections (DCSs) are shown in figures 2(a) – 2(d), respectively at impact energies 30, 50, 100 and 293 keV. Lastly, DCSs into  $n=2$  shell are also plotted in figure 2(e) at impact energies 60, 100 and 300 keV, respectively. The results for DCSs are given in table 2 and table 3.

In figure 1(a), we have also presented the calculated total single-electron capture cross sections both in prior and post form of BCCIS-4B method as a function of incident projectile energy from 20 to 11000 keV and compared only with the CDW-4B results of Belkic et al [13] where the dynamic correlation have been taken through the perturbation potential. The obtained total cross sections are found to be in excellent agreement with the results of Belkic et al [13] above 60 keV energy. The total cross section as a function of incident projectile energy for single-capture from helium by proton impact is displayed in figure 1(b) in the same energy range. The present computed results are compared with the experimental measurements of Shah and Gilbody [31], Shah et al [32], Welsh et al [27], Rudd et al [30], Allison [25], Horsdal-Pedersen et al [39], Schwab et al [40] and the theoretical results of Mancev and Milojevic [23], Mancev et al [16], Zapukhlyak et al [21], Schultz and Olson [9] and Winter [12]. The present numerical results obtained from post form are in excellent agreement with the experimental results in the whole energy region. We also find from table 1 that the post-prior discrepancy in the BCCIS-4B method is well within 20% in the entire energy range except from 400-1000 keV. Here we may also notice that the computed results agree favorably with the theoretical results of Zapukhlyak et al [21] using BGM calculation except at energy 30 keV. The theoretical results of Mancev and Milojevic [23] using the CB1-4B approximation overestimates the observed cross sections in the whole energy range. The results obtained from BDW-4B model of Mancev et al [16] have reasonable agreement with the present results above 80 keV. The CTMC results of Schultz and Olson [9] are not in fair agreement with the present results because classical treatment of a two-electron atom may not be very accurate. We have observed that the ground state capture cross sections dominate over other states. This is expected because of near energy resonance and velocity matching of the active electron in the initial and final state. However, it is evident from figure 1(a) and figure 1(b) that the present numerical results obtained from post form have superiority over the results from prior form in the whole energy range. This might

mean that the dynamic electron correlations which are connected in post form in our calculation play a very important role, especially at intermediate to high energies. Similar conclusion has been previously drawn by Belkic et al in Ref. [13]. The differential single-electron capture cross sections in post results of BCCIS-4B method are shown in figure 2(a) at incident energy 30 keV and compared with other theoretical results [29] obtained by the two-state two-centre atomic expansion method in the eikonal approximation and experimental results of Martin et al [29]. The present computed results show overall good agreement in shape and in absolute height with the experimental data in the wide range of scattering angles. However, it may be seen that the theoretical results obtained by the eikonal approximation [29] underestimate the present results from the scattering angles 0 to 1 mrad. Mancev et al [16] using BDW-4B method and Zapukhlyak et al [21] using BGM has also calculated the DCS at 50 keV energy and their results have been compared with our results which are shown in figure 2(b). It may be seen from figure 2(b) that the present results have good agreement with the measurements of Martin et al [29] and Schulz et al [36]. However, results from the BDW-4B method of Mancev et al [16] overestimate the present theoretical data at larger scattering angles (above 0.75 mrad) and the results from the BGM of Zapukhlyak et al [21] underestimate the present results at smaller scattering angles (below 1.25 mrad). The present computed results for the DCS at 100 keV are shown in figure 2(c). The two experimental findings [29,38] are depicted in the same figure. The cross sections of the BCCIS-4B approximation are seen to be in very good agreement with the experimental findings from the scattering angle of approximately 0.3 mrad to the 1.5 mrad. At smaller scattering angle (below 0.3 mrad) we find the present numerical results are not in satisfactory agreement with two sets of experimental findings [29,38] and other theoretical results [16,21,29]. In figure 2(d), we display the present results along with other available experimental [16,28] and theoretical data [16] for DCS at 293 keV. The present results are seen to be in fair agreement with all the measurements for the scattering angle less than 1.5 mrad. It is evident from this figure, a discrepancy occur between the cross section computed by means of the BCCIS-4B method and BDW-4B except in the large scattering angles. The results of DCSs for different projectile energies are given in table 2. DCSs for single capture into first excited state ( $n=2$ ) in the p-He collision system is shown in figure 2(e) and numerical results are reported in table 3 at projectile energies 60, 100 and 300 keV respectively. We compare our results with the

theoretical results of BGM [22] and the experimental measurement [35]. The agreement is also satisfactory. However, single capture processes in the p-He system are described fairly well by our theory. This provides further evidence of the role of electron-correlation effects.

#### **5.4. CONCLUSIONS**

We have calculated the total single-electron capture cross sections as well as angular differential cross sections for one electron processes in p-He collisions within the framework of BCCIS-4B approximation both in prior and post form at intermediate to high energies. The obtained cross sections are found to be in very good agreement with the available experimental data. The essence of the method lies in the fact that the total scattering wavefunction satisfies the proper boundary conditions; the continuum state of active electron with the stronger charge are taken into account, and the transition potential is faster falling than the Coulomb potential. The dynamic electron correlation with certain approximation has been included in our calculation.

**Table 1. Total cross sections (in  $10^{-16} \text{ cm}^2$ ) as a function of incident energy  $E$  (keV) for single-charge transfer in  $\text{H}^+ + \text{He} (1s^2)$ . The displayed results are obtained by means of the BCCIS-4B approximation. The integer in parenthesis indicates the power of ten by which the number has to be multiplied.**

Energy (keV)	$Q_{\text{if}}^-$	$Q_{\text{if}}^+$	Energy (keV)	$Q_{\text{if}}^-$	$Q_{\text{if}}^+$
20	2.50(+0)	2.10(+0)	500	6.60(-4)	8.50(-4)
30	2.01(+0)	1.90(+0)	600	2.71(-4)	3.80(-4)
40	1.51(+0)	1.47(+0)	700	1.29(-4)	1.90(-4)
50	1.20(+0)	1.12(+0)	800	6.71(-5)	9.81(-5)
60	9.10(-1)	8.97(-1)	900	3.63(-5)	5.30(-5)
70	6.90(-1)	6.78(-1)	1000	2.20(-5)	3.31(-5)
80	5.40(-1)	5.32(-1)	2000	6.19(-7)	7.00(-7)
90	4.11(-1)	3.93(-1)	3000	8.40(-8)	9.00(-8)
100	3.13(-1)	2.88(-1)	4000	1.81(-8)	2.10(-8)
150	8.76(-2)	8.68(-2)	5000	5.60(-9)	6.00(-9)
200	3.22(-2)	3.50(-2)	8000	3.40(-10)	4.00(-10)
300	6.24(-3)	7.82(-3)	10000	9.82(-11)	1.11(-10)
400	1.80(-3)	2.50(-3)	11000	5.00(-11)	6.00(-11)

**Table 2. Differential cross sections (DCSs) ( $\text{cm}^2/\text{sr}$ ) into ground state as a function of the scattering angle  $\theta$  (mrad) at the incident energies  $E= 30, 50, 100$  and  $293$  keV respectively for the single-electron capture cross sections in  $\text{H}^+ + \text{He} (1s^2)$  collisions. The numbers in the brackets denote multiplicative powers of ten.**

Scattering angle $\theta$ (mrad)	Incident energies E in keV (post)			
	30	50	100	293
0.0000	4.91(-10)	7.53(-10)	4.82(-11)	7.60(-12)
0.0667	4.28(-10)	5.65(-10)	4.60(-11)	6.35(-12)
0.1333	3.40(-10)	3.98(-10)	3.92(-11)	4.08(-12)
0.2000	2.69(-10)	2.51(-10)	3.12(-11)	2.11(-12)
0.2667	2.13(-10)	1.63(-10)	2.30(-11)	9.62(-13)
0.3333	1.72(-10)	1.04(-10)	1.61(-11)	4.06(-13)
0.4000	1.41(-10)	7.20(-11)	1.08(-11)	1.71(-13)
0.4667	9.72(-11)	4.72(-11)	7.03(-12)	7.20(-14)
0.5333	6.67(-11)	2.90(-11)	4.44(-12)	3.48(-14)
0.6000	4.59(-11)	1.67(-11)	2.76(-12)	2.18(-14)
0.6670	2.96(-11)	9.07(-12)	1.79(-12)	1.63(-14)
0.7333	2.05(-11)	5.64(-12)	1.16(-12)	1.14(-14)
0.8000	1.47(-11)	3.92(-12)	9.17(-13)	9.30(-15)
0.8667	1.03(-11)	2.91(-12)	7.37(-13)	7.80(-15)
0.9333	7.48(-12)	2.54(-12)	6.36(-13)	6.30(-15)
1.0000	5.85(-12)	2.21(-12)	5.31(-13)	5.10(-15)
1.0667	4.74(-12)	1.95(-12)	4.05(-13)	4.40(-15)
1.1333	3.85(-12)	1.71(-12)	3.14(-13)	3.70(-15)
1.2000	3.39(-12)	1.48(-12)	2.49(-13)	3.00(-15)
1.2667	3.20(-12)	1.27(-12)	1.93(-13)	2.50(-15)
1.3333	2.79(-12)	1.10(-12)	1.64(-13)	2.00(-15)

1.4000	2.59(-12)	9.50(-13)	1.38(-13)	1.70(-15)
1.4667	2.35(-12)	8.60(-13)	1.15(-13)	1.40(-15)
1.5333	2.08(-12)	7.70(-13)	9.60(-14)	1.10(-15)
1.6000	1.95(-12)	6.90(-13)	8.10(-14)	9.80(-16)
1.6667	1.87(-12)	6.10(-13)	7.00(-14)	8.00(-16)
1.7333	1.81(-12)	5.30(-13)	6.10(-14)	7.00(-16)
1.8000	1.75(-12)	4.70(-13)	5.20(-14)	6.00(-16)
1.8667	1.68(-12)	4.20(-13)	4.30(-14)	5.00(-16)
1.9333	1.47(-12)	3.70(-13)	3.60(-14)	4.30(-16)
2.0000	1.27(-12)	3.20(-13)	2.80(-14)	3.70(-16)

**Table 3. Differential cross sections (DCSs) ( $\text{cm}^2/\text{sr}$ ) into excited states ( $n \geq 2$ ) as a function of the scattering angle  $\theta$  (mrad) at the incident energies  $E= 60, 100$  and  $300$  keV respectively for the single-electron capture cross sections in  $\text{H}^+ + \text{He} (1s^2)$  collisions. The numbers in the brackets denote multiplicative powers of ten.**

Scattering angle $\theta$ (mrad)	Incident energies E in keV (post)		
	60	100	300
0.0000	3.44(-11)	2.87(-13)	4.08(-18)
0.0667	3.21(-11)	2.57(-13)	2.91(-18)
0.1333	2.76(-11)	2.05(-13)	1.79(-18)
0.2000	2.18(-11)	1.44(-13)	8.98(-19)
0.2667	1.58(-11)	9.18(-14)	3.97(-19)
0.3333	1.08(-11)	5.40(-14)	6.27(-19)
0.4000	7.12(-12)	3.03(-14)	6.67(-20)
0.4667	4.49(-12)	1.68(-14)	2.77(-20)
0.5333	2.82(-12)	9.31(-15)	1.13(-20)
0.6000	1.75(-12)	5.28(-15)	5.45(-21)

0.6670	1.10(-12)	3.02(-15)	2.66(-21)
0.7333	7.13(-13)	1.88(-15)	1.53(-21)
0.8000	4.83(-13)	1.25(-15)	9.93(-22)
0.8667	3.43(-13)	8.84(-16)	7.21(-22)
0.9333	2.57(-13)	6.66(-16)	5.68(-22)
1.0000	1.98(-13)	5.30(-16)	4.58(-22)
1.0667	1.68(-13)	4.45(-16)	3.73(-22)
1.1333	1.43(-13)	3.69(-16)	3.14(-22)
1.2000	1.25(-13)	3.20(-16)	2.62(-22)
1.2667	1.11(-13)	2.81(-16)	2.23(-22)
1.3333	1.00(-13)	2.49(-16)	1.86(-22)
1.4000	9.10(-14)	2.20(-16)	1.61(-22)
1.4667	8.20(-14)	1.94(-16)	1.36(-22)
1.5333	7.40(-14)	1.72(-16)	1.15(-22)
1.6000	6.70(-14)	1.53(-16)	1.01(-22)
1.6667	6.20(-14)	1.36(-16)	8.70(-23)
1.7333	5.70(-14)	1.22(-16)	7.30(-23)
1.8000	5.20(-14)	1.08(-16)	6.50(-23)
1.8667	4.70(-14)	9.60(-17)	5.80(-23)
1.9333	4.20(-14)	8.40(-17)	5.10(-23)
2.0000	3.80(-14)	7.20(-17)	4.30(-23)

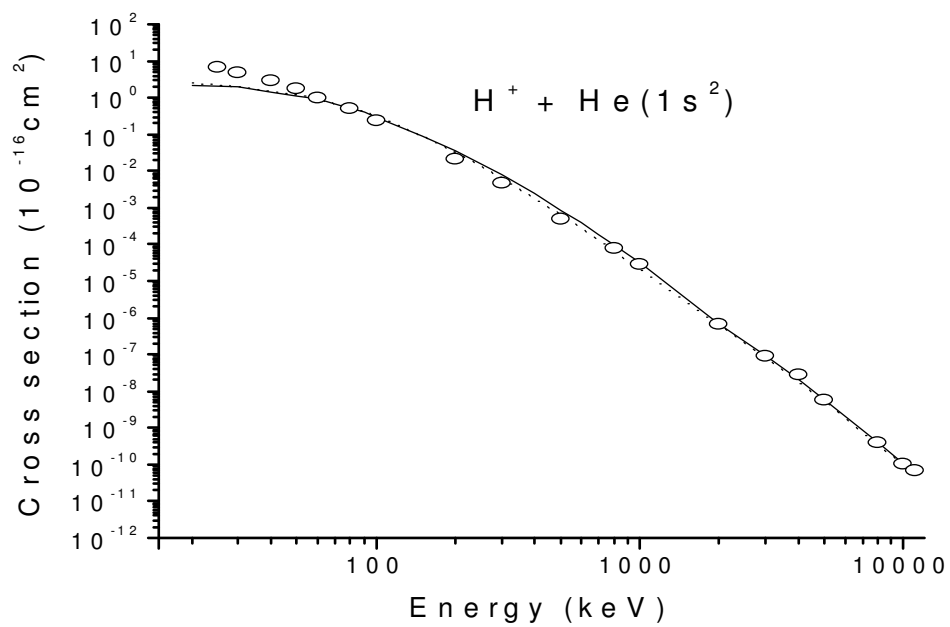


**Figure 1(a).** Total cross sections (in  $\text{cm}^2$ ) as a function of the incident energy  $E$  (keV) for reaction  $H^+ + He \rightarrow H + He^+$ .

Theory: solid line, present results (post form of BCCIS-4B); dotted line, present results (prior form of BCCIS-4B); circle, CDW-4B results of Belkic et al [13] (taken from graph).

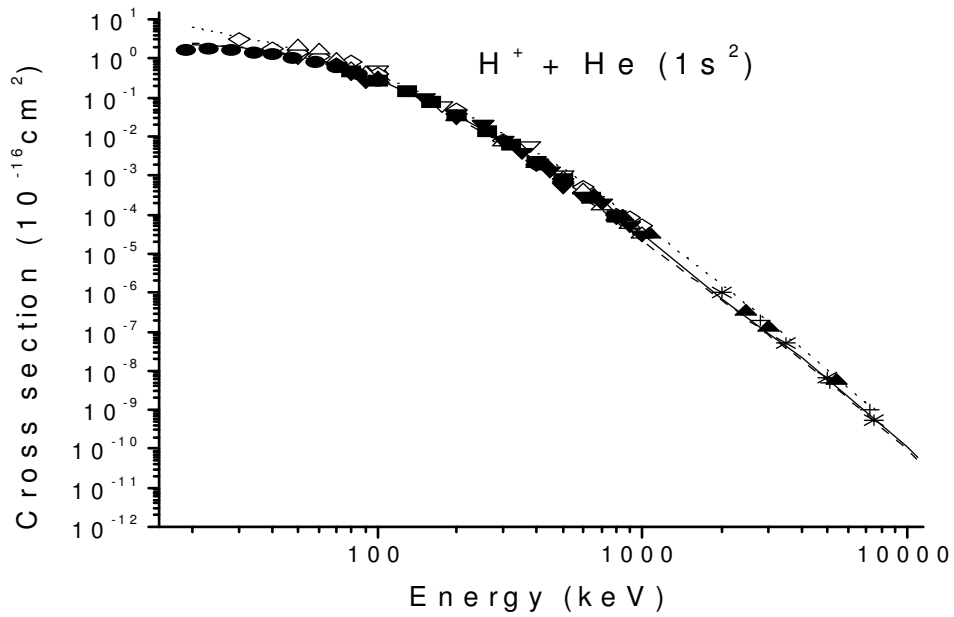


**Figure 1(b).** Total cross sections (in  $\text{cm}^2$ ) as a function of the incident energy  $E$  (keV) for reaction  $H^+ + He \rightarrow H + He^+$ .

Theory: solid line, present results (post form of BCCIS-4B); dashed line, present results (prior form of BCCIS-4B); dotted line, CB1-4B results of Mancev [23];  $\circ$ , couple state results of Winter [12];  $\Delta$ , BDW results of Mancev et al [16];  $\nabla$ , CTMC results of Schultz and Olson [9]; diamond shape, BGM results of Zapukhlyak [21].

Experiments: ■, results of Shah and Gilbody [31]; solid diamond, results of Rudd et al [30]; ●, results of Shah et al [32]; ▲, results of Welsh et al [27]; ▼, results of Allison [25]; +, results of Horsdal-Pedersen et al [39]; \*, results of Schwab et al [40].

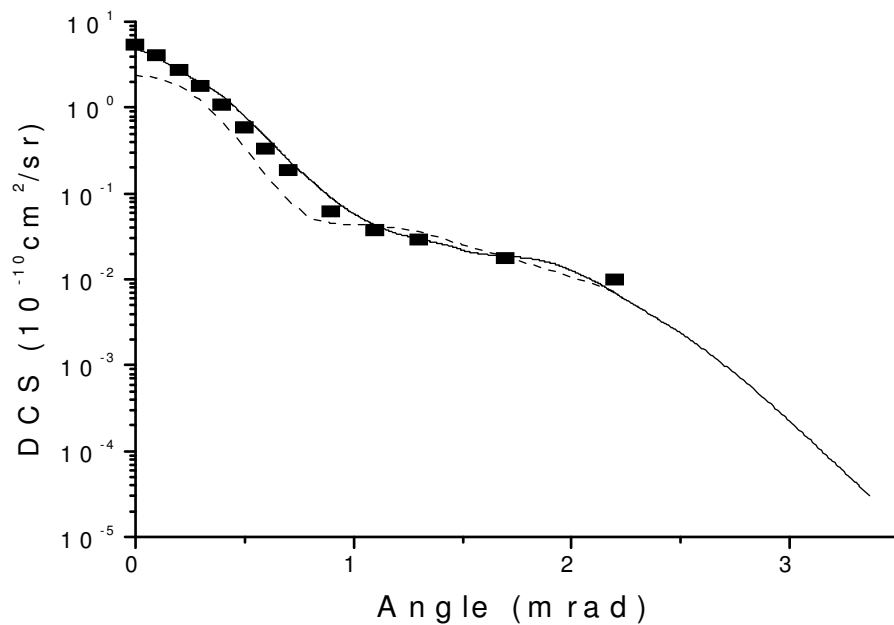


**Figure 2(a).** Comparison of the differential single-electron-capture cross sections in  $H^+ + He$  collisions for projectile energy 30 keV.

Theory: solid line, present results (post form of BCCIS-4B); dotted line, eikonal results of Martin et al [29].

Experiment: ■, results of Martin et al [29].

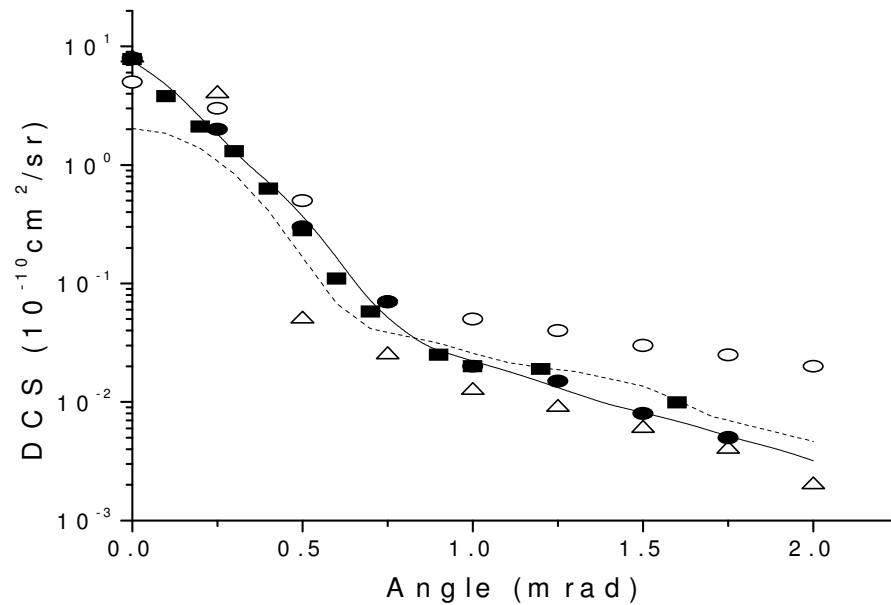


**Figure 2(b).** Comparison of the differential single-electron-capture cross sections in  $H^+ + He$  collisions for projectile energy 50 keV.

Theory: solid line, present results (post form of BCCIS-4B); dotted line, eikonal results of Martin et al [29];  $\circ$ , BDW-4B results of Mancev et al [16];  $\Delta$ , BGM results of Zapukhlyak [21].

Experiment:  $\blacksquare$ , results of Martin et al [29];  $\bullet$ , results of Schulz et al [36].

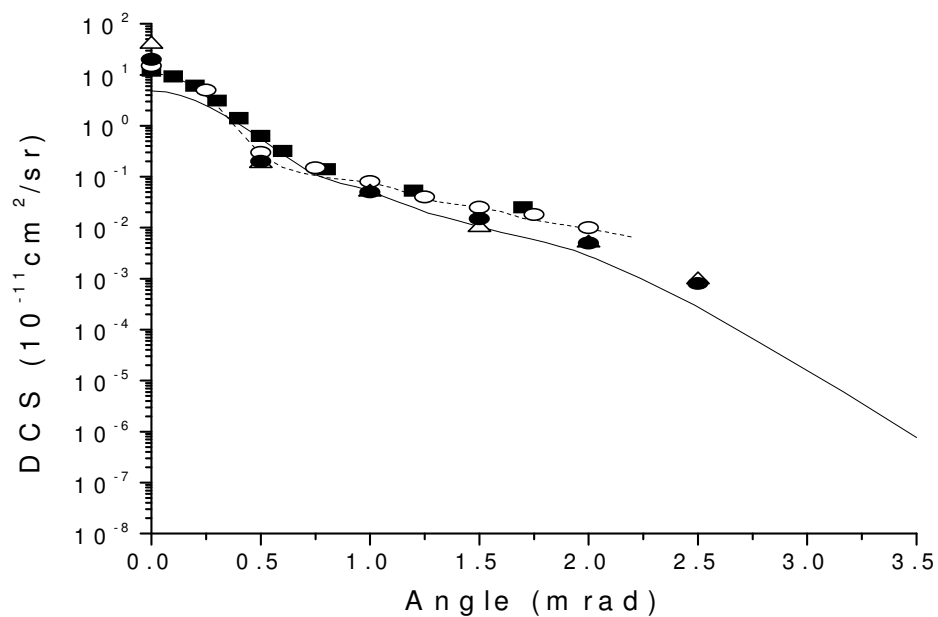


**Figure 2(c).** Comparison of the differential single-electron-capture cross sections in  $H^+ + He$  collisions for projectile energy 100 keV.

Theory: solid line, present results (post form of BCCIS-4B); dotted line, eikonal results of Martin et al [29]; ○, BDW-4B results of Mancev et al [16]; △, BGM results of Zapukhlyak [21].

Experiments: ■, results of Martin et al [29]; ●, results of Schoffler et al [38].

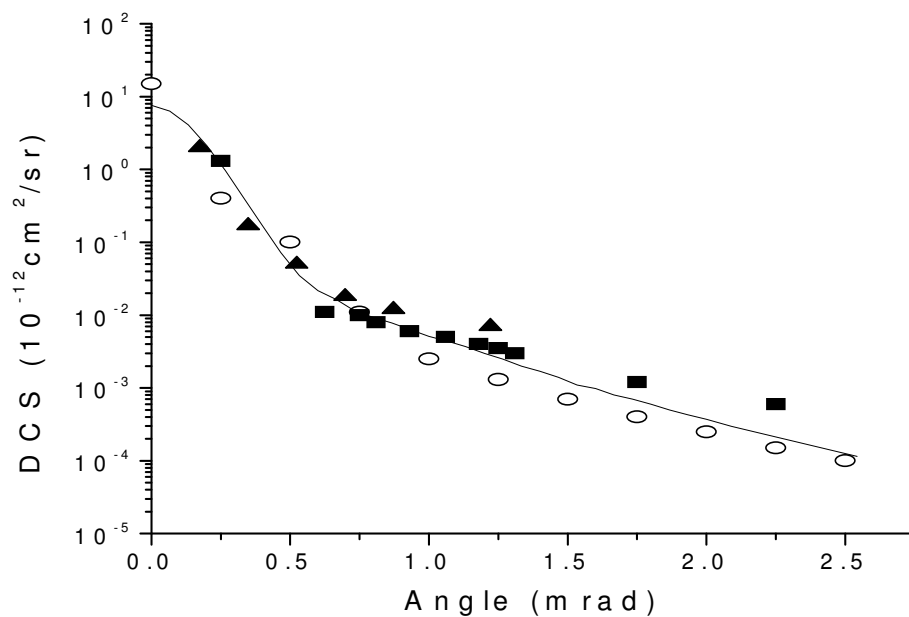


**Figure 2(d).** Comparison of the differential single-electron capture cross sections in  $H^+ + He$  collisions for projectile energy 293 keV.

Theory: solid line, present results (post form of BCCIS-4B); ○, BDW-4B results of Mancev et al [16].

Experiments: ■, results of Mancev et al [16]; ▲, results of Bratton et al [28].

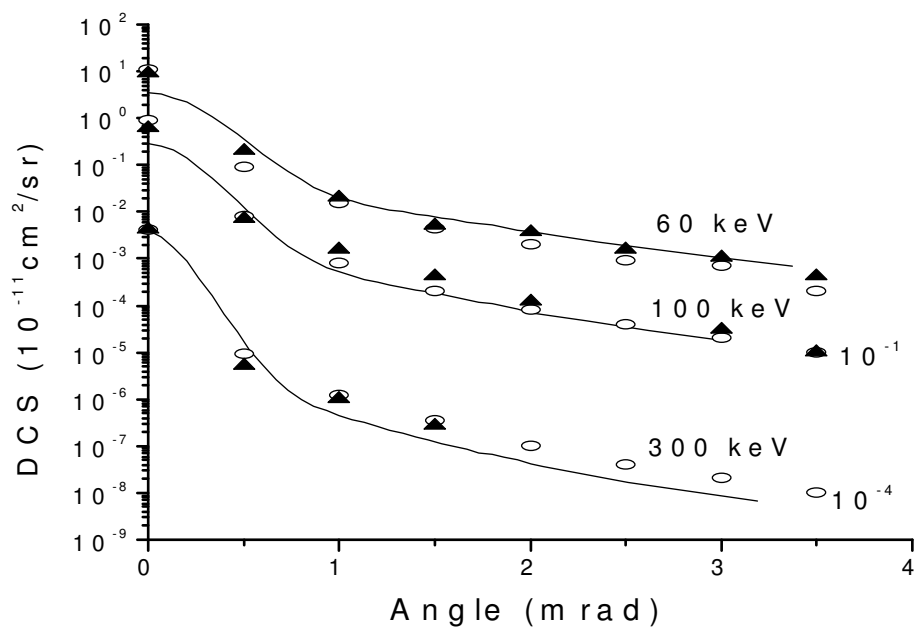


**Figure 2(e).** Comparison of the differential single-electron-capture cross sections in  $H^+ + He$  collisions for projectile energies 60, 100 and 300 keV.

Theory: solid line, present results (post form of BCCIS-4B);  $\circ$ , BGM results of Zapukhlyak et al [22].

Experiment:  $\blacktriangle$ , results of Schoffler [35].

## REFERENCES

- [1] Belkic Dz, Gayet R and Salin A 1979 *Phys.Rep.***56**, 279
- [2] Belkic Dz, Mancev I and Hanssen J 2008 *Rev. Mod. Phys.***80**, 249
- [3] Belkic Dz 2009 *Quantum Theory of High Energy Ion-Atom Collisions* (Taylor & Francis, London)
- [4] Belkic Dz 2004 *Principles of Quantum Scattering Theory* (Institute of Physics, Bristol)
- [5] Bransden B H and McDowell M R C, 1992 *Charge Exchange and the Theory of Ion-Atom Collisions* (Clarendon Press, Oxford)
- [6] McGuire J 1997 *Electron Correlation Dynamics in Atomic Collisions* (Cambridge University Press, Cambridge)
- [7] Dewangan D P and J. Eichler 1986 *J. Phys.* **B19**, 2939
- [8] Dewangan D P and Eichler J 1994 *Phys. Rep.***247**, 59; 1987 *J. Comm. At. Mol. Phys.***21**, 1
- [9] Schultz D R and Olson R E 1988 *Phys. Rev.* **A38**, 1866
- [10] Sidorovich V A, Nikolaev V S and McGuire J H 1985 *Phys. Rev.* **A31**, 2193
- [11] Dunseath K M and Crothers D S F 1991 *J. Phys.* **B24**, 5003
- [12] Winter T G 1991 *Phys. Rev.* **A44**, 4353
- [13] Belkic Dz, Gayet R, Hanssen J, Mancev I and Nunez A 1997 *Phys. Rev.* **A56**, 3675
- [14] Mancev I 1999 *Phys. Rev.* **A60**, 351
- [15] Mancev I 2003 *J. Phys. B: At. Mol. Opt. Phys.***36**, 93

- [16] Mancev I, Mergel V and Schmidt L 2003 *J. Phys. B: At. Mol. Opt. Phys.***36**, 2733
- [17] Schulz M, Moshammen R, Fischer D, Kollmus H, Madison D H, Jones S and Ullrich J 2003 *Nature* (London) **422**, 48
- [18] Abufager P N, Martinez A E, Rivarola R D and Fainstein P D 2004 *J. Phys. B: At. Mol. Opt. Phys.***37**, 817
- [19] Mancev I 2005 *EuroPhys. Letter.***69**, 200
- [20] Mancev I 2005 *J. Comput. Mech. Sci. Eng. (JC MSE)* **89**, 73
- [21] Zapukhlyak M, Kirchner T, Hasan A, Tooke B and Schulz M 2008 *Phys. Rev. A***77**, 012720
- [22] Zapukhlyak M and Kirchner T 2009 *Phys. Rev. A***80**, 062705
- [23] Mancev I and Milojevic N 2010 *Phys. Rev. A***81**, 022710
- [24] Ghosh S, Dhara A, Mandal C R and Purkait M 2008 *Phys. Rev. A***78**, 042708
- [25] Allison S 1958 *Phys. Mod. Rev.***30**, 1137
- [26] Williams J F 1967 *Phys. Rev.* **157**, 97
- [27] Welsh L M, Berkner K H, Kaplan S N and Pyle R V 1967 *Phys. Rev.***158**, 85
- [28] Bratton T R, Cocke C L and Macdonald J R 1977 *J. Phys. B: At. Mol. Phys.***10**, L517
- [29] Martin P J, Arnett K, Blankenship D M, Kvale T J, Peacher J L, Redd E, Sutcliffe V C, Park J T, Lin C D and McGuire J H 1981 *Phys. Rev. A***23**, 2858
- [30] Rudd M E, Dubois R D, Toburen L H, Ratcliffe C A and Goffe T V 1983 *Phys. Rev. A***28**, 3244
- [31] Shah M B and Gilbody H B 1985 *J. Phys. B: At. Mol. Phys.***18**, 899

- [32] Shah M B, McCallion P and Gilbody H B 1989 *J. Phys. B: At. Mol. Opt. Phys.***22**, 3037
- [33] Mergel V, Dorner R, Khayyat Kh, Achler M, Weber T, Jagutzki O, Ludde H J, Cocke C L and Schmidt-Bocking H 2001 *Phys. Rev. Lett.***86**, 2257
- [34] Loftager P 2002 *Private Communication*
- [35] Schoffler M 2006 *Ph.D. thesis, Johann Wolfgang Goethe-Universität, Frankfurt am Main;*<http://publikationen.uni-frankfurt.de/volltexte/2006/3536/>
- [36] Schulz M, Vajnai T and Brand J A 2007 *Phys. Rev. A***75**, 022717
- [37] Schoffler M S, Titze J N, Schmidt L Ph H, Jahnke T, Jagutzki O, Schmidt-Bocking H and Dorner R 2009 *Phys. Rev. A***80**, 042702
- [38] Schoffler M S, Titze J, Schmidt L Ph H, Jahnke T, Neumann N, Jagutzki O, Schmidt-Bocking H, Dorner R and Mancev I 2009 *Phys. Rev.* **79**, 064701
- [39] Horsdal-Pedersen E, Cocke C L and Stockli M 1983 *Phys. Rev. Lett.***50**, 1910
- [40] Schwab W, Baptista G B, Justiniano E, Schuch R, Vogt H and Weber E W 1987 *J. Phys. B: At. Mol. Phys.***20**, 2825
- [41] Lewis R R 1956 *Phys. Rev.* **102**, 537
- [42] Mukherjee S C, Roy K and Sil N C 1975 *Phys. Rev. A***12**, 1719

**ELECTRON CAPTURE CROSS SECTION IN COLLISION OF  
MULTI-CHARGED NEON IONS WITH GROUND STATE  
HYDROGEN AND HELIUM**

## 6.1. INTRODUCTION

Large amount of atomic data are required for modeling the structure and dynamics of high temperature plasmas occurring both naturally in space and artificially in fusion devices [1,2]. Among the atomic species, numerous investigations over few decades have been performed regarding the rare gases [3]. Neon is frequently introduced in tokomaks as a diagnostic element for probing fusion plasmas. Charge transfer reactions between partially or fully stripped charged ions and neutral atoms are of interest to researchers trying to understand line emissions produced in laboratory plasmas and more recently, in non-terrestrial sources such as comets [4]. The resulting charge transfer process leads to line emission that can be used as a diagnostic tool to measure various parameters of plasma such as temperature, velocity, electron density and the charge states of the ions present. Moreover collision between multiple charged ions and atomic targets has been studied [5-12].

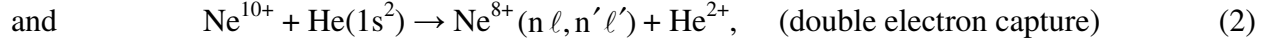
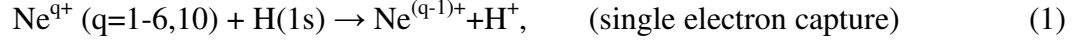
Ryufuku and Watanabe [13] have studied the single charge transfer cross sections in collisions of  $\text{Ne}^{10+}$ ,  $\text{Si}^{14+}$  and  $\text{Ca}^{20+}$  with H atom in the framework of unitarized-distorted-wave approximation (UDWA) method. They give a scaling rule from the observation of theoretical results and also investigated the partial cross sections for electron transfer into the individual orbital of the projectiles. A classical model [14] is proposed for the electron capture process in collision of highly charged ions with atomic hydrogen at low and intermediate impact energies. In this model they have investigated the role of classically allowed electron transitions in determining the cross section for the electron capture process. It was shown that in the case of highly charged fully stripped ions, these transitions become possible at large internuclear separations and consequently their contribution to the cross section is significant. For ionic charges  $Z_p \leq 10$ , the proposed model is valid in the intermediate region. Das et al [15] have calculated the charge transfer cross sections in collisions of completely stripped ions of nuclear charges  $Z_p = 3-8, 10$  in the energy range 200-700 keV/amu. They have applied a single channel distorted wave approximation and found that for a fixed charge state, the maximum contribution of cross sections will occur at smaller values of principal quantum number as the projectile energy increases. A three-body CTMC method [16,17] has been used to examine details of the charge transfer process between the highly charged bare projectile ions and neutral hydrogen.

This calculations show clear deviation from the population of states with large angular momentum quantum numbers to states characterized by low values as the collision energy is lowered. These deviations begin at collision energies somewhere below 500 keV/amu depending on the ion. Errea et al [18] have calculated the total and partial cross sections for capture and ionization in collisions of highly charged ions on neutral hydrogen using molecular-close-coupling and impact -parameter classical trajectory Monte Carlo method. These data are of crucial importance to analyze physical state of the actual tokamak plasmas in which Ne- ionic impurities are deliberately introduced to enhance energy and particle confinement. They found the CTMC calculation does not provide accurate partial capture cross sections compare to the molecular calculation at low energy and low values of principal quantum number (n). Later they [19] extended their CTMC calculations to such reactions at low velocities and also highlighted the limitations of the classical method. They have shown that classical and semi-classical mechanisms are essentially the same, although at low velocities the method is unable to describe the fall of the cross section. Recently Errea et al [20] have calculated the total and partial cross sections for capture and ionization in collision of highly charged ions with hydrogen in the energy range 30-300 keV/amu. They specially focus on capture into high-lying states of the projectile, which are much more important in diagnostics of fusion plasmas. It is to be mentioned that most of the cross sections data have been calculated in collision of fully stripped neon ions with hydrogen. Charge transfer cross sections into each individual sub-shell are not available. Under the context, we are motivated to study the single charge transfer reaction involving  $\text{Ne}^{q+}$  ( $q=1-6,10$ ) with hydrogen atom in the intermediate to high energy using quantum mechanical and classical method. We have also chosen to study the double charge transfer reaction in collision of fully stripped neon ions with helium atom.

The organization of the paper is as follows. Theoretical formulation has been described in Sec.2. Results and discussions are the contents of Sec.3. In Sec.4 we add some concluding remarks. Atomic units are used throughout unless otherwise mentioned.

## 6.2. THEORY

The reactions under the study may generally be represented by



**6.2.1. Classical formulation:** Let the cartesian co-ordinates of the active electron with respect to the target ion (T) are  $q_1, q_2$  and  $q_3$  respectively. Let the same quantities are  $q_4, q_5$  and  $q_6$  respectively for the incoming projectile ion (P) with respect to the centre of mass of the target system. So  $\vec{r}_{ij}$  ( $i, j = e, T, P$ ), the distance between any pair of two particles may easily be expressed in terms of  $q_i$  ( $i = 1, 6$ ) provided mass ( $M_T$ ) of the residual target ion, mass ( $M_P$ ) of the projectile ion and electron mass are known. Let  $p_i$  ( $i = 1, 6$ ) are the canonical momenta conjugate to the rectangular co-ordinate  $q_i$  ( $i = 1, 6$ ). So the classical hamiltonian of the three system (for equ<sup>n</sup>. 1) may be written as

$$H = \sum_{i=1}^3 \frac{p_i^2}{2\mu} + \sum_{j=4}^6 \frac{p_j^2}{2M} + V_{Te}(\vec{r}_{Te}) + V_{Pe}(\vec{r}_{Pe}) + V_{TP}(\vec{r}_{TP}) \quad (3)$$

where  $\mu = \frac{M_T}{M_T + 1}$ ,  $M = \frac{M_P(M_T + 1)}{M_P + M_T + 1}$

and  $V_{ij}$  ( $i, j = e, T, P$ ) is the two body pair interaction between  $i$ -th and  $j$ -th particle. So the Hamilton's equations of motion may be written as

$$p_i = \mu \dot{q}_i, \quad i=1,2,3 \quad (4a)$$

$$p_i = M \dot{q}_i, \quad i=4,5,6 \quad (4b)$$

$$\dot{p}_i = -\frac{1}{r_{Pe}} \frac{\partial V}{\partial r_{Pe}} \mu (\mu q_i - q_{i+3}) - \frac{1}{r_{Te}} \frac{\partial V}{\partial r_{Te}} q_i - \frac{1}{r_{TP}} \frac{\partial V}{\partial r_{TP}} \frac{\mu}{M_T} \left( \frac{\mu}{M_T} q_i + q_{i+3} \right), \quad i=1,2,3 \quad (4c)$$

$$\dot{p}_i = -\frac{1}{r_{Pe}} \frac{\partial V}{\partial r_{Pe}} (q_i - \mu q_{i-3}) - \frac{1}{r_{TP}} \frac{\partial V}{\partial r_{TP}} \left( q_i + \frac{\mu}{M_T} q_{i-3} \right), \quad i=4,5,6 \quad (4d)$$

where  $V = V_{Te}(\vec{r}_{Te}) + V_{Pe}(\vec{r}_{Pe}) + V_{TP}(\vec{r}_{TP})$  .

This set of twelve equations given by (4a) - (4d) describes the motion of the whole system in center of mass frame of the active electron and residual target ion. The interaction of the active electron with the target is uniquely determined by the Coulomb potential. But for the partially stripped charged projectile ions of neon, the model potential [21] is taken in the form of

$$V_{\text{mod}}(\vec{r}) = -\frac{Z_0}{r} - \frac{e^{-z_3 r}}{r} (z_1 + z_2 r), \quad z_1 = Z_P - Z_0.$$

Here  $z_0$ ,  $z_P$  and  $z_1$  are respectively asymptotic charge, nuclear charge and screened charge of the projectile.  $z_2$  and  $z_3$  are two arbitrary parameters chosen variationally with respect to Slater basis set in such a way that corresponding Hamiltonian of the active electron in the final state is diagonalised to reproduce correct binding energies. These binding energies of the active electron of different projectile ions are calculated from the tables of Clementi and Roetti [22] and works of Clark and Abdallah [23]. In an attempt to make the parameters  $z_3$  and  $z_2$  to be unique as far as possible, we have tested the virial theorem with an accuracy of 0.001 % with respect to the chosen Slater basis set. In doing so, we have found the values of  $z_3$  and  $z_2$  which are given in Table 1. It may be mentioned here that we have not included the polarization potential term because we have found that, the effect of such part beyond cut off potential has very little effect on the totality and enhances the consumption of computational time only. The method of calculation has been described in detail elsewhere [21].

## 6.2.2. Quantum mechanical formulation:

**6.2.2.1. Single charge transfer:** The total Hamiltonian of the three body system for the reaction

$$(1) \text{ may be written as } H = H_0 + V_{Te}(\vec{r}_T) + V_{Pe}(\vec{r}_P) + V_{TP}(\vec{R})$$

where

$$H_0 = -\frac{1}{2\mu_T} \nabla_{R_T}^2 - \frac{1}{2a} \nabla_{r_T}^2 = -\frac{1}{2\mu_P} \nabla_{R_P}^2 - \frac{1}{2b} \nabla_{r_P}^2$$

$$a = \frac{M_T}{1+M_T}, \quad b = \frac{M_P}{1+M_P}, \quad \mu_T = \frac{M_P(1+M_T)}{1+M_P+M_T}, \quad \mu_P = \frac{M_T(1+M_P)}{1+M_P+M_T}$$

$$V_{Te}(\vec{r}_T) = -\frac{1}{r_T}, \quad V_{TP}(\vec{R}) = -\frac{Z_0}{R}, \quad V_{Pe}(\vec{r}_P) = -\frac{Z_0}{r_P} - \frac{e^{-Z_3 r_P}}{r_P} (z_1 + z_2 r_P).$$

The post form of the transition amplitude in the framework of 3-body boundary corrected continuum intermediate state approximation (BCCIS-3B) [24] may be written as

$$T_{if}^{(+)} = \langle \psi_f | V_f | \psi_i^+ \rangle = N \iint d\vec{r}_P d\vec{R}_P e^{-i\vec{k}_f \cdot \vec{R}_P} {}_1F_1 \left\{ -i\alpha_3; 1; i \left( \vec{k}_f R_P + \vec{k}_f \cdot \vec{R}_P \right) \right\} \varphi_f^* \left( \frac{Z_T}{R_P} - \frac{Z_T}{r_T} \right) \times$$

$$e^{i\vec{k}_i \cdot \vec{R}_T} {}_1F_1 \left\{ i\alpha_1; 1; i b \left( v_i r_P + \vec{v}_i \cdot \vec{r}_P \right) \right\} {}_1F_1 \left\{ -i\alpha_2; 1; i a \left( \vec{k}_i R_P - \vec{k}_i \cdot \vec{R}_P \right) \right\} \varphi_i(\vec{r}_T) \quad (5)$$

where  $N = e^{\frac{\pi}{2}(a_1 - a_2 - a_3)} \Gamma(1 - i\alpha_1) \Gamma(1 + i\alpha_2) \Gamma(1 + i\alpha_3)$ ,  $\alpha_1 = \alpha_2 = \frac{Z_P}{v_i}$ ,  $\alpha_3 = \frac{Z_T(Z_P - 1)}{v_f}$ .

Using the integral representation of confluent hypergeometric function, equation (5) may be

written as  $T_{if}^{(+)} = \left( \frac{Z_T^3}{\pi} \right)^{\frac{1}{2}} Z_T \frac{CN}{(2\pi i)^3} \left( \frac{\partial^2}{\partial \lambda \partial \beta} - \frac{\partial^2}{\partial \lambda \partial \varepsilon} \right) \oint dt_3 t_3^{-i\alpha_3 - 1} (t_3 - 1)^{i\alpha_3} \oint dt_2 t_2^{-i\alpha_2 - 1} (t_2 - 1)^{i\alpha_2} \times$

$$\oint dt_1 t_1^{i\alpha_1 - 1} (t_1 - 1)^{-i\alpha_1} J, \quad (6)$$

where  $J = \ell \lim_{\varepsilon \rightarrow 0} \iint d\vec{r}_P d\vec{R}_P e^{i(t_3 \vec{k}_f - \vec{k}_f - a t_2 \vec{k}_i) \cdot \vec{R}_P + i \vec{k}_i \cdot \vec{R}_T + i b t_1 \vec{v}_i \cdot \vec{r}_P} \frac{e^{-\alpha R_P}}{R_P} \frac{e^{-\lambda_1 r_P}}{r_P} \frac{e^{-\beta r_T}}{r_T}, \quad (7)$

$$\alpha = \varepsilon - i a k_i t_2 - i k_f t_3, \quad \lambda_1 = \lambda - i b v_f t_1, \quad \beta = Z_T.$$

Here the  $\lambda$  is the exponential parameter in the final state wavefunction and the constant  $C$  originate from the final bound state wavefunction.

Using Fourier transforms techniques and following Lewis [25] the space integration  $J$  of the equation (7) can be evaluated. Following Sinha and Sil [26], the integral  $J$  may be reduced as

$$J = \frac{16\pi^2}{b^2} \int_0^\infty \frac{dx}{\alpha_1 x^2 + 2\beta_1 x + \gamma_1}, \quad (8)$$

where  $\alpha_1, \beta_1, \gamma_1$  are linear functions of  $t_1$  and  $t_2$ . Thus we can write  $\alpha_1 x^2 + 2\beta_1 x + \gamma_1$  as  $A + Bt_1 + Ct_3 + Dt_1 t_3$ , where  $A, B, C, D$  are functions of  $t_2$ , and  $x$ . Hence by applying Cauchy's residue theorem, equation (6) can be reduced into the following form

$$T_{if}^{(+)} = z_T \left( \frac{z_T^3}{\pi} \right)^{\frac{1}{2}} \left( \frac{NC}{2\pi i} \right) \frac{16\pi^2}{b^2} \ell \lim_{\varepsilon \rightarrow 0} \left( \frac{\partial^2}{\partial \lambda \partial \beta} - \frac{\partial^2}{\partial \lambda \partial \varepsilon} \right) \oint dt_2 t_2^{-i\alpha_2-1} (t_2-1)^{i\alpha_2} \int_0^\infty k dx. \quad (9)$$

Finally we have performed the  $t_2$  and  $x$  integrations numerically [27].

**6.2.2.2. Double charge transfer:** The post form of the transition amplitude in the framework of 4-body boundary corrected continuum intermediate state approximation (BCCIS-4B) for the reaction (2) may be written as [28]

$$T_{if}^{(+)} = \langle \chi_f^- | \frac{2Z_T}{R} - \frac{Z_T}{x_1} - \frac{Z_T}{x_2} | \psi_i^{BCCIS-4B(+)} \rangle \quad (10)$$

where  $\chi_f^{(-)}$  is the distorted wavefunction in the exit channel, and  $\psi_i^{BCCIS-4B(+)}$  is the two-electron coulomb wavefunction in the entrance channel. So the equ<sup>n</sup> (10) can be written as

$$T_{if}^{BCCIS-4B(+)} = N_1 \iiint d\vec{x}_1 d\vec{x}_2 d\vec{R} e^{-i\vec{k}_f \cdot \vec{R}_p} \varphi_f(\vec{s}_1, \vec{s}_2) {}_1F_1(i\alpha_1; 1; z_1) {}_1F_1(i\alpha_2; 1; z_2) {}_1F_1(-i\alpha_3; 1; z_3) \times \\ {}_1F_1(-i\alpha_4; 1; z_4) \left( \frac{2Z_T}{R} - \frac{Z_T}{x_1} - \frac{Z_T}{x_2} \right) e^{i\vec{k}_i \cdot \vec{R}_T} \varphi_i(\vec{x}_1, \vec{x}_2) \quad (11)$$

where  $z_1 = i b_1 (v_i s_1 + \vec{v}_i \cdot \vec{s}_1)$ ,  $z_2 = i b_1 (v_i s_2 + \vec{v}_i \cdot \vec{s}_2)$ ,  $z_3 = i (\vec{k}_i \cdot \vec{R}_p - \vec{k}_i \cdot \vec{R}_p)$ ,  $z_4 = i (\vec{k}_f \cdot \vec{R}_p + \vec{k}_f \cdot \vec{R}_p)$

$$N_1 = e^{\frac{\pi}{2}(\alpha_1 + \alpha_2 - \alpha_3 - \alpha_4)} \Gamma(1 - i\alpha_1) \Gamma(1 - i\alpha_2) \Gamma(1 + i\alpha_3) \Gamma(1 + i\alpha_4), \quad \alpha_1 = \alpha_2 = \frac{Z_P}{b_3 v_i},$$

$$\alpha_3 = \frac{Z_P Z_T}{b_1 v_i}, \quad \alpha_4 = \frac{Z_T (Z_P - 2)}{v_f}, \quad b_1 = \frac{M_P}{2 + M_P}, \quad b_3 = \frac{2 + M_P}{1 + M_P}.$$

The integral representation of the hypergeometric function is given by

$${}_1F_1(i\alpha; 1; z) = \frac{1}{2\pi i} \oint dt (t-1)^{-i\alpha} t^{i\alpha-1} e^{tz}.$$

Using the integral representation of confluent hypergeometric function, the Fourier transform, the Feynman parametric integral and following Lewis [25], Sinha and Sil [26], equation (11) becomes

$$T_{if}^{BCCIS-4B(+)} = \frac{N}{(2\pi i)^2} .32 \pi^3 \oint dt_2 t_2^{i\alpha_2-1} (t_2-1)^{-i\alpha_2} \oint dt_3 t_3^{-i\alpha_3-1} (t_3-1)^{i\alpha_3} D \ell \lim_{\varepsilon \rightarrow 0} \int_0^1 \frac{dx}{\Delta} \int_0^\infty dy K, \quad (12)$$

where D is the appropriate parametric differential operator used to generate the singly excited state wavefunctions and K may be written as

$$K = \frac{1}{A} \left( \frac{A}{A+B} \right)^{i\alpha_2} \left( \frac{A}{A+C} \right)^{-i\alpha_3} {}_2F_1 \left\{ i\alpha_2; -i\alpha_3; 1; \frac{BC-AD}{(A+B)(A+C)} \right\}.$$

Equation (9) contains two-dimensional integral, Lewis, and a complex contour integration, but the equation (12) contains four-dimensional integrals such as Lewis, Feynman and two complex contour integrations. The complex contour integrations is converted to real integral [27] and is integrated using Gauss-Laguerre quadrature method. Finally, integration over the scattering angles has been performed with the Gauss-Legendre quadrature method.

### 6.3. RESULTS AND DISCUSSION

We have performed quantum mechanical ( post form of BCCIS approximation) and classical calculations (CTMC) in collision of multiply charged  $Ne^{q+}$  ( $q=1-6,10$ ) ions with ground

state atomic hydrogen in the impact energy range  $50 \leq E \leq 1000$  keV/amu ( $v = 1.41$  a.u to  $6.33$  a.u). Total charge transfer cross sections have been obtained by summing over all contributions into each shell up to principal quantum number  $n=4$  and the contribution to each individual sub-shell is determined by multiplying the calculated cross sections by a Pauli blocking factor [29]. All our calculated results are given in graphical form (Figures 1-8). The variation of double charge transfer cross sections in collision of fully stripped  $\text{Ne}^{10+}$  ions with helium atoms in the energy range 80-2000 keV/amu (1.79 a.u to 8.95 a.u) are plotted in Figure 9 using the post form of BCCIS-4B approximation [28,30]. The variation of double-to-single capture cross sections with projectile energies is shown in Figure 10. State-selective results are also displayed in Table 2 for  $\text{Ne}^{10+} + \text{He}$  collision.

### 6.3.1. Single charge transfer and ionization

In Figure 1(a)-1(c), the calculated total capture cross sections along with the cross sections for capture into a specific  $n$ -state and  $\ell$ -state are plotted for projectile ion  $\text{Ne}^+$ . We have seen that the major contribution to the total capture cross section comes from capture into the  $n=2$  state and contribution from  $n>2$  is negligible at energies greater than 300 keV/amu. We have not considered the capture into  $1s$  state of the projectile as it is a completely filled state. Due to unavailability of any experimental results, we have only compared with the results obtained by CTMC method. In Figure 1(a), the CTMC results agree with the present BCCIS results below 300 keV / amu. We have plotted the variation of cross sections with principal quantum number ( $n$ ) in Figure 1(b) and angular momentum quantum number ( $\ell$ ) in Fig.1(c) for  $\text{Ne}^+ + \text{H}$  collision. We found the contribution of charge transfer cross sections obtained by the BCCIS approximation for  $n=4$  comes from  $d$ - and  $f$ -states at  $E < 400$  keV/amu and maximum from  $p$ -state at energy  $E > 400$  keV/amu. But in Figure 2(a), we have seen the contribution is maximum for  $n=3$  at  $E < 400$  keV/amu and for  $n=2$  at  $E \geq 400$  keV/amu. In Figure 2(c), the contribution of charge transfer cross sections for given principal quantum number  $n=4$ , is maximum at  $d$ -state. Same feature is obtained from the CTMC calculations. Energy variation of total single electron capture cross sections have been presented in figures 3(a), 4(a), 5(a) and 6(a) for collisions of  $\text{Ne}^{q+}$  ( $q = 3 - 6$ ) with H atoms respectively. We have compared our computed results with the CTMC results of Maynard et al [31]. From these figures we may find that our computed results

are in reasonable agreement with the results of Maynard et al. For  $\text{Ne}^{3+}$  and  $\text{Ne}^{4+}$  ions in Figure 3(b) and Figure 4(b), present BCCIS results shows that major contribution of total charge transfer cross sections comes from  $n=3$  and  $n=4$  at low energy range. But CTMC results have their peak values at  $n=3$  state in the low energy range and at  $n=2$  state in the high energy range for both charge state  $q=3,4$ . For  $q=3-6$  charge states (in Figure 3(c), Figure 4(c), Figure 5(c), and Figure 6(c)), both the results (BCCIS and CTMC) have almost identical  $\ell$ -distributions for  $n=4$  state i.e their peak values occur at the d-shell. The total cross sections as a function of incident projectile energy for collision of the  $\text{Ne}^{10+}$  ion with the hydrogen atom are displayed in figure 7(a). The present results are compared with the theoretical works of Maynard et al [31], Perez et al [17], Ryufuku and Watanabe [13], Das et al [15] and the experimental works of Meyer et al [32]. Our calculated results are not in satisfactory agreement with the other theoretical findings. From figures 3(b), 4(b), 5(b) and 6(b) respectively, it has been shown that the cross sections increase with  $n$  for increasing charge state. However contribution from  $n>5$  shell is quite significant for  $\text{Ne}^{10+} + \text{H}$  collision which is shown in Figure 7(b). For this reason, discrepancy appeared in Figure 7(a). We may also find that for higher excited shells (identified higher values of  $n$ ) higher  $\ell$  sub-shells (d and f sub-shells) contribute significantly and lower  $\ell$  sub-shells (s and p) have small contribution. The capture peak in the individual shell and sub-shells may be explained in terms of the nearest matching of the binding energy and momentum distribution of the active electron in the initial and final state. The variation of ionization cross sections with energy is shown in Figure 8 for charge states  $q=1-6$  using only the CTMC method. Due to non-availability of any experimental result for such ions, we are unable to compare them in our investigation. From Figure 8, we may find that the peak of the ionization cross sections shift towards higher projectile energies as projectile charge increases because any electron removed from the H atom is preferentially captured by the strong Coulomb field of the projectile.

### 6.3.2. Double charge transfer

BCCIS-4B results for double electron capture by fully stripped  $\text{Ne}^{10+}$  in  $\text{He}(1s^2)$  collision are displayed in Figure 9. The experimental results of Kase et al [33] for collision of  $\text{Ne}^{2+}$  ion with He atom in the energy range 50-150 keV/amu have been compared with our present results for the same process. In Table 2, state selective results are given for capture into ground state

$(1s^2)^1S$  and into the first singly excited states. In all cases, calculations have been carried out using Lowdin wavefunctions [34] for helium in the initial channel and configuration interaction wavefunctions of Novikov and Senashenko [35] for the final state on the projectile. In figures, we have plotted present theoretical results which are obtained by summing the contributions from the ground state and from the 1st singly excited states. From this graph, it is evident that present ground state results slightly overestimate the experimental results of Kase et al [33]. But the results of excited states have reasonable discrepancies with the experiment. As we have already mentioned in our previous work [28], that for the low-charge states, the capture is favored only in the ground state and for highly charged ions, capture is usually favored to several excited states of the final states of the product ions. Due to unavailability of any experimental and other theoretical data, the double-to-single capture ratio with the projectile energy is plotted in Figure 10. From the figure we may find that the ratio increases with projectile energy and finally it gets almost saturated in the higher energy regime.

#### 6.4. CONCLUSIONS

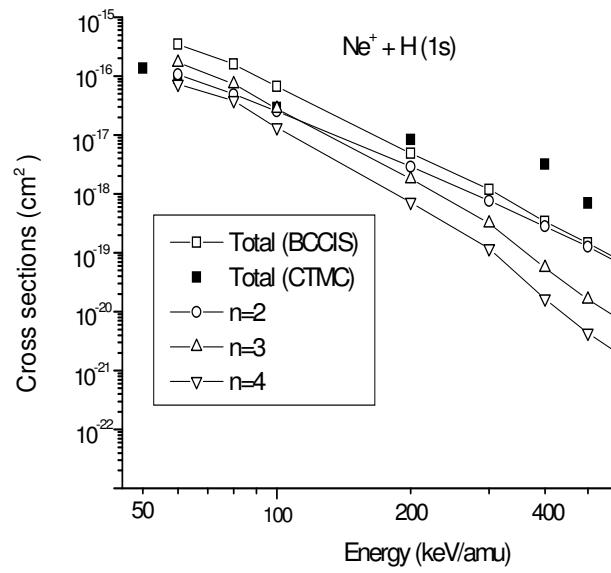
The main purpose of this paper is to present the theoretical data on absolute total capture cross section and sub-shell distribution of single and double electron capture cross sections of  $Ne^{q+}$  recoil ions by H and He atoms in the intermediate to high energies in the framework of BCCIS and CTMC methods. These data are of crucial importance to analyze the physical state of actual tokamak plasmas in which Ne ionic impurities are introduced to enhance energy and particle confinement. It is well known that the inclusion of intermediate continuum state is very much important to take into account to describe a charge transfer event. However, in the case of asymmetric collision where  $Z_P > Z_T$ , post form of BCCIS approximation is appropriate as projectile continuum states are to be taken into account. We have adopted model potential containing both a long-range part and a short-range part for the interaction of the active electron with the projectile ion. For  $Z_P > Z_T$ , the major contribution of total charge transfer cross sections comes from higher excited states.

**Table 1. Model potential parameters  $z_0$ ,  $z_1$ ,  $z_2$  and  $z_3$ .**

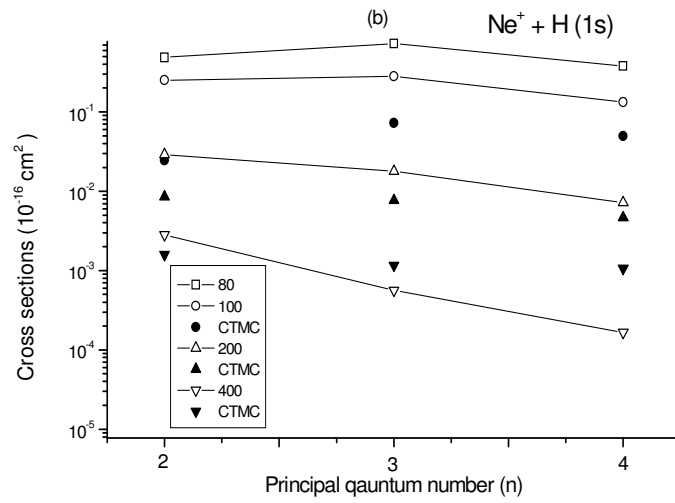
Ions	$\epsilon_i$	$z_0$	$z_1$	$z_2$	$z_3$
Ne <sup>+</sup>	-1.6042	1.0	9.0	2.6450	2.2280
Ne <sup>2+</sup>	-2.3809	2.0	8.0	1.8750	2.3180
Ne <sup>3+</sup>	-3.4025	3.0	7.0	1.8250	2.4180
Ne <sup>4+</sup>	-4.3240	4.0	6.0	1.7250	2.6180
Ne <sup>5+</sup>	-5.8230	5.0	5.0	1.6150	2.5170
Ne <sup>6+</sup>	-7.4986	6.0	4.0	2.0660	2.7170

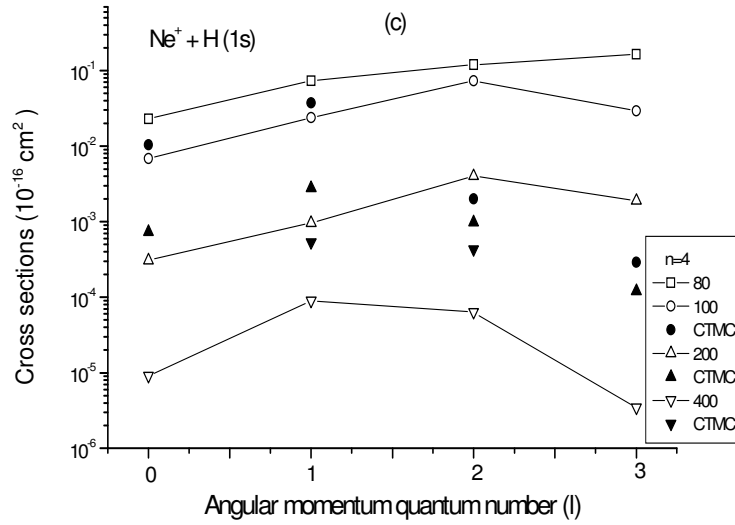
**Table 2. Theoretical cross sections (in units of  $10^{-16}$  cm<sup>2</sup>) as a function of energy for double electron capture reaction  $\text{Ne}^{10+} + \text{He}(1s^2) \rightarrow \text{Ne}^{8+}(nl, n'l') + \text{He}^{2+}$ .**

States	Energy (keV/amu)						
	80	100	200	400	500	1000	2000
(1s1s) <sup>1</sup> S	4.01(-2)	2.76(-2)	8.43(-3)	2.08(-3)	1.36(-3)	2.81(-4)	3.97(-5)
(1s2s) <sup>1</sup> S	3.05(-2)	2.18(-2)	1.25(-2)	6.04(-3)	2.96(-3)	6.32(-4)	8.50(-6)
(1s2p) <sup>1</sup> P	3.62(-2)	3.15(-2)	2.11(-2)	1.08(-2)	7.67(-3)	8.44(-4)	6.50(-5)
(1s3s) <sup>1</sup> S	2.14(-2)	1.80(-2)	9.06(-3)	3.15(-3)	1.25(-3)	4.71(-4)	3.01(-5)
(1s3p) <sup>1</sup> P	3.51(-2)	3.10(-2)	1.87(-2)	5.50(-3)	2.75(-3)	6.27(-4)	5.39(-5)
(1s3d) <sup>1</sup> D	4.27(-3)	4.00(-3)	3.11(-3)	7.84(-4)	3.49(-4)	6.00(-5)	5.82(-7)



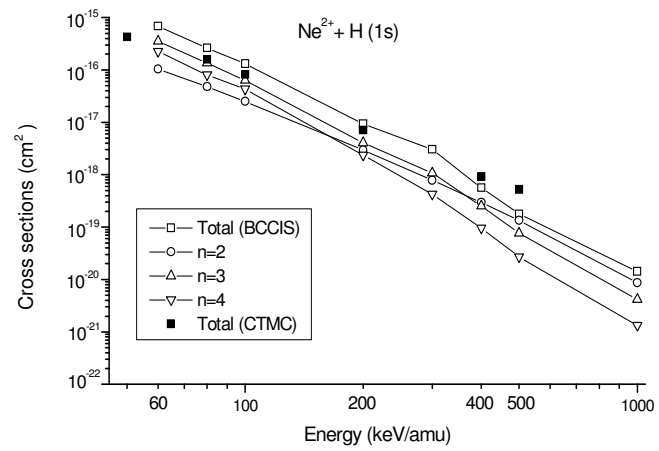
(a)



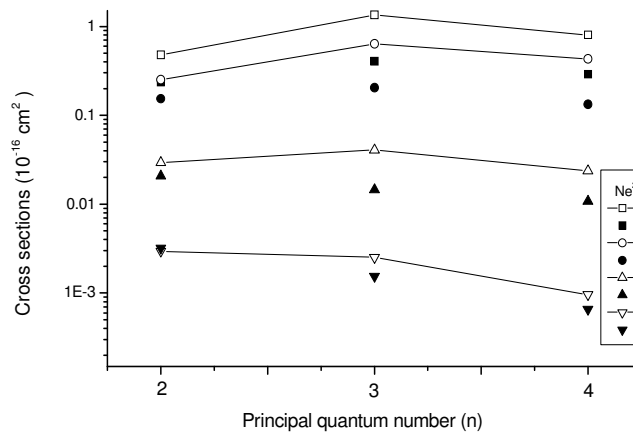


(c)

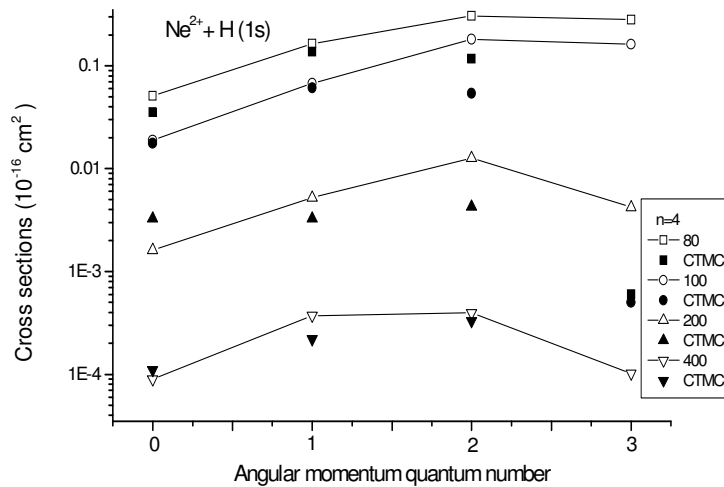
**Figure 1(a).** Variation of calculated total capture cross sections for the dominant  $n$ -states for the interaction  $\text{Ne}^+ + \text{H}(1s)$  with collision energy, **(b)** Capture cross sections from specific  $n$ -states by the projectile ion  $\text{Ne}^+$  and **(c)** Cross sections for electron capture to specific  $\ell$  values for  $\text{Ne}^+$  ion.



(a)

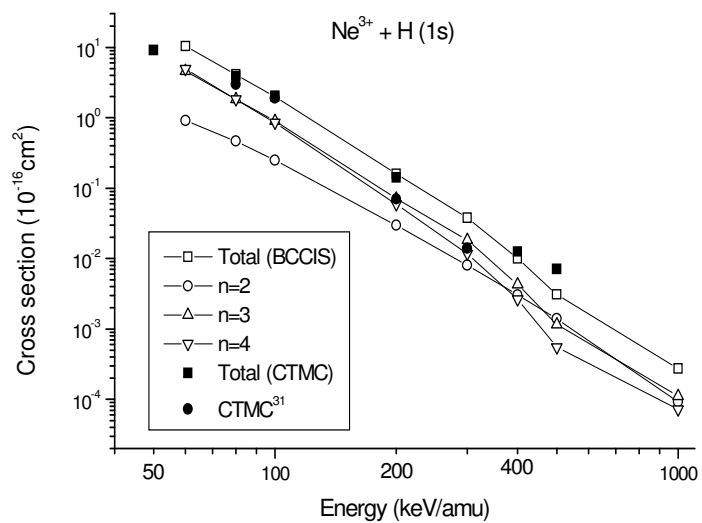


(b)

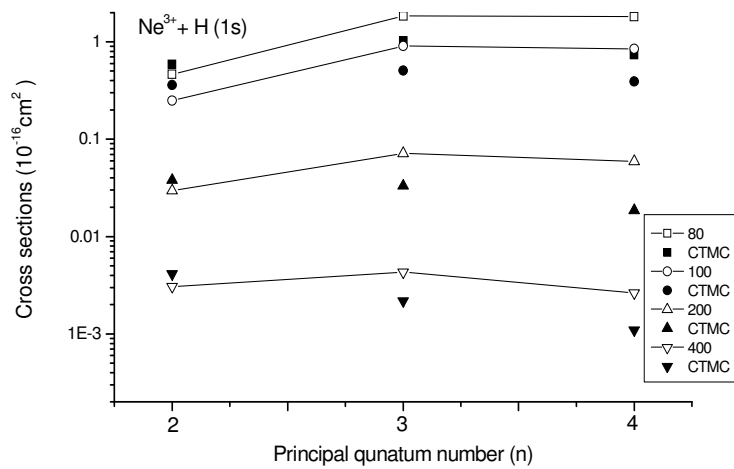


(c)

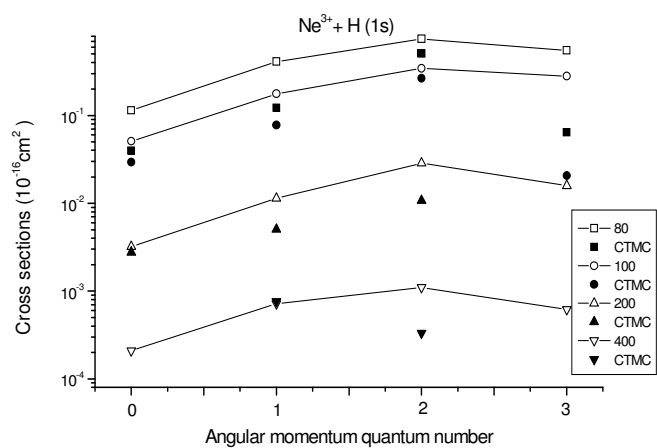
**Figure 2(a).** Variation of calculated total capture cross sections for the dominant n-states for the interaction  $\text{Ne}^{2+} + \text{H}(1s)$  with collision energy, **(b)** Capture cross sections from specific n-states by the projectile ion  $\text{Ne}^{2+}$  and **(c)** Cross sections for electron capture to specific  $\ell$  values for  $\text{Ne}^{2+}$  ion.



(a)

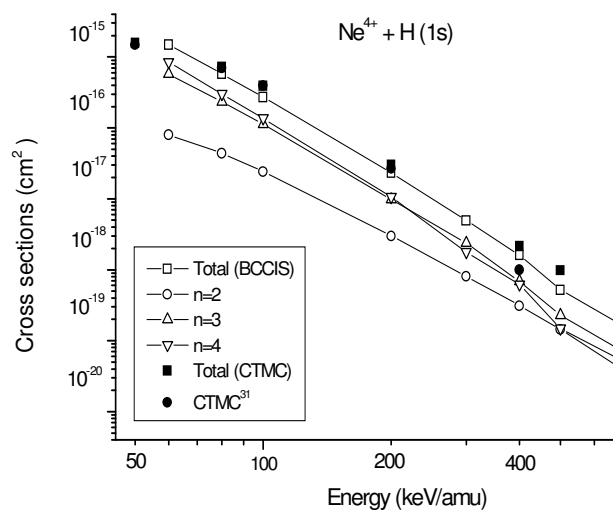


(b)

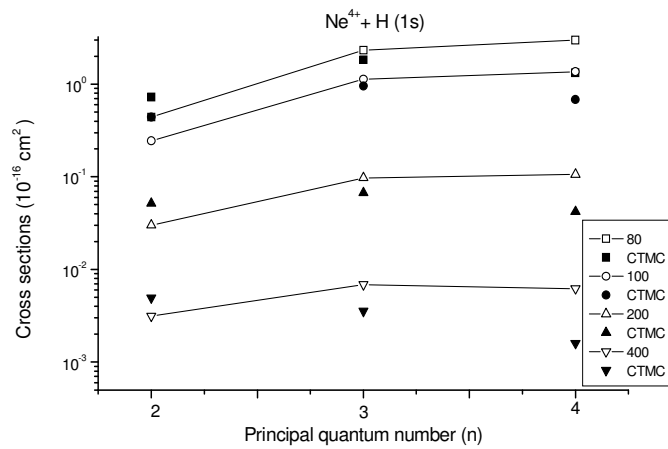


(c)

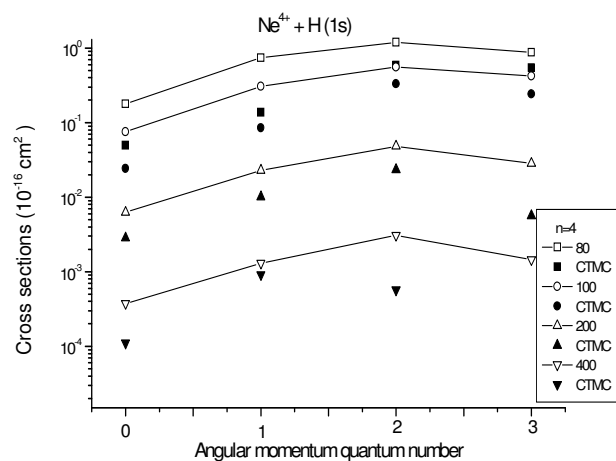
**Figure 3(a).** Variation of calculated total capture cross sections for the dominant n-states for the interaction  $\text{Ne}^{3+} + \text{H}(1s)$  with collision energy, **(b)** Capture cross sections from specific n-states by the projectile ion  $\text{Ne}^{3+}$  and **(c)** Cross sections for electron capture to specific  $\ell$  values for  $\text{Ne}^{3+}$  ion.



(a)

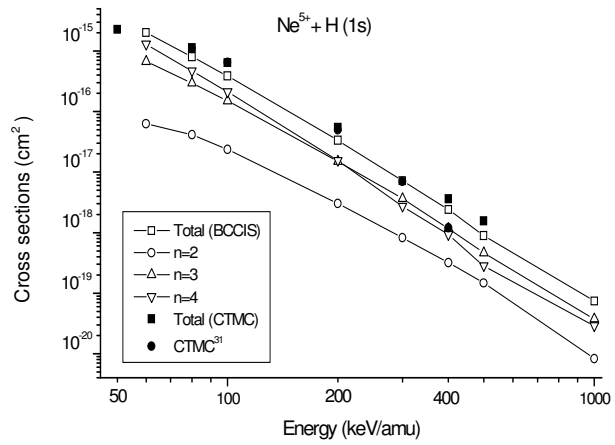


(b)

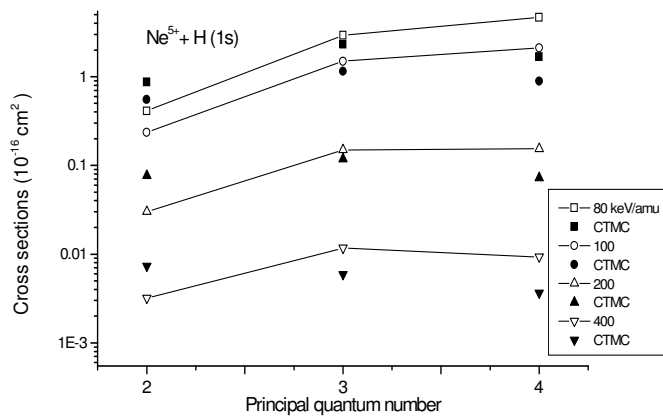


(c)

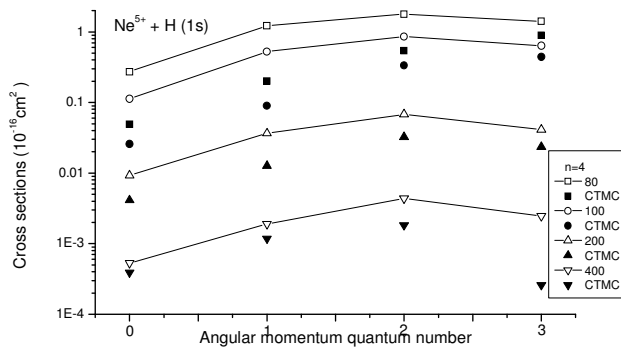
**Figure 4(a).** Variation of calculated total capture cross sections for the dominant  $n$ -states for the interaction  $\text{Ne}^{4+} + \text{H}(1s)$  with collision energy, **(b)** Capture cross sections from specific  $n$ -states by the projectile ion  $\text{Ne}^{4+}$  and **(c)** Cross sections for electron capture to specific  $\ell$  values for  $\text{Ne}^{4+}$  ion.



(a)

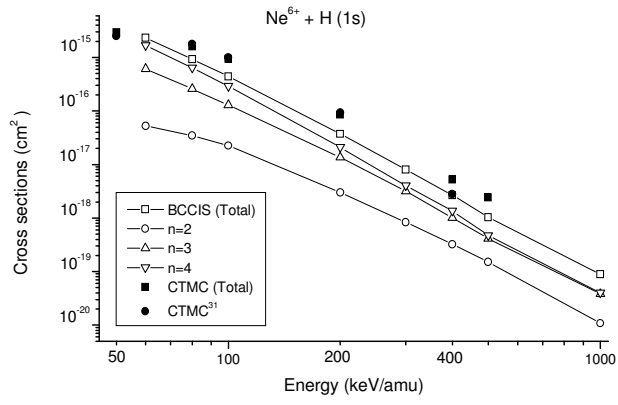


(b)

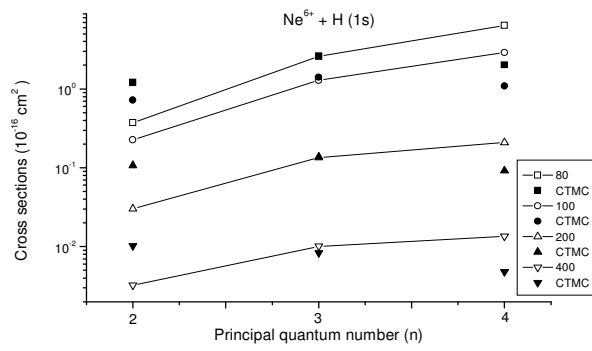


(c)

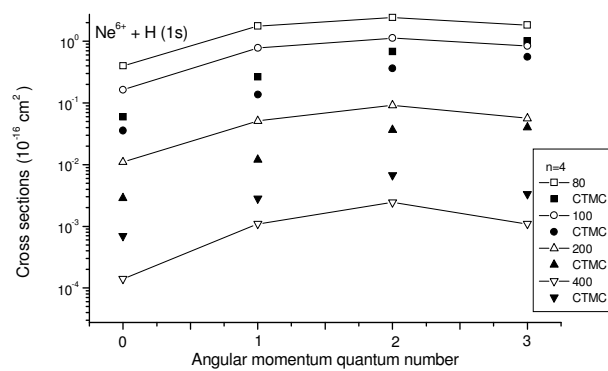
**Figure 5(a).** Variation of calculated total capture cross sections for the dominant n-states for the interaction  $\text{Ne}^{5+} + \text{H}(1s)$  with collision energy, **(b)** Capture cross sections from specific n-states by the projectile ion  $\text{Ne}^{5+}$  and **(c)** Cross sections for electron capture to specific  $\ell$  values for  $\text{Ne}^{5+}$  ion.



(a)

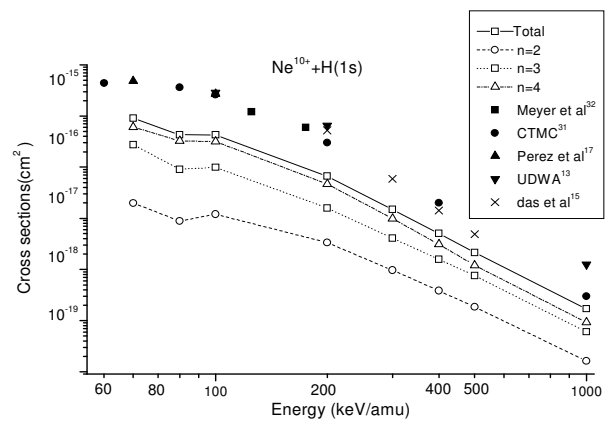


(b)

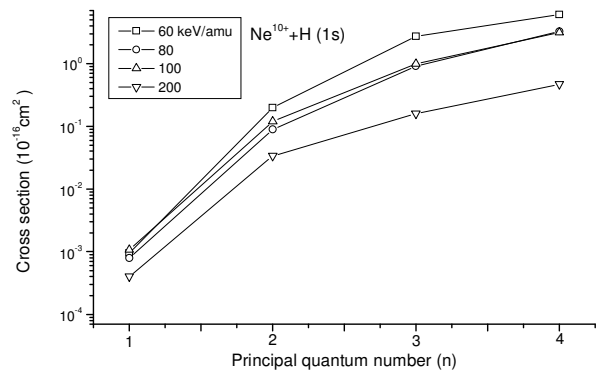


(c)

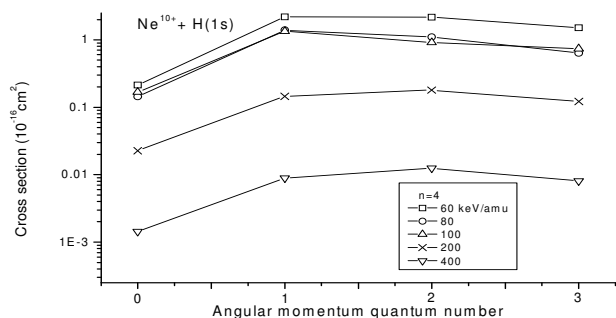
**Figure 6(a).** Variation of calculated total capture cross sections for the dominant  $n$ -states for the interaction  $\text{Ne}^{6+} + \text{H}(1s)$  with collision energy, **(b)** Capture cross sections from specific  $n$ -states by the projectile ion  $\text{Ne}^{6+}$  and **(c)** Cross sections for electron capture to specific  $l$  values for  $\text{Ne}^{6+}$  ion.



(a)

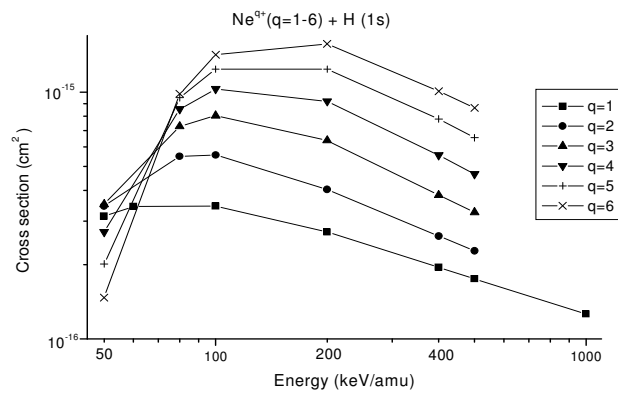


(b)



(c)

**Figure 7(a).** Variation of calculated total capture cross sections for the dominant n-states for the interaction  $\text{Ne}^{10+} + \text{H}(1s)$  with collision energy, **(b)** Capture cross sections from specific n-states by the projectile ion  $\text{Ne}^{10+}$  and **(c)** Cross sections for electron capture to specific  $\ell$  values for  $\text{Ne}^{10+}$  ion.



(a)

**Figure 8.** Calculated ionization cross sections for the interaction  $\text{Ne}^{q+}$  ( $q=1-6$ ) + H (1s) at collision energies ranging from 50 to 1000 keV/amu.

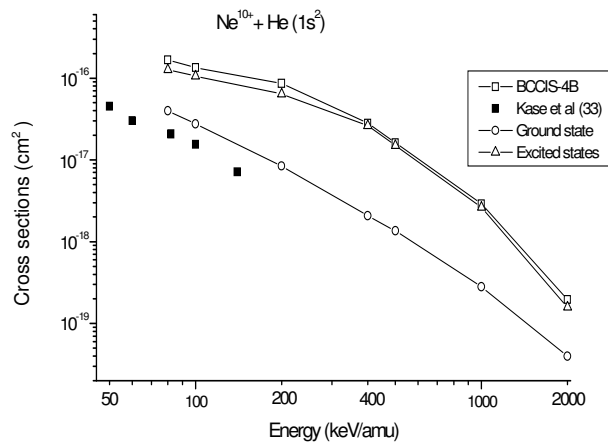


**Figure 9.** Calculated double capture cross sections for the interaction  $\text{Ne}^{10+}$  + He (1s<sup>2</sup>) at collision energies ranging from 80 to 2000 keV/amu.

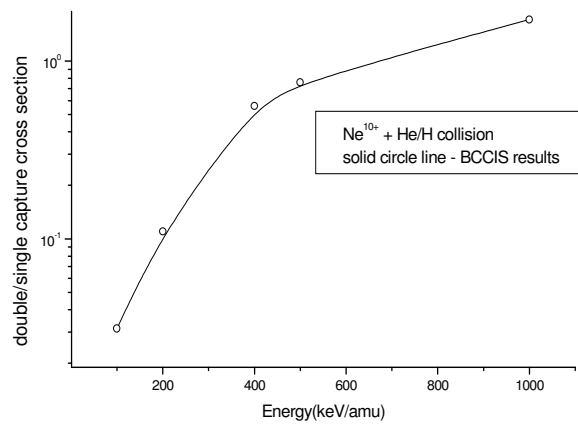


**Figure 10.** Calculated double-to-single capture cross sections for the interaction  $\text{Ne}^{10+} + \text{He} / \text{H}$  at collision energies ranging from 100 t

## REFERENCES

- [1] T D Mark and G H Dunn, *Electron impact ionization* (Vienna: Springer) (1985)
- [2] J Botero and J A Stephein, *Int. Bull. At. Mol. Data Fusion* 50-1, (1996)
- [3] R Rejoub, G B Lindsay and R F Stebbings *Phys. Rev.* **A65** 042713 (2002)
- [4] C M Lisse *Science* **277** 1625 (1997)
- [5] S Ghosh, A Dhara, M Purkait and C R Mandal *Indian J. Phys.* **84** 231(2010)

- [6] B B Dhal, L C Tribedi, U Tiwari, T G Lee, C D Lin, L Gulyas and P N Tandon *J. Phys.* **B33** 1069 (2000)
- [7] B B Dhal, L C Tribedi, U Tiwari, K V Thulasiram, P N Tandon, T G Lee, C D Lin and L Gulyas *Phys. Rev.* **A62** 022714 (2000)
- [8] Ajay Kumar, D Misra, A H Kelkar, U Kadhane, Y P Singh, G Lapicki, L Gulyas and L C Tribedi *J. Phys. B: At. Mol. Opt. Phys.* **39** 331 (2006)
- [9] S Ghosh, M Purkait, S Sounda, A Dhara and C R Mandal *Indian J. Phys.* **83** 1259(2009)
- [10] A Sharma *Indian J. Phys.* **84** 391(2010)
- [11] K C Rao, K G Bhushan, R Mukund, S M Rodrigues, S K Gupta and J V Yakhmi *Indian J. Phys.* **85** 1717(2011)
- [12] S Pal, Anshu and N Kumar *Indian J. Phys.* **85** 1729(2011)
- [13] H Ryufuku and T Watanabe *Phys. Rev.* **A20** 1828 (1979)
- [14] T P Grozdanov *J. Phys. B: At. Mol. Phys.* **13** 3835 (1980)
- [15] M Das, N C Deb and S C Mukherjee *Phys. Scr.* **54** 44 (1996)
- [16] R E Olson *Phys. Rev.* **A24** 1726 (1981)
- [17] J A Perez, R E Olson and P Beiersdorfer *J. Phys. B: At. Mol. Opt. Phys.* **34** 3063 (2001)
- [18] L F Errea, Clara Illescas, L Mendez, B Pons, A Riera and J Suarez *J. Phys. B: At. Mol. Opt. Phys.* **37** 4323 (2004)
- [19] L F Errea, Clara Illescas, L Mendez, B Pons, A Riera and J Suarez *Phys. Rev.* **A70** 052713 (2004)

- [20] L F Errea, Clara Illeseas, L Mendez, B Pons, A Riera and J Suarez *J. Phys. B: At. Mol. Opt. Phys.***39** L91 (2006)
- [21] M.Purkait, A Dhara, S Sounda and C R Mandal *J. Phys. B: At. Mol. Opt. Phys.***34** 755 (2001)
- [22] E Clementi and C Roetti *At. Data. Nucl. Data. Tab.***14** 185 (1974)
- [23] R E H Clark and J Abdallah Jr. *Phys. Scr.***T 62** 7 (1996)
- [24] S Sounda, A Dhara, M Purkait and C R Mandal *Eur. Phys. J. D***38** 257 (2006)
- [25] R R Lewis *Phys. Rev.***102** 537 (1956)
- [26] C Sinha and N C Sil *J. Phys. B: At. Mol. Phys.***11** L333 (1978)
- [27] A Roy, K Roy and N C Sil *J. Phys. B: At. Mol. Phys.***15** 1559 (1982); *Indian J. Phys.***B60** 418 (1986)
- [28] S Ghosh, A Dhara, C R Mandal and M Purkait *Phys. Rev.***A78** 042708 (2008)
- [29] J Eichler, A Tusji and I Ishihara *Phys. Rev.***A23** 2833 (1981)
- [30] S Ghosh, A Dhara, C R Mandal and M Purkait *FIZIKAA***18** 1 (2009)
- [31] G Maynard, R K Janev and K Katsonis *J. Phys. B: At. Mol. Opt. Phys.***25** 437 (1992)
- [32] F W Meyer, R A Phaneuf, H J Kim, P Hvelplund and P H Stelson *Phys. Rev.***A18** 515 (1979)
- [33] M Kase, A Kikuchi, A Yagishita and Y Nakai *J. Phys. B: At. Mol. Phys.***17** 671 (1984)
- [34] P Lowdin *Phys. Rev.***90** 120 (1953)
- [35] N V Novikov and V S Senashenko *Optics and Spectroscopy***86** 371 (1999)

**CHAPTER- 7**

**SINGLE-ELECTRON CAPTURE FROM HYDROGEN LIKE  
ATOMIC SYSTEMS**

## 7.1. INTRODUCTION

In recent years much work has been devoted to the study of single-electron capture by multi charged ions interacting with few- electron atoms. When many active electrons are involved in high energy ion- atom collisions, one has to face the question of the influence of electronic correlations on the magnitude of cross section for the process. The study of inter-electronic correlation has played a central role in atomic collision physics for a long time [1]. Not only this research is motivated by the quest for a better understanding of the fundamental few-body dynamics, but it has also practical implications for applied field, such as plasma physics and fusion research. For a long time, theoretical and experimental efforts concentrated on the energy dependence of total cross sections (TCSs) for a single-electron transfer from single-electron target atoms/ ions colliding with hydrogenlike projectiles. In this respect, previous theoretical work consists of calculations in the framework of three-body formalism such as the continuum distorted wave (CDW-3B) approximation of Belkic [2], coupled-channel calculations of Ford et al [3], Oppenheimer-Brinkman-Kramers (OBK) approximation [4,5], classical trajectory Monte Carlo (CTMC) method [6,7], CDW-3B and continuum intermediate state (CIS) approximations [8] and two-centre atomic orbital close-coupling method of Liu et al [9]. Some of these three-body models show a satisfactory agreement with experimental data, but these models completely neglect electronic correlations. In the present paper we shall be particularly interested in processes of the single-electron capture, in which the two electrons take part. Such processes involve scattering between the two hydrogen-like atoms. However, different quantum mechanical four-body formalisms for such reactions have been proposed. Different four-body theories such as boundary corrected first Born approximation (CB1-4B) of Mancev [10,11], CIS approximation of Banyard and Shirtcliffe [12], CTMC method of Becker and MacKellar [13], atomic-orbital expansion method of Fritsch and Lin [14], time-dependent Hartree-Fock approximation (TDHF) of Henne et al [15], CDW-4B method [16,17], CDW-4B and CB1-4B method of Mancev [18,19]. In the present theoretical investigation, we have focused our attention on charge transfer of hydrogen-like ions/ atom by the impact of H, He<sup>+</sup> and Li<sup>2+</sup> ions in the incident energy range between 20 and 5000 keV/amu.

The total and partial single-electron capture cross sections in  $\text{He}^+ - \text{He}^+$  collision has been studied within the two-electron form of the atomic-orbital expansion method [14]. The calculated results are in very close agreement with experimental data at lower energies. Cross sections for single-electron capture in the collision of partially and completely stripped projectile ions with hydrogen-like atoms were calculated by Belkic [2] in the framework of three-body CDW approximation at incident energies ranging from 25 keV to 10 MeV. In this method, the dynamic correlations have been neglected. The calculation shows that in the low energy range, the computed results are not in satisfactory agreement. The problem of single charge exchange in collision of hydrogen-like atoms with ground state hydrogen-like atom / ion was investigated by Mancev [10] in the framework of CB1-4B theory within the distorted wave four-body formalism. In such investigation, they have studied the sensitivity of the total cross sections to the choice of ground state wave function for helium-like atoms and the influence of non-captured electron on the final results. However, the agreements of the obtained results with the experimental findings are not satisfactory in the low energy range. Mancev [11] also investigated the cross sections for single-electron transfer from helium atoms by the impact of hydrogen atoms and helium ions using same method. They have used an independent particle model with one-electron Roothan-Hartree-Fock (RHF) orbital for the target atom. Agreement of the obtained results with the experimental data for  $\text{He}^+ + \text{He}$  collision is not satisfactory in the whole energy range. Becker and Mackellar [13] have developed a general four-body version of CTMC and calculated the electron transfer and ionization for  $\text{He}^+ + \text{H}$  and  $\text{H} + \text{H}$  collisions in the energy range 35-1000 keV, but there are substantial differences compared with the experimental results. The CDW-4B model [18] has been used to investigate the charge exchange between hydrogen-like projectiles and atoms. In this calculation, the effects of electron correlation have been explicitly taken into account in the complete perturbation potential. The calculation shows that below 200 keV/amu for  $\text{He}^+ + \text{He}$  collision and 150 keV for  $\text{He}^+ + \text{H}$  collision, respectively, the computed results are not in satisfactory agreement. Later, Mancev [19] investigated the total cross sections for charge transfer in  $\text{Li}^{2+}-\text{H}$  and  $\text{He}^+ - \text{He}^+$  collisions using the CB1-4B and CDW-4B in the energy range 10-5000 keV/amu. In this calculation, the dynamic correlation has been taken into account through the perturbation potential. The computed results are not in agreement with the experimental results in the energy range 10-300 keV/amu. Recently, electron capture by fast

Be<sup>q+</sup> (q=2,3) and B<sup>q+</sup> (q=3,4) ions in collisions with atomic hydrogen have been also studied by Liu et al [9] in the framework of the two-centre atomic orbital close coupling method (TC-AOCC) in the energy region from 0.1 keV/amu to 100 keV/amu. Total and sub-shells state-selective cross sections are compared with available experimental and other theoretical data. These results are quite satisfactory. In this context, Belkic et al [20] have extensively discussed different quantum mechanical four-body methods for various inelastic ion-atom collisions. Based on the success of four-body boundary corrected continuum intermediate state (BCCIS-4B) approximation [21], we are motivated to study the above mentioned processes in the framework of the BCCIS-4B theory at impact energies 20-5000 keV/amu.

The plan of this paper is as follows. We present the details of our calculations in Sec.II and discuss our computed results in Sec.III. Finally, we make our concluding remarks in Sec.IV. Atomic units will be used throughout unless otherwise stated.

## 7.2. THEORY

Single-electron capture in the process of the scattering between two hydrogen-like atomic systems may be written as

$$(Z_P; e_1)_{i_1} + (Z_T, e_2)_{i_2} \rightarrow (Z_P; e_1, e_2)_f + Z_T, \quad (1)$$

where  $Z_P$  and  $Z_T$  are, respectively, the nuclear charges of the projectile and the target. Here e, T and P represent active electron, target ion and projectile ion respectively.  $e_1$  and  $e_2$  are the two electrons initially bound to the projectile and target nucleus respectively. Finally the electron  $e_2$  is captured by the projectile but  $e_1$  occupies the same orbital before and after collision. Let  $\vec{s}_1$  and  $\vec{s}_2$  ( $\vec{x}_1$  and  $\vec{x}_2$ ) be position vectors of the first and second electrons ( $e_1$  and  $e_2$ ) relative to the nuclear charge of the projectile  $Z_P$  (target  $Z_T$ ). The inter-electronic coordinate is denoted by  $\vec{r}_{12} = \vec{s}_1 - \vec{s}_2 = \vec{x}_1 - \vec{x}_2$ .  $\vec{R}$  denotes the position vector of the projectile (P) relative to the target (T) nucleus. In the entrance channel, it is convenient to introduce  $\vec{R}_T$  as the position vector between

the center of mass of  $(Z_p; e_1)$  and  $(Z_T; e_2)$  system, and  $\vec{R}_p$  is the position vector of the center of mass of  $(Z_p; e_1, e_2)$  system relative to  $Z_T$ . The total Hamiltonian of the system may be written as

$$H = H_i + V_i = H_f + V_f \quad (2)$$

where  $H_{i,f}$  represents Hamiltonian in the entrance and exit channel respectively and  $V_{i,f}$  are the corresponding perturbation potentials, respectively. Let  $M_T$  ( $M_p$ ) be the mass of the target (projectile) nucleus. In the initial channel, one may write

$$H_i = -\frac{1}{2\mu_i} \nabla_{R_T}^2 + \frac{(Z_p-1)(Z_T-1)}{R_T} - \frac{1}{2a} \nabla_{x_2}^2 - \frac{Z_T}{x_2} - \frac{1}{2b} \nabla_{s_1}^2 - \frac{Z_p}{s_1}, \quad (3)$$

$$V_i = \frac{Z_p Z_T}{R} - \frac{Z_T}{x_1} - \frac{Z_p}{s_2} + \frac{1}{r_{12}} - \frac{(Z_p-1)(Z_T-1)}{R_T}$$

$$\approx Z_T \left( \frac{1}{R} - \frac{1}{x_1} \right) + Z_p \left( \frac{1}{R} - \frac{1}{s_2} \right) + \left( \frac{1}{r_{12}} - \frac{1}{R} \right).$$

When the aggregates P and T are far apart, they interact through a residual Coulomb potential  $\frac{(Z_p-1)(Z_T-1)}{R_T}$ . According to the prescriptions of collision theory [22], this asymptotic potential

has to appear in the initial channel Hamiltonian ( $H_i$ ). However, the initial perturbation potential  $V_i$  is obtained by subtracting the asymptotic potential from the total interaction potential between projectile and target. So, in the initial channel  $V_i$  decreases much faster than Coulomb interaction at large internuclear distance ( $\vec{R}$ ). In the exit channel, the target is a bare ion. Thus,  $H_f$  and  $V_f$  can be written as

$$H_f = -\frac{1}{2\mu_f} \nabla_{R_p}^2 + \frac{Z_T(Z_p-2)}{R_p} - \frac{1}{2b} \nabla_{s_1}^2 - \frac{1}{2b} \nabla_{s_2}^2 - \frac{Z_p}{s_1} - \frac{Z_p}{s_2} + \frac{1}{r_{12}},$$

$$V_f = \frac{Z_p Z_T}{R} - \frac{Z_T}{x_1} - \frac{Z_T}{x_2} - \frac{Z_T(Z_p - 2)}{R_p} \approx \frac{2Z_T}{R} - \frac{Z_T}{x_1} - \frac{Z_T}{x_2}, \quad (4)$$

where  $\mu_i = \frac{(1 + M_p)(M_T + 1)}{(2 + M_p + M_T)}$ ,  $\mu_f = \frac{M_T(2 + M_p)}{(2 + M_p + M_T)}$ ,  $a = \frac{M_T}{1 + M_T}$ ,  $b = \frac{M_p}{1 + M_p}$ .

The prior form of the scattering amplitude may be written in the form

$$T_{if}^{(-)} = \langle \psi_f^- | V_i | \psi_i \rangle \quad (5)$$

Here the wavefunction in the initial channel is given by

$$\psi_i(\vec{R}_T, \vec{x}_2, \vec{s}_1) = \varphi_T(\vec{x}_2) \varphi_p(\vec{s}_1) \chi_i^+(\vec{R}_T),$$

where  $\varphi_T(\vec{x}_2)$  and  $\varphi_p(\vec{s}_1)$  are the target bound state and the projectile bound state wavefunctions, respectively.  $\chi_i^+(\vec{R}_T)$  is the coulomb distorted wave for the relative motion of P and T in the centre of mass frame of the whole system which satisfies the equation

$$\left( -\frac{1}{2\mu_i} \nabla_{R_T}^2 + \frac{(Z_p - 1)(Z_T - 1)}{R_T} - \frac{k_f^2}{2\mu_i} \right) \chi_i^+(\vec{R}_T) = 0 \quad (6)$$

Solving this equation, we find

$$\chi_i^+(\vec{R}_T) = e^{-\frac{\pi}{2}\alpha_3} \Gamma(1 + i\alpha_3) e^{i\vec{k}_i \cdot \vec{R}_T} {}_1F_1\left\{-i\alpha_3; 1; i(\vec{k}_i R_T - \vec{k}_i \cdot \vec{R}_T)\right\} \quad (7)$$

where  $\alpha_3 = \frac{(Z_p - 1)(Z_T - 1)}{v_i}$ . Furthermore,  $\vec{k}_i$  is the initial wave vector. The electron in the projectile is passive. The passive electron plays the role of screening the projectile ion. However, the interaction of the target ion with the screened projectile ion and that between the active electron and the projectile core are described by the Coulomb continuum wavefunctions in the final channel. The Coulomb continuum wavefunction in the final channel  $\psi_f^{(-)}$  is given by

$$\psi_f^{(-)} = e^{\frac{\pi}{2}(\alpha_1 - \alpha_2)} \Gamma(1 + i\alpha_1) \Gamma(1 - i\alpha_2) e^{i\vec{k}_f \cdot \vec{R}_p} \varphi_f(\vec{s}_1, \vec{s}_2) {}_1F_1\{-i\alpha_1; 1; -i(v_f x_2 + \vec{v}_f \cdot \vec{x}_2)\} {}_1F_1\{i\alpha_2; 1; -i(k_f R_T + \vec{k}_f \cdot \vec{R}_T)\} \quad (8)$$

where  $\alpha_1 = \frac{Z_T}{v_f}$  ,  $\alpha_2 = \frac{Z_T(Z_p - 1)}{v_f}$ .

Here  $\varphi_f(\vec{s}_1, \vec{s}_2)$  is the bound state wavefunction of the atomic system ( $Z_p$ ;  $e_1, e_2$ ). The bound state wavefunction of  $\text{Li}^+$  or  $\text{He}$  i.e.  $\varphi_f(\vec{s}_1, \vec{s}_2)$  may be written as [23] a set of two electron hydrogenic configurations  $\varphi_{\lambda, \lambda'}(\vec{s}_1, \vec{s}_2)$ .

$$\varphi_{\lambda, \lambda'}(\vec{s}_1, \vec{s}_2) = \sum_{\lambda \leq \lambda'} a_{\lambda \lambda'}^f \varphi_{\lambda \lambda'}^f(\vec{s}_1, \vec{s}_2),$$

where  $\varphi_{\lambda \lambda'}^f$  is a configuration with the same symmetry as  $\varphi_f$ .

$$\varphi_{\lambda \lambda'}^f(\vec{s}_1, \vec{s}_2) = N_f \left\{ R_{n_\lambda l_\lambda}(s_1) R_{n_{\lambda'} l_{\lambda'}}(s_2) Y_{l_\lambda l_{\lambda'}}^{\text{LM}}(\hat{s}_1, \hat{s}_2) + (-1)^\delta R_{n_{\lambda'} l_{\lambda'}}(s_1) R_{n_\lambda l_\lambda}(s_2) Y_{l_{\lambda'} l_\lambda}^{\text{LM}}(\hat{s}_1, \hat{s}_2) \right\}. \quad (9)$$

Here the constant  $N_f = \frac{1}{\sqrt{2}}$  for  $\lambda \neq \lambda'$

$$= \frac{1 + (-1)^{L+S}}{4} \text{ for } \lambda = \lambda' \text{ and } \delta = L + S - l_\lambda - l_{\lambda'}.$$

$\hat{s}_k$  ( $k=1,2$ ) is the direction of the vector  $\vec{s}_k$ ,  $R_{n_\lambda l_\lambda}(s_k)$  and  $Y_{l_\lambda l_{\lambda'}}^{\text{LM}}(\hat{s}_1, \hat{s}_2)$  are radial hydrogenic function and spherical harmonics, respectively.

The transition amplitude in the post form can be written as

$$T_{if}^{(+)} = \langle \psi_f | V_f | \psi_i^+ \rangle \quad (10)$$

where  $\psi_f$  is the wave function in the final channel which is given by  $\psi_f = \varphi_f(\vec{s}_1, \vec{s}_2) \chi_f^-(\vec{R}_p)$ .  $\varphi_f(\vec{s}_1, \vec{s}_2)$  is the final bound-state wavefunction and  $\chi_f^-(\vec{R}_p)$ , the Coulomb distorted wave in the exit channel, is given by

$$\chi_f^-(\vec{R}_p) = e^{-\frac{\pi}{2}\alpha_3} \Gamma(1 - i\alpha_3) e^{i\vec{k}_f \cdot \vec{R}_p} {}_1F_1\{i\alpha_3; 1; -i(\vec{k}_f \cdot \vec{R}_p + \vec{k}_f \cdot \vec{R}_p)\} \quad (11)$$

where  $\alpha_3 = \frac{Z_T(Z_P - 2)}{v_f}$ .  $\vec{k}_f$  is the final wave vector. Here, the passive electron in the projectile plays the role of screening the projectile ion in the initial channel. However, the interaction of the active electron and the target ion with the screened projectile ion are described by the Coulomb continuum wavefunctions. So, the wavefunction in the initial channel may be given by

$$\psi_i^+ = e^{\frac{\pi}{2}(\alpha_1 - \alpha_2)} \Gamma(1 - i\alpha_1) \Gamma(1 + i\alpha_2) e^{i\vec{k}_i \cdot \vec{R}_T} \varphi_i(\vec{x}_2, \vec{s}_1) {}_1F_1\{i\alpha_1; 1; i(v_i s_2 + \vec{v}_i \cdot \vec{s}_2)\} {}_1F_1\{-i\alpha_2; 1; ia(\vec{k}_i \cdot \vec{R}_p - \vec{k}_i \cdot \vec{R}_p)\}, \quad (12)$$

$$\text{where } \alpha_1 = \frac{(Z_P - 1)}{v_i}, \quad \alpha_2 = \frac{Z_T(Z_P - 1)}{v_i}.$$

Here  $\varphi_i(\vec{x}_2, \vec{s}_1) = \varphi_T(\vec{x}_2) \varphi_p(\vec{s}_1)$ .  $\varphi_T(\vec{x}_2)$  and  $\varphi_p(\vec{s}_1)$  are the hydrogen-like wavefunction for the target and the projectile respectively. The transition amplitudes in the prior and post forms for single- electron capture in the BCCIS-4B theory may be written as

$$\begin{aligned} T_{if}^{\text{BCCIS}(-)} = N \iiint d\vec{s}_1 d\vec{x}_2 d\vec{R} e^{i\vec{k}_i \cdot \vec{R}_T - i\vec{k}_f \cdot \vec{R}_p} \varphi_f^*(\vec{s}_1, \vec{s}_2) {}_1F_1\{i\alpha_1; 1; i(v_f x_2 + \vec{v}_f \cdot \vec{x}_2)\} \times \\ {}_1F_1\{-i\alpha_2; 1; i(\vec{k}_f \cdot \vec{R}_T + \vec{k}_f \cdot \vec{R}_T)\} \left\{ Z_T \left( \frac{1}{R} - \frac{1}{x_1} \right) + Z_P \left( \frac{1}{R} - \frac{1}{s_2} \right) + \left( \frac{1}{r_{12}} - \frac{1}{R} \right) \right\} \times \\ \varphi_i(\vec{x}_2, \vec{s}_1) {}_1F_1\{-i\alpha_3; 1; i(\vec{k}_i \cdot \vec{R}_T - \vec{k}_i \cdot \vec{R}_T)\}, \quad (13) \end{aligned}$$

where  $N = e^{\frac{\pi}{2}(\alpha_1 - \alpha_2 - \alpha_3)} \Gamma(1 - i\alpha_1) \Gamma(1 + i\alpha_2) \Gamma(1 + i\alpha_3)$ ,  $\alpha_1 = \frac{Z_T}{V_f}$ ,  $\alpha_2 = \frac{Z_T(Z_P - 1)}{V_f}$  and

$$\alpha_3 = \frac{(Z_P - 1)(Z_T - 1)}{V_i}.$$

and  $T_{if}^{BCCIS(+)} = N \iiint d\bar{s}_1 d\bar{s}_2 d\bar{R} e^{i\bar{k}_i \cdot \bar{R}_T - i\bar{k}_f \cdot \bar{R}_p} \varphi_f^*(\bar{s}_1, \bar{s}_2) \times {}_1F_1\{-i\alpha_3; 1; i(k_f R + \bar{k}_f \cdot \bar{R})\} \times$

$$\left( \frac{2Z_T}{R} - \frac{Z_T}{x_1} - \frac{Z_T}{x_2} \right) \times \varphi_i(\bar{x}_2, \bar{s}_1) {}_1F_1\{i\alpha_1; 1; i(v_i s_2 + \bar{v}_i \cdot \bar{s}_2)\} {}_1F_1\{-i\alpha_2; 1; ia(k_i R_p - \bar{k}_i \cdot \bar{R}_p)\}, \quad (14)$$

where  $N = e^{\frac{\pi}{2}(\alpha_1 - \alpha_2 - \alpha_3)} \Gamma(1 - i\alpha_1) \Gamma(1 + i\alpha_2) \Gamma(1 + i\alpha_3)$ ,  $\alpha_1 = \frac{(Z_P - 1)}{V_i}$ ,  $\alpha_2 = \frac{Z_T(Z_P - 1)}{V_i}$ ,

$$\text{and } \alpha_3 = \frac{Z_T(Z_P - 2)}{V_f}.$$

Using the integral representation of confluent hypergeometric function, the technique of Fourier transform, Feynman parametric integral such as  $\frac{1}{a'b'} = \int_0^1 \frac{dx}{[a'x + (1-x)b']^2}$  and applying the Lewis integral [24], respectively, equation (13) and (14) can be expressed in both prior and post forms as

$$T_{if}^{BCCIS(\pm)} = 32C' N \frac{1}{2\pi i} \oint dt_3 t_3^{-i\alpha_3 - 1} (t_3 - 1)^{i\alpha_3} \ell \lim_{\beta_1, \varepsilon_1 \rightarrow 0} D(\beta_1, \delta_2, \gamma_1, \gamma_2, \varepsilon_1) \int_0^1 \frac{dx}{\Delta} \int_0^\infty dy K \quad (15)$$

where  $K = -\frac{1}{A} \left( \frac{A}{A+B} \right)^{i\alpha_1} \left( \frac{A}{A+D} \right)^{-i\alpha_2} {}_2F_1\left\{i\alpha_1; -i\alpha_2; 1; \frac{P}{Q}\right\}$ ,  $P = BD - AC$ ,  $Q = (A+B)(A+D)$ ,

$$\Delta^2 = \left\{ \frac{\bar{k}_f}{2 + M_p} - (1-b)\bar{k}_i \right\}^2 x(1-x) + \lambda_1^2 x + (1-x)\beta_1^2, \quad \lambda_1 = \gamma_1' + \gamma_1 \quad \text{for the prior form and}$$

$$\Delta^2 = \left\{ \frac{\bar{\mathbf{k}}_f}{2 + M_p} - \frac{\bar{\mathbf{k}}_i}{1 + M_T} \right\}^2 x(1-x) + \lambda_1^2 x + (1-x)\beta_1^2 \text{ for the post form.}$$

Here A, B, C and D in prior form (-) and post form (+) are given by

$$A^\pm = A_1^\pm y^2 + 2y(\beta^\pm A_1^\pm + A_{22}^\pm + A_{23}^\pm) + A_3^\pm,$$

$$B^\pm = B_1^\pm y^2 + 2y(\beta^\pm B_1^\pm + B_{22}^\pm + B_{23}^\pm) + B_3^\pm,$$

$$C^\pm = C_1^\pm y^2 + 2y(\beta^\pm C_1^\pm + C_{22}^\pm + C_{23}^\pm) + C_3^\pm,$$

$$D^\pm = D_1^\pm y^2 + 2y(\beta^\pm D_1^\pm + D_{22}^\pm + D_{23}^\pm) + D_3^\pm,$$

where in prior form,  $\beta^- = \gamma_2$ ,

$$A_1^- = \mathbf{q}_-^2 + (\delta_2 + \Delta + \varepsilon_1)^2 - 2\bar{\mathbf{q}}_- \cdot \bar{\mathbf{v}}_f t_1 - 2i v_f t_1 (\delta_2 + \Delta + \varepsilon_1),$$

$$B_1^- = -2\bar{\mathbf{q}}_- \cdot \bar{\mathbf{k}}_f + 2\bar{\mathbf{v}}_f \cdot \bar{\mathbf{k}}_f t_1 - 2ik_i (\delta_2 + \Delta + \varepsilon_1) - 2v_f k_f t_1,$$

$$C_1^- = 2\bar{\mathbf{q}}_- \cdot \bar{\mathbf{k}}_i - 2\bar{\mathbf{v}}_f \cdot \bar{\mathbf{k}}_i t_1 - 2ik_i (\delta_2 + \Delta + \varepsilon_1) - 2v_f k_i t_1,$$

$$D_1^- = -2k_i k_f - 2\bar{\mathbf{k}}_i \cdot \bar{\mathbf{k}}_f,$$

$$A_{22}^- = \beta_2^- \{ \mathbf{q}_-^2 + (\Delta + \varepsilon_1)^2 + \gamma_2^2 \}, \quad B_{22}^- = -2\beta_2^- \{ \bar{\mathbf{q}}_- \cdot \bar{\mathbf{k}}_f + ik_f (\Delta + \varepsilon_1) \},$$

$$C_{22}^- = 2\beta_2^- \{ \bar{\mathbf{q}}_- \cdot \bar{\mathbf{k}}_i - ik_i (\Delta + \varepsilon_1) \}, \quad D_{22}^- = -2\beta_2^- (k_i k_f + \bar{\mathbf{k}}_i \cdot \bar{\mathbf{k}}_f),$$

$$A_{23}^- = (\Delta + \varepsilon_1) P_{23}^-, \quad B_{23}^- = -ik_f P_{23}^-, \quad C_{23}^- = -ik_i P_{23}^-, \quad D_{23}^- = 0$$

$$A_3^- = E_{11}^- \{ \mathbf{q}_-^2 + (\Delta + \varepsilon_1 + \gamma_2)^2 \}, \quad B_3^- = -E_{11}^- \{ 2\bar{\mathbf{q}}_- \cdot \bar{\mathbf{k}}_f + 2ik_f (\Delta + \varepsilon_1 + \gamma_2) \}$$

$$C_3^- = E_{11}^- \{2\bar{q}_- \cdot \bar{k}_f - 2ik_i(\Delta + \varepsilon_1 + \gamma_2)\}, \quad D_3^- = -2E_{11}^- \{\bar{k}_i \cdot \bar{k}_f + k_i k_f\}.$$

The terms  $\bar{q}_-$ ,  $\beta_2^-$ ,  $P_{23}^-$  and  $E_{11}^-$  can be explicitly written as

$$\bar{q}_- = \bar{k}_f \left(1 - \frac{x}{2 + M_T}\right) - (1 + bx - x)\bar{k}_i, \quad \beta_2^- = \delta_2 - i v_f t_1,$$

$$P_{23}^- = \left\{ \frac{\bar{k}_f}{2 + M_P} + (1 - a)\bar{k}_i \right\}^2 + \delta_2^2 + \gamma_2^2 - 2\bar{v}_f \cdot \left\{ \frac{\bar{k}_f}{2 + M_P} + (1 - a)\bar{k}_i \right\} t_1 - 2i v_f \delta_2 t_1,$$

$$E_{11}^- = P_{23}^- + 2\delta_2 \gamma_2 - 2i v_f \gamma_2 t_1,$$

and in post form,  $\beta^+ = \delta_2$ ,

$$A_1^+ = q_+^2 + (\gamma_2 + \Delta + \varepsilon_1)^2 + 2\bar{q}_+ \cdot \bar{v}_i t_1 - 2i v_i (\gamma_2 + \Delta + \varepsilon_1) t_1,$$

$$B_1^+ = 2\bar{q}_+ \cdot \bar{k}_i - 2ik_i(\gamma_2 + \Delta + \varepsilon_1),$$

$$C_1^+ = -2\bar{q}_+ \cdot \bar{k}_f - 2\bar{v}_i \cdot \bar{k}_f t_1 - 2ik_f(\gamma_2 + \Delta + \varepsilon_1) - 2v_i k_f t_1,$$

$$D_1^+ = -2\bar{k}_i \cdot \bar{k}_f - 2k_i k_f,$$

$$A_{22}^+ = \lambda_2^+ \{q_+^2 + (\Delta + \varepsilon_1)^2 + \delta_2^2\}, \quad B_{22}^+ = \lambda_2^+ \{\bar{q}_+ \cdot \bar{k}_i - 2ik_i(\Delta + \varepsilon_1)\},$$

$$C_{22}^+ = \lambda_2^+ \{\bar{q}_+ \cdot \bar{k}_f - 2ik_f(\Delta + \varepsilon_1)\}, \quad D_{22}^+ = -2\lambda_2^+ \{\bar{k}_i \cdot \bar{k}_f + k_i k_f\},$$

$$A_{23}^+ = (\Delta + \varepsilon_1)P_{23}^+, \quad B_{23}^+ = -ik_i P_{23}^+, \quad C_{23}^+ = -ik_f P_{23}^+, \quad D_{23}^+ = 0,$$

$$A_3^+ = E_{11}^+ \{q_+^2 + (\delta_2 + \Delta + \varepsilon_1)^2\}, \quad B_3^+ = 2E_{11}^+ \{\bar{q}_+ \cdot \bar{k}_i - ik_i(\delta_2 + \Delta + \varepsilon_1)\},$$

$$C_3^+ = -2E_{11}^+ \{\bar{q}_+ \cdot \bar{k}_f + ik_f(\delta_2 + \Delta + \varepsilon_1)\}, \quad D_3^+ = -2E_{11}^+ \{\bar{k}_i \cdot \bar{k}_f + k_i k_f\}.$$

The terms  $\bar{q}_+$ ,  $\lambda_2^+$ ,  $P_{23}^+$  and  $E_{11}^+$  can be explicitly written as

$$\bar{q}_+ = \bar{k}_f \left(1 - \frac{x}{2 + M_p}\right) - \bar{k}_i \left(1 - \frac{x}{1 + M_p}\right), \quad \lambda_2^+ = \gamma_2 - i v_i t_1$$

$$P_{23}^+ = \left\{ \frac{\bar{k}_f}{2 + M_p} + \frac{\bar{k}_i}{1 + M_T} \right\}^2 + \delta_2^2 + \gamma_2^2 - 2 \bar{v}_i \cdot \left( \frac{\bar{k}_f}{2 + M_p} + \frac{\bar{k}_i}{1 + M_T} \right) t_1, \quad E_{11}^+ = P_{23}^+ + 2 \delta_2 \gamma_2 - 2 i v_i \delta_2 t_1.$$

Here the constant  $C'$  originates from the initial and final bound state wavefunctions.  $D(\beta_1, \delta_2, \gamma_1, \gamma_2, \varepsilon_1)$  is a parametric differential operator used to generate the excited-state wavefunctions.  $\delta_2, \gamma_1$  and  $\gamma'_1, \gamma_2$  are the orbital component of the initial and final bound state wavefunctions. Finally, the total cross sections in prior form ( $Q_{if}^{(-)}$ ) and post form ( $Q_{if}^{(+)}$ ) are given by

$$Q_{if}^{(\pm)}(\pi a_0^2) = \frac{\mu_i \mu_f}{4 \pi^2} \cdot \frac{k_f}{k_i} \int \left| T_{if}^{BCCIS(\pm)} \right|^2 d\Omega \quad (16)$$

where  $d\Omega$  is the solid angle around  $\bar{k}_i$ .

The transition amplitude contains three-dimensional integrals such as Lewis, Feynman and a complex contour integration. The final real form of this complex contour integration (in  $t_3$ ) in equation (15) may be written [25] as

$$\begin{aligned} & \frac{1}{2 \pi i} \oint dt_3 t_3^{-i \alpha_3 - 1} (t_3 - 1)^{i \alpha_3} f(t_3) dt_3, \quad t_3 \rightarrow \tau \\ & = \frac{e^{\pi \alpha_3} - e^{-\pi \alpha_3}}{2 \pi i} \int_0^\infty \left[ e^{i \alpha_3 \tau} \varphi\left(\frac{1}{e^\tau + 1}\right) + e^{-i \alpha_3 \tau} e^{-\tau} \varphi\left(\frac{1}{e^{-\tau} + 1}\right) \right] / (1 + e^{-\tau}) d\tau + f(0) \end{aligned} \quad (17)$$

where  $e^\tau = (1 - t_3)/t_3$ ,  $\tau$  being the transformed integration variable, and  $\varphi(t_3) = f(t_3) - f(0)$ .

The real two-dimensional integration in  $y$  and  $\tau$  is finally carried out numerically. To evaluate the double integral ( $y$  and  $\tau$ ), we first perform the  $y$  integration by Gauss quadrature method with different fixed values of  $\tau$  which are the Gauss Laguerre quadrature points required for the subsequent  $\tau$  integration. The Feynman integral has been evaluated numerically with the 48-point Gauss-Legendre quadrature method. Finally, integration over the scattering angles has been performed with the 48-point Gauss-Legendre quadrature method. However, it may be mentioned that cross sections have finally been evaluated with an accuracy of 0.1%.

### 7.3. RESULTS AND DISCUSSION

The total single-electron capture cross sections for the process of the scattering between two hydrogen-like atomic systems were obtained by summing over all contributions (ground state ( $1s^2$ ), singly excited states  $1s2s$ ,  $1s2p$ ) from individual shells and sub-shells upto  $n=2$ , except  $H + H$  collision as the  $H^-$  ion does not have any stable excited states. So only one state is to be taken into account in the capture process. The variation of single-electron capture cross sections of ground state hydrogen like ions by the impact of different projectile ions as a function of the incident energy ranging from 20-5000 keV/amu are plotted in Figs 1-4, respectively using both prior and post forms of BCCIS-4B approximation. Post-prior discrepancy does not exceed 20% for all interactions above 70 keV/amu. Numerical computations are carried out for the following reactions.



The present results obtained for the reaction (18) are presented in Fig.1 in both forms of BCCIS-4B approximation. Our computed results for total single-electron capture cross sections have also been compared with the measurements of McClure [26], Schryber [27], Hill et al [28] and the

theoretical results of Mancev [10] obtained by CB1-4B method, the continuum-intermediate-states approximation (CIS) of Banyard and Shirtcliffe [12], CDW method of Moore and Banyard [29] using Hartree-Fock (HF) function, the first Born approximation of Mapleton [30] and the couple-state results of Wang et al [31]. The agreement between BCCIS-4B theory and experimental results [26,27,28] are found to be satisfactory in both low and intermediate energy range. Additional experimental results at higher impact energies are very much needed to provide a better test of our formalism. The CB1-4B results of Mancev [10] obtained by means of the Hylleraas wave function [32] for  $H(1s^2)$  have a trend of departing from experimental data below 200 keV as collision energy decreases. This is expected because the formulation does not include intermediate continuum states which are very much important for the description of a charge transfer event. It is also observed that the present computed results using Hylleraas wave function [32] agree with the theoretical results of Moore and Banyard [29], but agreement is not satisfactory with the CIS method of Banyard and Shirtcliffe [12] using HF function in the low energy region. The reason may be attributed to the fact that CIS method does not satisfy proper boundary condition. However, the results of Mapleton [30] obtained by the two parameter wavefunction of Chandrasekhar [33] in the first Born approximation overestimate the present findings at low energies. This feature is obvious because first Born approximation is valid at high energies. In Fig.2, we have displayed the present results for another symmetric collision of  $He^+$  with  $He^+$  as a function of incident projectile energy. The present data are compared with the existing experimental results of Murphy et al [34], Melchert et al [35], Schmidt-Bocking and Dorner [36] (for the reverse reaction:  $He^{2+} + He(1s^2) \rightarrow He^+(1s) + He^+(1s)$ ) and only the theoretical results of Mancev [19]. However, our calculated results are in better agreement with the experimental results [34,35] in comparison to other theoretical results [19] particularly at lower side of the energy region under consideration, but agreement is poor with other experimental results [36] who have measured the cross sections for the reverse reaction. This discrepancy may be attributed to the principle of detail balancing. The theoretical results of Mancev using the CB1-4B [19] approximation agrees with the experimental results of Schmidt-Bocking and Dorner [36] (data taken from Ref. [10]), whereas the results obtained by the CDW-4B model [19] overestimate the experimental results [34-36] below 150 keV/amu. In the CDW-4B method, the electronic continuum intermediate states are included in both channels through

the Coulomb waves but not being included in the CB1-4B method. However, the CDW-4B and CB1-4B approximation may not be accurate at low energies. We have also observed that the ground state capture is dominant as for symmetric collision. This is expected because of energy resonance and velocity matching of the active electron in the initial and final states. We find from Fig.1 and Fig.2 the post-prior discrepancy is within 20% above 60 keV/amu for H + H collision and throughout the whole energy region for He<sup>+</sup> + He<sup>+</sup> collision.

Now, we shall study our computed results for the asymmetric reactions given by (20) and (21). In Fig.3, we have displayed the present results along with other available experimental and theoretical data for collision He<sup>+</sup> + H. From Fig.3, it is evident that the present computed results show overall good agreement with the experimental results [37-39]. The results obtained by CDW-4B approximation [18] overestimate the present computed results below 500 keV as the CDW-4B approximation may not be valid in the low energy range. The CTMC results of Becker and MacKeller [13] overestimate all the available results to a significant extent because classical treatment of a two-electron collision system may not be accurate. It may be seen from Fig.3 that the present results show good agreement with the theoretical results of Mancev [10] in the whole energy range. In such case post-prior discrepancy is less than 20% above 70 keV/amu. For Li<sup>2+</sup> + H collision, the present computed results in both forms are presented in graphical form in Fig.4. We have compared our theoretical results with only the experimental results [40] and theoretical results [4,6,19]. It is evident that the present results show good agreement with the experimental results. However, a comparison of the CDW-4B and CB1-4B models of Mancev [19] with the measurements shows that the theoretical curves underestimate experimental data, especially at lower impact energy (less than 400 keV/amu). The results obtained by the method of three-body formalism of BCCIS approximation in prior form and CTMC method [6] have similar trend with the present BCCIS-4B model. In both these methods [6], the interactions of the active electron in the target with incoming projectile ions have been taken by a suitable potential containing both a long-range part and a short-range part. However, such a BCCIS-3B model cannot yield any information about the relative significance of the role of the dynamic electron-electron correlation in collisions under study. As may be expected, the theoretical results of Eichler et al [4] using Oppenheimer-Brinkman-Kramers (OBK) approximation are not in agreement with the present results. We have observed that maximum contribution of total capture cross sections

occur at  $n=2$  state for  $\text{Li}^{2+} + \text{H}$  collision in the low energy range. The capture peak in the individual state may be explained in terms of the binding energy matching and the momentum distribution of the active electron in the initial and final state respectively.

#### **7.4. CONCLUSIONS**

We have calculated cross sections for the capture of  $1s$  electron by hydrogen-like projectile ions using the BCCIS-4B approximation in both the prior and post forms in the collision energy range of 20-5000 keV/amu. The present computed results are in satisfactory agreement with the experimental observations. The reasons for such success are the following: (i) the continuum state of active electron have been taken into account properly; (ii) the boundary condition for the scattering wavefunction has also been satisfied; and (iii) the potential is faster falling than the coulomb potential. In the presented four body formalisms, the dynamic electron correlations are automatically included through the perturbation potentials. However more experimental data covering higher energies is needed for the above mentioned interactions both for the development of refined theory and their applications in other branches of physics.

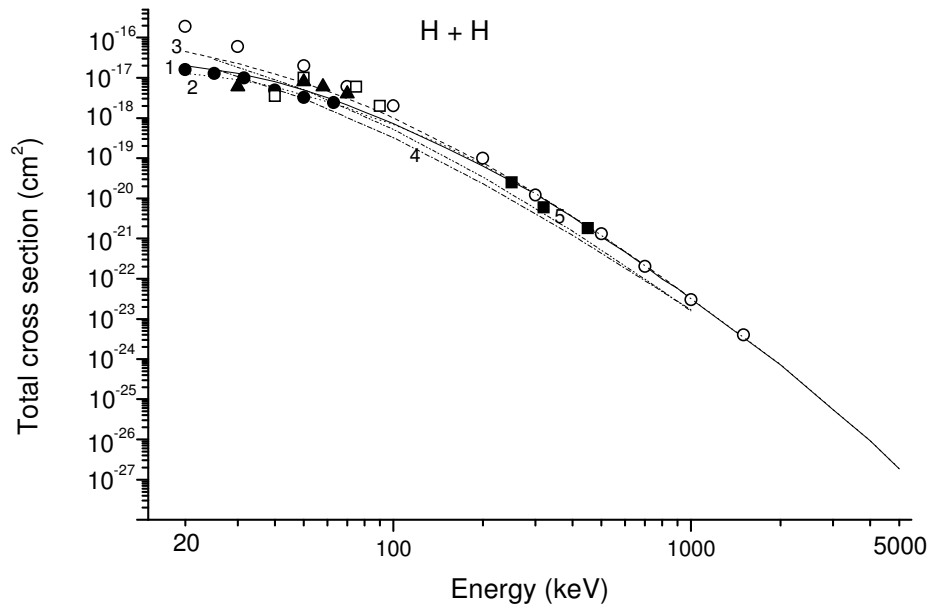


FIG. 1. Total cross sections (in  $\text{cm}^2$ ) as a function of the incident energy  $E$  (keV) for reaction  $H + H(1s) \rightarrow H^- + H^+$ .

Theory: solid line, 1: present results (prior form of BCCIS-4B); dotted line, 2: present results (post form of BCCIS-4B); dashed line, 3: CB1-4B results of Mancev [10]; dash-dotted line, 4: CIS-HF results of Banyard and Shirtcliffe [12]; dash-dot-dotted line, 5: CDW-HF results of Moore and Banyard [29]; open circle, first Born results of Mapleton [30]; open square, couple state results of Wang et al [31].

Experiments:  $\bullet$ , results of McClure [26];  $\blacksquare$ , results of Schryber [27];  $\blacktriangle$ , results of Hill et al [28].

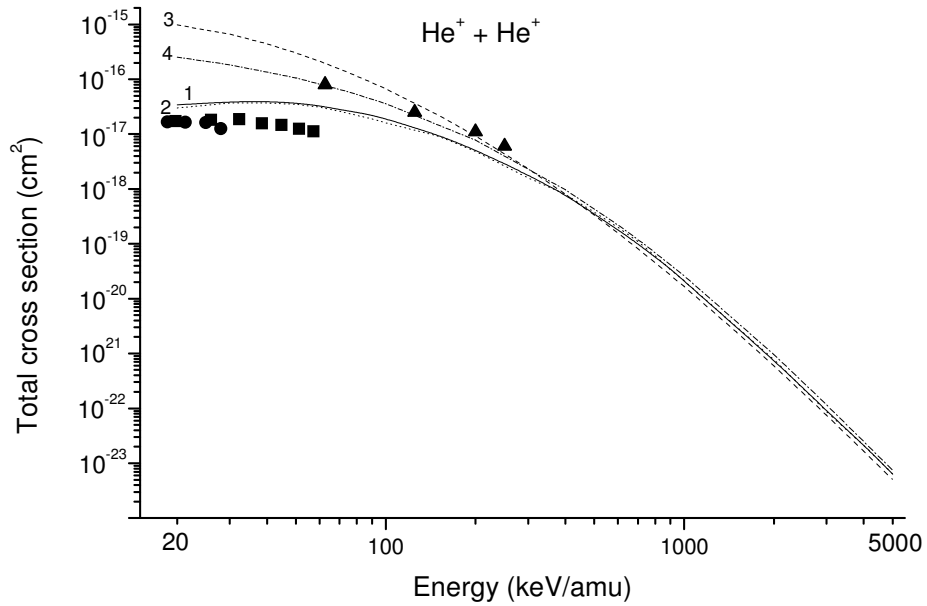


FIG. 2. Total cross sections (in cm<sup>2</sup>) as a function of the incident energy  $E$  (keV/amu) for reaction  $\text{He}^+ + \text{He}^+ \rightarrow \text{He} + \text{He}^{2+}$ .

Theory: solid line, 1: present results (prior form of BCCIS-4B); dotted line, 2: present results (post form of BCCIS-4B); dashed line, 3: prior form of CDW-4B results of Mancev [19]; dash-dotted line, 4: post form of CB1-4B results of Mancev [19].

Experiments: ■, results of Murphy et al [34]; ●, results of Melchert et al [35]; ▲, results of Schmidt-Bocking and Dorner [36] (data taken from Mancev [10]).

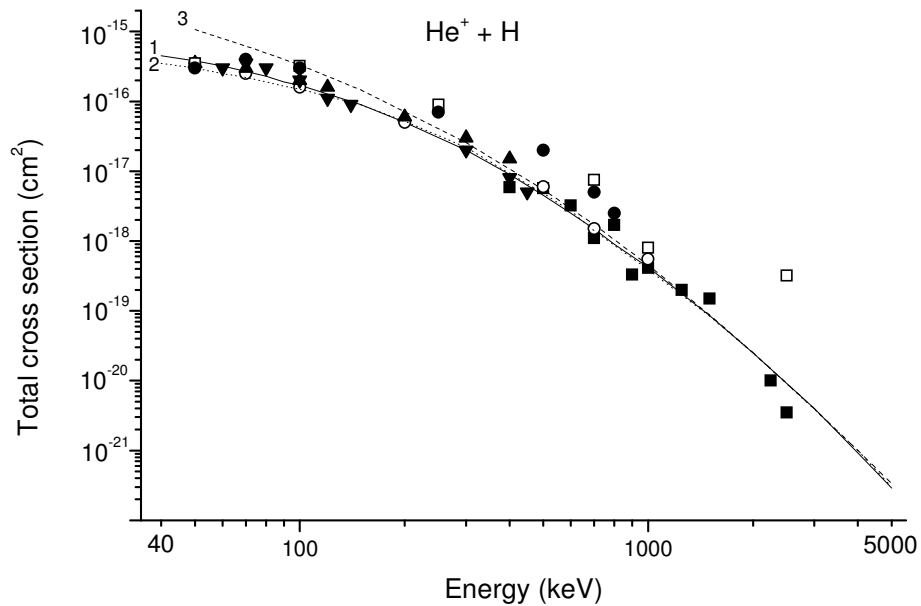


FIG. 3. Total cross sections (in  $\text{cm}^2$ ) as a function of the incident energy  $E$  (keV) for reaction  $\text{He}^+ + \text{H}(1s) \rightarrow \text{He} + \text{H}^+$ .

Theory: solid line, 1: present results (prior form of BCCIS-4B); dotted line, 2: present results (post form of BCCIS-4B); dashed line, 3: CDW-4B results of Mancev [18]; open square, CTMC results of Becker and MacKellar [13]; open circle, CB1-4B results of Mancev [10].

Experiments:  $\blacktriangle$ , results of Olson et al [7];  $\blacktriangledown$ , results of Shah and Gilbody [37];  $\bullet$ , results of Phaneuf et al [38];  $\blacksquare$ , results of Hvelplund and Andersen [39];

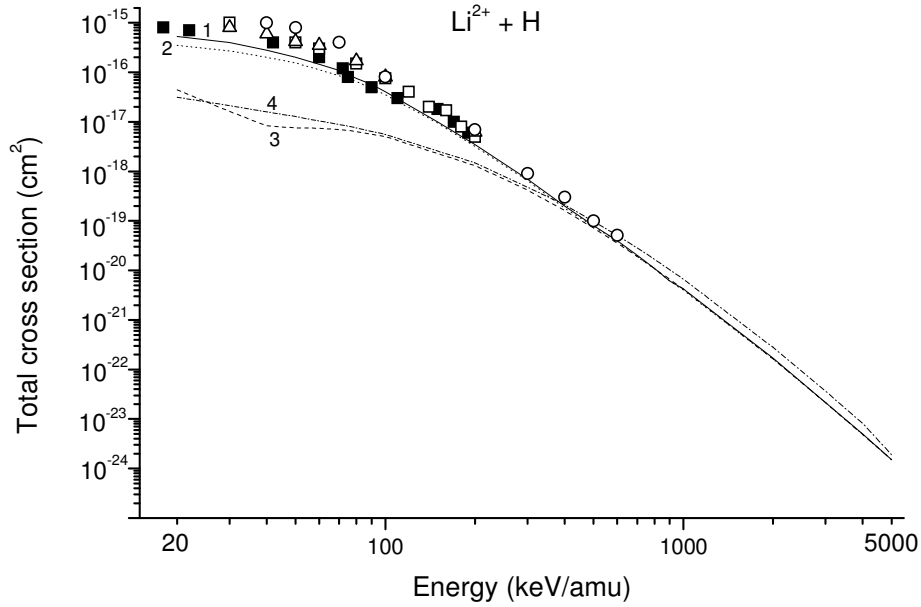


FIG. 4. Total cross sections (in  $\text{cm}^2$ ) as a function of the incident energy  $E$  ( keV/amu ) for reaction  $\text{Li}^{2+} + \text{H}(1s) \rightarrow \text{Li}^+ + \text{H}^+$ .

Theory: solid line, 1: present results (prior form of BCCIS-4B); dotted line, 2: present results (post form of BCCIS-4B); dashed line, 3: prior form of CDW-4B results of Mancev [13]; dash-dotted line, 4: post form of CB1-4B results of Mancev [19]; open square, BCCIS-3B results of Purkait [6]; open triangle, CTMC results of Purkait [6]; open circle, results of Eichler et al [4].

Experiments: ■, results of Shah et al [40].

## REFERENCES

- [1] J. McGuire, *Electron correlation dynamics in Atomic Collisions* (Cambridge University Press, Cambridge, 1997).
- [2] Dz. Belkic, Phys. Scr. **43**, 561 (1991).
- [3] A. L. Ford, J. Reading, and R. L. Becker, J. Phys. B **15**, 3257 (1982).
- [4] J. K. M. Eichler, A. Tsuji, and T. Ishihara, Phys. Rev. A **23**, 2833 (1981).
- [5] D. S. F. Crothers and N. T. Todd, J. Phys. B **13**, 2277 (1980).
- [6] M. Purkait, Nucl. Instrum. Methods Phys. Res. B **207**, 101 (2003).
- [7] R. E. Olson, A. Salop, R. A. Phaneuf, and F.W. Meyer, Phys. Rev. A **16**, 1867 (1977).
- [8] Dz. Belkic, J. Phys. B **10**, 3491 (1977).
- [9] L. Liu, D. Jakimovski, J. G. Wang, and R. K. Janev, J. Phys. B: At. Mol. Opt. Phys. **43**, 144005 (2010).
- [10] I. Mancev, Phys. Scr. **51**, 762 (1995).
- [11] I. Mancev, Phys. Rev. A **54**, 423 (1996).
- [12] K. E. Banyard and G. W. Shirtcliffe, Phys. Rev. A **22**, 1452 (1980).
- [13] R. L. Becker and A. D. MacKellar, J. Phys. B: At. Mol. Phys. **12**, L345 (1979).
- [14] W. Fritsch and C. D. Lin, Phys. Lett. A **123**, 128 (1987).
- [15] A. Henne, A. Toepter, H. J. Ludde, and R. M. Dreizler, J. Phys. B: At. Mol. Phys. **19**, L361 (1986).

- [16] R. Gayet and J. Hanssen, *J. Phys. B: At. Mol. Opt. Phys.* **25**, 825 (1992).
- [17] R. Gayet, J. Hanssen, and L. Jacqui, *J. Phys. B: At. Mol. Opt. Phys.* **28**, 2193 (1995). [18] I. Mancev, *Phys. Rev. A* **75**, 052716 (2007).
- [19] I. Mancev, *Eur. Phys. J. D* **51**, 213 (2009).
- [20] Dz. Belkic, I. Mancev, and J. Hanssen, *Rev. Mod. Phys.* **80**, 249 (2008).
- [21] R. Samanta, M. Purkait, and C. R. Mandal, *Phys. Rev. A* **83**, 032706 (2011).
- [22] Dz. Belkic, R. Gayet, and A. Salin, *Phys. Rep.* **56**, 279 (1979).
- [23] H. Bachau, R. Gayet, J. Hanssen, and A. Zerarka, *J. Phys. B: At. Mol. Opt. Phys.* **25**, 839 (1992).
- [24] R. R. Lewis, *Phys. Rev.* **102**, 537 (1956).
- [25] C. Mitra and N. C. Sil, *Phys. Rev. A* **14**, 1009 (1976).
- [26] G. McClure, *Phys. Rev.* **166**, 22 (1968).
- [27] U. Schryber, *Helv. Phys. Acta.* **40**, 1023 (1967).
- [28] J. Hill, J. Geddes, and H.B. Gilbody, *J. Phys. B: At. Mol. Phys.* **12**, 2875 (1979).
- [29] J. C. Moore and K. E. Banyard, *J. Phys. B* **11**, 1613 (1978).
- [30] R. Mapleton, *Phys. Rev.* **117**, 479 (1960); *ibid*, *Proc. Phys. Soc.* **85**, 841 (1965).
- [31] J. Wang, J.P. Hansen, and A. Dubois, *J. Phys. B: At. Mol. Opt. Phys.* **33**, 241 (2000).
- [32] E. Hylleraas, *Z. Phys.* **54**, 347 (1929).
- [33] S. Chandrasekhar, *Astrophys. J.* **100**, 176 (1944).

- [34] J. G. Murphy, K. F. Dunn, and H. B. Gilbody, *J. Phys. B: At. Mol. Opt. Phys.* **27**, 3687 (1994).
- [35] F. Melchert, K. Rink, K. Rinn, E. Salzbom, and N. Grun, *J. Phys. B: At. Mol. Phys.* **20**, L223 (1987).
- [36] H. Schmidt-Bocking and H. Dorner, 1994 (from Mancev [10] ).
- [37] M. B. Shah and H. B. Gilbody (Private Communication).
- [38] R. A. Phaneuf, F. W. Meyer, R. H. Mc Knight, R. E. Olson, and A. Salop, *J. Phys. B: At. Mol. Phys.* **10**, L425 (1977).
- [39] P. Hvelplund and A. Andersen, *Phys. Scr.* **26**, 375 (1982).
- [40] M. B. Shah, T. V. Goffe, and H. B. Gilbody, *J. Phys. B* **11**, L233 (1978).